Inelastic Response of Torsionally Unbalanced Multistorey Shearwall Buildings Designed Using Elastic Static and Dynamic Analyses

by

CHERYL DALE SEWELL

BASc., University of British Columbia, 1996

A THESIS SUBMITTED IN PARTIAL FULFILLMENT OF

THE REQUIREMENTS FOR THE DEGREE OF

MASTER OF APPLIED SCIENCE

in

THE FACULTY OF GRADUATE STUDIES

Department of Civil Engineering

We accept this thesis as conforming
to the required standard

THE UNIVERSITY OF BRITISH COLUMBIA

August 2000

Abstract

Damage to buildings during recent earthquakes caused by increased torsional response supports the need to improve upon the existing building code design guidelines through developing a better understanding of the response of asymmetric buildings with the intent to restrict the construction of torsionally precarious structures. The effects of torsion on building response is a complex problem for even single storey structures because so many parameters are involved in the description of linear and nonlinear torsional response. Discrepancies exist between the results of many previous studies due to the number of factors governing torsional response. Researchers also have varying opinions as to how to effectively incorporate torsional effects into analytical models for building design. These controversies contribute to the fact that there are wide variations between the torsional provisions of major world design codes. Current building codes torsional provisions are only applicable to buildings which are essentially uniform vertically with relatively symmetric floor plans.

Most studies examining torsional response of multistorey buildings focus on shear frame structures. This study investigates the adequacy of elastic design methods to predict and control the increased displacement and ductility demand on edge-elements of vertically uniform, multistorey, shear core buildings, designed to yield in flexure, with varying degrees of asymmetric stiffness distribution. A comparison is made between the elastic and nonlinear time history response of models designed using three elastic methods of determining element strength; the NBCC static torsional provisions (*NBC*), revised static torsional provisions proposed by Humar and Kumar (*H/K*), and a dynamic analysis with a statically applied torsional moment of $0.1b$ (*Dyn*+*T1*) where b is the length of the building perpendicular to the direction of earthquake motion.

The elastic static methods grossly overestimate nonlinear displacements of elements on both the stiff- and flexible-edges for torsionally flexible structures. The elastic response spectrum analysis (RSA) with shifted centre of mass (CM) best estimates inelastic displacements for all elements. Inelastic displacements of stiff- and flexible-edge elements generally increase with increasing torsional flexibility for structures with a torsional to lateral frequency ratio, $\Omega < 1$. Deformation demand increases with the magnitude of static stiffness eccentricity for the flexible-edge elements. The inelastic displacements of stiff-edge elements of torsionally stiff structures (for $\Omega = 1.25$) increase for the *Dyn*+*T1* and sometimes for the *H/K* design method, leading to large ductility demands for these elements. The *NBC* design method best controls the displacements and, therefore, ductility demand of stiff wall elements at $\Omega = 1.25$. The displacement response of structures with a lateral period ≥ 2 seconds is relatively insensitive to the design method used for determining element strength distribution. The ductility demand of the flexible wall elements is below the design target for all methods of design.

Dynamic magnification of base shear and storey shear forces, found by the nonlinear analyses, due to the contribution from higher modes can be more than double those predicted by elastic analysis, regardless of the elastic method employed in determining wall strengths. Also, the inelastic moment demand from the nonlinear dynamic time history analyses varies substantially from that predicted by the elastic analyses. Higher mode effects are evident in the moment and shear envelopes of the stiff and flexible walls and are more pronounced for the buildings with a lateral period ≥ 2 seconds.

Table of Contents

List of Figures

List of Tables

List of Symbols

A_x	amplification factor specified in UBC 1997
AUS	Australian Building Code
a	building plan dimension, measured parallel to direction of earthquake ground motion
b	building plan dimension, measured perpendicular to direction of earthquake ground motion
BST	base shear–torque surface
CM	floor centre of mass
CR	floor centre of rigidity
CS	storey shear centre
δ_i	floor displacement at i^{th} storey
e	arbitrary value of eccentricity
e_1	additional supplementary eccentricity used by the Eurocode 8
e_a	accidental eccentricity
e_d	design eccentricity
e_e	effective edge eccentricity
e_r	(strength) resistance eccentricity
e_s	static stiffness eccentricity between CM and CR
e_{d1}, e_{d2}	design eccentricities
EC8	Eurocode 8
F_i	floor force at level i

GC	geometric centroid of floor plan
I_{cm}	polar moment of inertia about the *CM*
J	adjustment factor for NBCC storey moments
K	total lateral stiffness parallel to the direction of earthquake motion
k_i	elastic stiffness of lateral load resisting element i ($i = 1, 2$, or 3)
Ko	initial stiffness of hysteresis model
Ku	stiffness degradation of hysteresis model
K_x	total lateral stiffness in x-direction
K_y	total lateral stiffness in y-direction
k_{yi}	is the lateral stiffness of the i^{th} element in the y-direction,
$K_{\theta r}$	rotational stiffness about CR
L	vertical length/height of the wall
l_d	development length
l_w	length of the lateral resisting wall element
m	lumped floor mass
MES	mass eccentric system
M_b	base moment
M_I	design value of bending moment
M_t	torsional moment resulting from design eccentricity
M_y	yield moment
n	the number of resisting planes in the y-direction and number of stories
NEHRP	National Earthquake Hazards Reduction Program
NBCC	National Building Code of Canada
NZS	New Zealand Standard
q	behaviour factor

Q	approximated seismic base shear force
Q_I	design value for shear force
R	force reduction factor for determining inelastic design strengths
r_k	resilience radius - term used by the Eurocode 8, which is identical to the stiffness radius of gyration about the CR
r_m & r_r	mass radii of gyration taken about CM and CR, respectively
RSA	response spectrum analysis
Sad_{max}	peak value of the design acceleration spectrum, and
$Sad(T_1)$	spectral acceleration corresponding to the fundamental lateral period
SE	super-element
SES	stiffness eccentric system
SST	story shear and torque response histories
TB	torsionally balanced building
TH	time history
TU	torsionally unbalanced building
T	fundamental lateral period
T_i	i^{th} storey torque
T_y	uncoupled lateral period in the y-direction in seconds
T_z	torque in the z-axis
T_θ	uncoupled torsional period in seconds
UBC	Uniform Building Code
V_o	base shear in the torsionally balanced (TB) building
V_x & V_y	base shear in the x- and y-axis
x_i	is the distance to the i^{th} element in a plane parallel to the x axis
α, δ	coefficients to represent effect of torsional dynamic amplification in torsional design eccentricity equations

δ_{max}, δ_{avg}	maximum and average diaphragm displacements of the structure under applied design lateral forces
β	coefficients to represent magnitude of accidental eccentricity in torsional design eccentricity equations
Δ_{max}	maximum displacement recorded for an equivalent elastic system
Δ_u	ultimate or peak displacement
Δ_y	displacement at yield
γ	first hysteresis parameter of the hysteresis model
γ_c	correction factor for EC8 code design
λ_u	third hysteresis parameter of the hysteresis model
μ_Δ	displacement ductility
μ_θ	rotational ductility
ρ_k	normalized torsional stiffness radius of gyration
ω	dynamic magnification factor for shear
ω_y & ω_x	uncoupled lateral frequency in the *y*- and *x*-direction (rad/s)
ω_θ, $\omega_{\theta r}$	uncoupled torsional frequency (rad/s) with torsional inertia calculated about CM and CR, respectively
Ω, Ω_r	uncoupled torsional to lateral frequency ratios taken about the CM and CR, respectively, defined as ω_θ / ω_y and $\omega_{\theta r} / \omega_y$ respectively
θ_i	i^{th} storey rotation
θ_p	peak plastic rotation

Acknowledgements

I am deeply indebted to my advisor, Dr. Don Anderson, whose wealth of experience and knowledge peaked my curiousity in structures and earthquake engineering during my undergraduate degree. His enthusiasm and generosity throughout my studies is greatly appreciated.

I would like to thank Dr. Carlos Ventura, who reviewed the final draft of this thesis and provided valuable guidance for my directed study in the initial stages of my research. I would also like to thank him for distracting me with other intriguing projects along the way which deepened my interest in earthquake engineering. I would also like to thank Dr. Kang-Ning Li for providing the program CANNY-E and for his continuous support in assisting with the various difficulties that arose during structural modelling.

The financial support for this research was provided by a research scholarship from NSERC, the Natural Science and Engineering Research Council of Canada. Without this support I could not have considered continuing my university education at this time.

Finally, I would like to thank my family for supporting me in every possible way during my studies. My parents, Irvin and Agnes, have offered contiuous support in my endeavors and I will always cherish their pride in everything I do. My husband Bill, worked back to back with me on his Ph.D. disertation – the dueling computers – essentially every night this last year. His devotion and dedication to his own work fueled me to completion. And finally, my beautiful daughter Simone, who joined me at the comencement of the writing stage of this thesis, came into this world on March 6th, 2000.

1 Introduction

1.1 General

A considerable number of asymmetric buildings have suffered severe damage and collapse in recent large magnitude earthquakes. The cause can usually be attributed to inadequate element strength and/or lack of ductile detailing for the excessive demand imposed on lateral resisting elements due to torsional response during strong ground motion. The coupling between the lateral and torsional modes of asymmetric buildings leads to nonuniform displacement demand on the lateral resisting elements, which is of great significance in when sizing and detailing structural elements for earthquake resistance. The occurrence of structural failures supports the need for a better understanding of building response to improve upon existing building code design guidelines and restrict the construction of torsionally precarious structures.

The increased response of asymmetric structures to strong ground motion has been the subject of many studies in past years. Numerous studies have been conducted on elastic and inelastic torsional response of single storey buildings. Some studies extend to simple multistorey shear frame buildings, however, few incorporate the response of shear wall or shear core structures. To investigate the current state of research, several recent analytical studies examining elastic and inelastic torsional effects and proposals for new treatment of torsion were reviewed. An attempt was made to identify inconsistencies between results of the studies and to search for areas in need of further investigation.

The main objectives of this study are:

- to develop an understanding of the elastic and inelastic response of multistorey shear wall buildings to earthquake records,
- to compare various parameters of the elastic and inelastic response of structures with lateral resisting element strengths distributed according to different dynamic and quasi-static design methods,
- and to comment on the applicability of the NBCC-95 torsional provisions for multistorey asymmetric shear wall buildings.

1.2 Sources of Torsional Response

The sources of torsional response can be broken into two categories, (1) natural torsion and (2) accidental torsion. Natural torsion is considered to be the resulting torsional response due to coupling between the lateral and torsional motions of buildings with inherent plan asymmetry. The dynamic forces acting on a structure during an earthquake are a function of the mass inertia and are considered to act through the centre of mass, CM, at each floor level. If the centre of mass and centre of rigidity, CR, of each floor do not coincide torsional motion results when the structure is subjected to ground shaking.

Accidental torsion is a result of all the unforeseen variability in the structural properties of the building and the input ground motions which lead to changes in the torsional response. The actual distribution of mass in a building is likely different than the commonly adopted assumption that building mass is concentrated at the floors and uniformly distributed. Accidental torsion is to account for the uncertainty in determining the locations of CM and CR as well as the uncertainty in determining lateral load resisting element stiffness and strengths due to variability in material properties, element dimensions, fabrication, quality control, construction methods, and previous load history. This implies that even nominally symmetric structures are inherently asymmetric to some degree. Other sources of accidental torsion are variations of stiffness with time, possible additional inelastic action, torsional vibrations due to base rotational motion and spatial variations in ground motion, and other unforeseen sources of torsion.

1.3 Literature Review

Exhaustive parametric studies have been conducted on single story asymmetric structures to develop an understanding of the change in displacement response due to building asymmetry and lateral torsional coupling. The effects of torsion are influenced by a large number of governing parameters and is an inherently complex problem for even single story buildings. The complex nature of torsion and torsional coupling make it difficult to compare studies or extract general trends from results that can be applied to asymmetric structures other than for the particular ones studied. From this brief review of previous research on elastic and inelastic torsional response of buildings it is apparent that the conclusions derived are not always consistent and may be model specific rather than generally valid for all structures.

Few studies encompass multistorey asymmetric buildings due to the already complex nature of the single storey structures and mainly only cover a special class of uniformly asymmetric multistory buildings where the CM and CR lie in two vertical axes. It is not obvious how to extend these results to irregular or highly asymmetric multistorey buildings.

Code torsional provisions are based on the original studies of torsion examining the elastic response of simple single storey asymmetric structures. The early studies focused on the maximum torsional moment as the important response parameter for establishing torsional response (Tso & Dempsey, 1980). Torsional effects were defined by the ratio of the dynamic to static torques, termed the dynamic eccentricity, which was considered to be the measure of torsional coupling. Tso & Dempsey found that coupling effects in the elastic range were significant for structures with an uncoupled torsional to lateral frequency ratio near one. Based on these findings they recommended that structures with an uncoupled torsional to lateral frequency ratio close to one be avoided.

In subsequent studies, Dempsey and Tso (1982) and Tso (1983) found that maximum edge displacement provided a better means of assessing torsional response. They established the concept of effective edge eccentricity, e_e, defined as the shortest distance from the CR to a point through which the static shear force would act to produce displacements identical to those obtained through a dynamic analysis. Comparisons of the two methods showed that for a given structure, e_e was about 50 – 75% of the dynamic eccentricity. This difference was due to the fact that the maximum edge displacements due to peak lateral motion and peak torsional response were not likely to occur simultaneously.

Many studies on the elastic response of buildings have been used to evaluate torsional provisions in seismic codes. As a result, torsional provisions of major world building codes have been amended several times with the intent of defining more rational expressions for the design eccentricity equations. The study by Tso (1983) led to the current form of the design eccentricity equations found in the NBCC torsional provisions. Cheung & Tso (1987) verified that the static provisions established for single storey structures could be extended to simple multistorey structures with limited asymmetry, where the CR and CM on each floor lie essentially on two vertical axes over the height of the building. They found that the NBCC static code procedures do provide reasonable estimates of seismic torsional effects for regular asymmetric multistorey structures. However, for irregular asymmetric multistorey structures, with CR scattered about a vertical axis, a dynamic modal analysis is the only reliable tool for estimating the torsional response. Static code procedures can not be relied upon to provide estimates of response for general asymmetric structures.

More recently researchers have focused on investigations of the inelastic response of asymmetric single storey structures. Initially, the response of asymmetric systems was compared to that of similar but symmetric reference models exhibiting purely translational behaviour in both the elastic an inelastic ranges (Tso and Sadek, 1985; Sadek and Tso, 1989; Goel & Chopra, 1990, 1991; Tso & Ying, 1992). This lead to the classification of two types of eccentric model systems, mass eccentric systems MES, and stiffness eccentric systems SES, which were found to behave quite differently when excited into the inelastic range. The MES creates eccentricity in the system by altering the mass distribution (or location of CM) while maintaining a constant stiffness distribution to the lateral resisting elements. The SES introduces eccentricity by modifying the stiffness distribution to the lateral resisting elements while keeping the mass distribution constant. The conclusions drawn from these studies were often contradictory and could not be considered valid for general structures but rather restricted to the particular system studied and the associated design assumptions. Despite the contradictions between conclusions drawn from various studies, they have been important in the developing of a general understanding of the behaviour of asymmetric systems.

Tso and Sadek (1985) found that contrary to findings of earlier research by Kan & Chopra (1981) based on elastic response of asymmetric systems, the coincidence of the uncoupled torsional and lateral frequencies in the inelastic range did not lead to a large increase in response. They also concluded that a) asymmetric systems do not respond primarily in translation when excited into the inelastic range, as found in previous studies, but rather exhibit significant torsional response, b) variations in the ratio of uncoupled torsional to lateral frequencies had little effect on displacement ductility demand of edge elements, however, peak displacement of eccentric systems decreased with increased torsional stiffness c) the ductility demand on flexible-edge elements in asymmetric systems can increase by as much as 100% and displacement demand by as much as 300% over a symmetric system, and d) both ductility demand and edge displacements increase with increased static eccentricity as expected. Tso and Sadek (1985) also showed that a 3-element model is more representative of an actual structure than the 2-element model adopted in some earlier studies because the model with 3 elements becomes statically indeterminate and the changes in torsional frequency are achieved through variations in torsional stiffness rather than purely through changes in the polar moment of inertia of the floor slab.

The influence of strength eccentricity on torsional response was examined in further studies. Sadek and Tso (1989) proposed that strength or resistance eccentricity, e_r, be considered as an alternate measure of asymmetry. They showed that for a given stiffness eccentricity, the torsional response of the system decreased with decrease in strength eccentricity. Bruneau and Mahin (1991) found that stiffness symmetric structures with asymmetric strength distribution exhibit torsional response in the inelastic range. Tso and Ying (1990) examined the difference in response between inelastic SES and MES models with element strengths distributed proportional to their stiffness (ignoring torsion) referred to as the "proportional model" and models with element strengths determined including the effects of torsion as required by code torsional provisions referred to as the static "equilibrium model". The first method leads to a strength eccentricity, e_r, equal to the stiffness eccentricity, $e_r = e_s$. The second method, which is essentially an examination of the NBCC design eccentricity equations, lead to a strength eccentricity $e_r \cong 0$. They concluded that (1) flexible-edge elements in a SES and stiff-edge elements in a MES can experience large additional ductility demand; (2) the ductility demand for flexible-edge elements of a SES is greater for systems with $e_r = e_s$ than systems with $e_r \cong 0$; (3) flexible-edge elements in both SES and MES exhibit a large increase in displacement demand; (4) for systems with $e_r \cong 0$, flexible-edge elements of SES exhibit minimal additional ductility demand but display additional displacement demand of up to 3 times that of a similar symmetric system; (5) for all models the flexible-edge element strength should be adequately increased to account for the additional displacement and ductility demand due to torsional effects and stiff-edge element strength should not be drastically decreased; (6) additional displacement demand is relatively insensitive to lateral period or means of determining strength distribution; (7) strength eccentricity alone is not an effective criterion for specification of strength distribution to all classes of eccentric systems.

Subsequent studies confirmed that elements on the flexible side of the building are most vulnerable to additional ductility demand for SES (Tso & Ying, 1992) and elements on the stiff side are most susceptible for MES (Goel & Chopra, 1990). Goel and Chopra (1990) also examined the influence of a number of additional parameters on the inelastic response of single-storey asymmetric structures and concluded the following: (1) contributions to torsional stiffness from resisting elements located perpendicular to the direction of ground motions substantially decreased torsional response for short period, acceleration-sensitive structures, however, their influence is small for medium and long period structures; (2) the number of resisting planes oriented in the direction of ground motion has little influence on the response of systems with $e_r \cong e_s$ and on the displacement response for systems with $e_r << e_s$, however, element ductility demand of the latter could be greatly affected; (3) strength symmetric systems with $e_r \cong 0$ experience much lower effects of torsional coupling as compared to systems with $e_r \cong e_s$.

Tso and Zhu (1992) reiterated that SES and MES possess different requirements for strength eccentricity to minimize additional ductility demand and strength eccentricity alone is not a sufficient measure for determining strength distribution for all types of asymmetric structures. They stated that although the classification of eccentric systems into SES and MES is logical for the understanding of torsional response, it is not practical for the development of design guidelines. They also criticized the use of a symmetric reference model since the ductility demand on elements of the symmetric and asymmetric systems are not considered to be directly comparable because the stiffness distribution, mass distribution, and lever arms from the CR to the wall elements the varied between the models. To alleviate these issues, Tso and Zhu (1992) proposed a new form of reference system that is derived directly from the asymmetric system. It is not required to be symmetric but purely torsionally balanced – defined as having the same stiffness distribution as the asymmetric or torsionally unbalanced system but with the mass distribution altered such that the CM and CR coincide. Since the eccentricity of the unbalanced system is due to stiffness asymmetry in plan and to changes in mass distribution from the reference model, the comparison incorporates both forms of eccentricity and the problem of classifying the unbalanced system as SES or MES is avoided.

In this study, Tso and Zhu (1992) examined the ductility demand on a broad range of 3-element, single storey systems with strengths distributed according to the torsional provisions of NBCC-90, NZS-84, and UBC-88. They defined the static eccentricity and the second moment of stiffness distribution – the normalized torsional stiffness defined as $\rho_k = \frac{1}{b}\sqrt{\frac{K_{\theta r}}{K}}$ as the important parameters affecting torsional response – where b is the dimension of the structure perpendicular to the direction of ground motion, $K_{\theta r}$ is the torsional stiffness about the CR, and K is the lateral stiffness parallel to the direction of ground motion. They determined that (1) there is always additional displacement demand on the flexible-edge element which is a function of the torsional stiffness, the static eccentricity, and the distance from the CR but it is essentially independent of the method of determining element strength distribution; (2) flexible-edge elements of systems designed without torsional provisions (stiffness proportional strength distribution) always exhibit additional ductility demand, however, systems designed based on any of the three code torsional provisions limit flexible-edge ductility demand; (3) substantial strength reduction of stiff-edge elements is allowed for torsionally flexible systems by the UBC-88 and NZS-84 which resulted in a significant additional ductility demand on stiff-edge elements. They also showed that the first two modal periods (first lateral in the direction of interest and first torsional), for a torsionally coupled system always lie outside the frequency range bounded by the fundamental uncoupled lateral and torsional periods – above the higher uncoupled frequency and below the lower uncoupled frequency. This follows the fundamental theory of vibrations (Thompson, 1971) which states that the coupled frequencies always lie outside the uncoupled frequencies. The form and adequacy of the various current code torsional provisions is discussed in greater detail in Chapter 2.

In a separate study, Zhu and Tso (1992) investigated the factors affecting strength distribution of asymmetric structures based on the torsional provisions of various codes. They expressed the element strength as the element strength of a similar torsionally balanced system multiplied by a strength factor. The strength factor is a function of the design coefficients of the particular code specified design eccentricity equations and three system parameters: the location of the element relative to the CR, the normalized torsional stiffness as defined previously and, the static eccentricity of the structure. They proposed a relaxation of the NBCC torsional provisions for the flexible side elements by reducing the first coefficient of the design equations from 1.5 to 1.0 as per the NZS and UBC. The form of the design equations for code torsional provisions is discussed in Chapter 2.

In its present form, adopted in the 1985 version, the NBCC torsional provisions require the explicit determination of the CR location. While the eccentricity concept is widely accepted and implemented into most code torsional provisions, the definition of eccentricity differs between codes (Tso, 1990). Determining eccentricity is a simple task for single storey structures since all possible definitions of eccentricity, centre of rigidity, shear centre, and centre of twist coincide, however, it is not easily extended to general multistorey buildings. Tso (1990) clarified two definitions of eccentricity applied to multistorey buildings adopted by code torsional provisions and shows that if the proper definitions are employed, both methods produce the same storey torsional moments. These methods are discussed in greater detail in Section 2.2.4. Goel and Chopra (1993) attempted to alleviate the problem of determining CR locations by developing a means of determining equivalent static element storey forces of multistorey asymmetric structures without locating CR, but this requires a 3D analysis.

The concept of accidental torsion has been studied in detail by De La Llera and Chopra (1992, 1994a, b, c, d, e, 1995a) to ascertain how accurately the method of increasing the design eccentricity by a constant value for the accidental torsion incorporated by most codes predicts the "true" increase in response due to all sources of accidental torsion. These studies focus on developing a more accurate estimation of accidental torsion due to rotational motion of building foundation, uncertainty in stiffness of structural elements, uncertainty in location of CM, uncertainty in stiffness and mass distributions of stories other than the one analyzed and stiffness uncertainty in elements perpendicular to the direction of ground motion assuming linear elastic behaviour of buildings. The uncertainty in the system parameters were defined and characterized using known and inferred experimental data. Then the response of nominally symmetric plan systems were examined using an approximate analytical model for probability distribution of the system response and a series of Monte Carlo simulations based on sampling the probability distributions of the desired structural parameter. The effects of base rotational excitation on building response was studied using recorded motions obtained from 30 buildings in California. They concluded that (1) together the effects of uncertainty in element stiffness and location of CM account for approximately 70% of the increase in response due to accidental torsion. Since both of these are best modelled by perturbations of the static eccentricity, this gives justification to using the dynamic method of calculating effects due to accidental torsion by shifting the CM some distance away from its nominal position; (2) the increase in response resulting from a dynamic analysis shifting the CM $\pm 0.05b$ followed a trend similar to the estimated "true" increase in response due to the combined effects of all sources of accidental eccentricity; (3) the response obtained from applying equivalent static forces at a distance equal to the accidental eccentricity, e_a, from the CM did not follow the same trend; (4) a dynamic analysis incorporating 5% accidental eccentricity adequately estimates the combined "true" effects of accidental torsion with a probability of exceedance of approximately 30%. Using an accidental eccentricity of 10%, as required by the NBCC, would give more conservative results closer to the combined "true" mean-plus-one standard deviation values and a lower probability of exceedance; (5) accidental torsion effects are greater for symmetric systems than for eccentric systems.

In most studies, the adequacy of code torsional provisions is judged on their ability to limit element ductility demand in eccentric or torsionally unbalanced models to no greater than those of a similar but non-eccentric or torsionally balanced reference model. Significantly different results are obtained for ductility demand, deformation at edge elements and yield strengths, depending on the method of incorporation of accidental torsion. There is a difference in opinion between researchers as to whether accidental torsion should be included in the distribution of strengths in models used to evaluate code torsional provisions (Correnza *et al* 1992, 1995; Tso, 1993). It is not clear how to incorporate accidental torsion for effective evaluation of existing design procedures since the effects cannot be easily simulated in either the reference or analytical model without some extensive form of probabilistic simulation. Chandler and Duan (1991) believe that since the accidental torsion effects cannot be easily simulated in the analysis then they should be omitted in the element strength distribution of both the reference and analytical models for consistency. This method of comparison would only evaluate the static eccentricity portion of the torsional provisions. A similar approach adopted by Correnza *et al* (1992) is to include accidental torsion allowances in both the reference model and eccentric model. With this approach the reference model becomes code dependant since the percentage of accidental torsion applied is code specific.

Wong and Tso (1994) argue that in order to fully evaluate code torsional provisions the analytical model element strengths should include the accidental torsion allowance, however the reference model should remain free of torsion to maintain a unique reference against which it is possible to clearly quantify the torsional effects of the code. The inclusion of accidental torsion introduces eccentricity into the reference model which could exhibit substantial torsional responses when excited into the inelastic range. The inelastic displacements of the reference model would be a combination of translational and torsional motions and comparing the displacements of an asymmetric system to this reference model would not give a clear illustration of the isolated torsional contribution to edge displacement or ductility (Tso, 1993). Also, the accidental torsional provisions differ among codes which would result in different reference models depending upon the code being evaluated.

The treatment of accidental torsion effects (whether they are incorporated into the reference model or not) can result in significant differences in distribution of element strengths and comparison of the results. It is very important to consider the form of reference model when evaluating the response results.

The extension of the static torsional provisions is generally accepted for a special class of uniformly asymmetric multistorey buildings, where the CR and CM of each storey lie on two vertical axes over the height of the building, since the determination of CR locations is identical as for single storey structures. A number of researchers have extrapolated the findings for single storey structure and applied the static methods of distributing element strength to irregular, asymmetric, multistorey models and investigated the adequacy of these methods through performing 3D inelastic dynamic analyses. Duan and Chandler (1993) investigated the inelastic response of a special class of asymmetric multistorey frame buildings designed according to the NBCC-90, UBC-88, Mexican code 87, Eurocode 8 and NZS-92. They concluded that, contrary to findings for elastic systems, the torsional provisions did not adequately control additional ductility demand on edge elements in the inelastic range. Based on a comparison between codified static and elastic dynamic analyses, Tso and Yao (1994) state that the static approach assumes the majority of response comes from the first mode, and higher mode contributions cannot be simulated by the static approach. Higher mode contributions become more significant as building irregularity increases and the static approach can underestimate the forces induced in the edge frames. De La Llera & Chopra (1992, 1994a, 1996) showed that observations and conclusions drawn for single storey asymmetric structures were valid for the special class of uniform multistorey buildings, however, the torsional response of irregular multistorey buildings with discontinuities in torsional stiffness between floors is much more difficult to predict.

Tso and Wong (1995) investigated the ability of three codes, NBCC-90, UBC-91 and NZS-92 to estimate the inelastic displacements at the flexible-edge of torsionally unbalanced, TU, single storey structural systems and found that only the NZS always gave conservative estimates. They also concluded that the elastic response spectrum analysis incorporating accidental torsion effects by shifting the CM by $\pm 0.1b$ is a viable means of conservatively estimating flexible-edge displacements.

Chopra and De La Llera (1995b) developed a conceptual aid to assist designers in understanding the performance (torsional/translational behaviour) of various asymmetric structural configurations. They created a means to construct a base shear–torque surface, abbreviated BST, whose boundaries define the limits of the elastic response of a structure. The base shear and torque response histories are plotted in a force space with base shear V_x and V_y in the x- and y-axis and torque, T_z, in the z-axis. The base shear and torque at each instant of the response of a structure to earthquake loads define one point in this space. The boundary of these points are defined by a surface which corresponds to all the possible combinations of shear and torque for inelastic response that depict the collapse mechanisms of the system. The interior of this surface contains all the possible combinations for elastic behaviour of the structure.

In a subsequent study, Chopra and De La Llera (1994a, 1996) extended the concept of the BST surface to uniform multistory asymmetric structures and developed story shear and torque response histories, abbreviated SST, for various different structural configurations to establish a means of understanding the governing parameters for the complicated nature of inelastic seismic behaviour of general multistory systems. The SST surfaces combined with the associated yield surfaces can act as useful conceptual aids in the preliminary design stage to ensure that asymmetric structures have adequate torsional stiffness to avoid the formation of torsional mechanisms. A further study (De La Llera & Chopra, 1995c) lead to the development of a simplified model for analysis and design of multistorey buildings consisting of a single super-element (SE) per storey possessing the elastic and inelastic properties of the entire storey. The SE model incorporates an accurate representation of the SST surfaces which enable it to capture the fundamental features of the inelastic behaviour of the structure. The accuracy of the SE was found to be adequate for most design purposes. The maximum error in peak response due to the simplifications of the SE was less than 20% for the structures examined.

Based on the results of previous studies, Bertero (1995) suggests that detrimental torsional effects can be escaped if a building is designed to eliminate the possibility of a torsional mechanisms forming during inelastic response to seismic loads. This view is also supported by Paulay (1997a) in his recent papers reviewing the adequacy of current torsional provisions.

With the goal to avoid torsional mechanisms, Bertero developed a method to determine the reduction of building strength resulting from inelastic torsion applying classical theorems of plastic analysis to a simplified auxiliary structure. The auxiliary structure is made to possess the same properties for total strength as the original structure for both orthogonal directions, torsional strength and location of CM and CR. This method can be applied to a special class of uniform multistory buildings with identical floor plans where the CM and CR fall on the same two vertical lines. The limitation on perimeter elemental strength to avoid the formation of a torsional mechanism can be identified in the preliminary design stages.

In recent studies Paulay (1997b & c) investigated the elasto-plastic torsional response of asymmetric structures. He developed a conceptual model with elastic-perfectly plastic wall elements. Based on the deformation capacity and torsional restraint of the system the development of a torsional mechanism may occur when pushed into the inelastic range. Paulay proposed that structures without torsional restraint perpendicular to the direction of earthquake motion should be avoided. A subsequent study by Farah (1998) found Paulay's approach to be overly conservative. The development of torsional mechanisms did not occur during inelastic time history analyses as Paulay hypothesized and the predicted magnitudes of displacement ductility and displacement demand were not attained.

Humar (1998) and Humar & Kumar (1999) proposed alterations to the NBCC code torsional provisions to encompass some of the results of recent studies. They maintained the current approach for treatment of torsional effects through altering the design eccentricity equations. The proposed alterations provide separate equations for flexible and stiff-edge elements.

The proposed design eccentricity equations are as follows:

For flexible-edge elements: $e_d = e_s + 0.1b$

For stiff-edge elements: $e_d = e_s - 0.1b\Omega \geq 1$

$e_d = -0.1b\Omega < 1$

where e_d is the design eccentricity, e_s is the static stiffness eccentricity, and Ω is the ratio of the torsional to lateral uncoupled fundamental frequencies. These equations include an accidental eccentricity allowance of $\pm 0.05b$. The remaining eccentricity is to account for natural torsion. Humar concluded that a good design would avoid low values of Ω which would eliminate torsionally flexible structures with lateral resisting elements located only near the geometric centre of the building. The new proposed design eccentricity equations require calculation of the frequency ratio, Ω, however, this can be adequately estimated by the Rayleigh method and would be a good indicator of excessively torsionally flexible systems.

The ultimate goal of research examining the torsional response of asymmetric structures is to develop universally accepted guidelines for the design of ductile asymmetric structures to be incorporated into building codes, however, this is yet to be achieved. The effects of plan asymmetry on elastic response of buildings has been well established, but these results are not necessarily directly applicable to determining design forces for the majority of buildings which are intended to deform well into the inelastic range when subjected to strong ground motion. The many governing parameters influencing the nonlinear response of asymmetric structures further complicate the investigation of such systems. Some of these parameters identified for single storey inelastic models in previous studies are planwise strength distribution, strength asymmetry, element overstrength factor, mass eccentricity, number of resisting planes parallel to the direction of ground motion, contribution to torsional stiffness from resisting elements perpendicular to the direction of ground motion, torsional to lateral frequency ratio, bidirectional ground motion, and the dominant frequency content of the earthquake records. Despite the efforts of previous research to identify the controlling structural parameters of inelastic torsional behaviour, no clear relationships have yet been identified. The discrepancies between conclusions drawn from the numerous studies has led to variations between major world seismic code torsional provisions.

1.4 Scope

Several researchers have conducted exhaustive parametric studies on the various aspects affecting the torsional response of single storey and uniformly asymmetric multistorey frame buildings. The main issues addressed in this thesis, identified from the review of these studies as requiring further investigation, are as follows:

1. Do the current NBCC static torsional provisions adequately control element ductility demand. How does the ductility demand determined from the NBCC design compare with that from a dynamic analysis with shifted CM, a dynamic analysis with statically applied torsional moments, and the static method proposed by Humar and Kumar?

2. Do the current NBCC static torsional provisions adequately estimate inelastic displacements of stiff- and flexible-edge elements for uniformly asymmetric multistorey shear wall buildings. How do the displacement predictions from the NBCC static code provisions compare with those estimated by a dynamic analysis with shifted CM, a dynamic analysis with statically applied torsional moments, and the static method proposed by Humar and Kumar.

3. How dependent are the inelastic displacements and ductilities of multistorey shear wall buildings on the method used for determining element design strengths? What effect does

variation in building period have on the inelastic response of asymmetric multistorey shear wall buildings?

4. Typically researchers assess the adequacy of torsional design provisions on their ability to limit displacement and ductility demand in an asymmetric or torsionally unbalanced model, to that of an equivalent torsionally balanced model. It is implicitly assumed that the inelastic torsionally balanced models always displays controlled behaviour, i.e. the displacement and ductility demands are as assumed in the design. However, only the normalized results are typically displayed and it is not explicitly evident that the torsionally balanced behaviour is indeed controlled in the inelastic range.

   The review of past studies brings up the following questions: Is the inelastic torsionally balanced displacement response always near the elastic torsionally balanced displacement estimations, and is the ductility demand of the torsionally balanced models always about equal to the design R value assumed in the NBCC code provisions? Are the normalized displacement demand and normalized ductility demand appropriate parameters for defining the response due to plan asymmetry?

5. What is the magnitude of dynamic magnification of shear forces in lateral resisting shear wall elements of asymmetric buildings designed to yield in flexure.

The main purpose of this investigation is to provide a general understanding of torsional effects on the response of uniformly asymmetric and symmetric multistorey shear wall buildings and to verify some of the major parameters influencing the torsional response. This study also reviews and compares the treatment of torsional effects by major world design codes and their implementation into design practise.

2 Current Code Torsional Provisions

2.1 General

Code torsional provisions are derived from a large number of parametric studies examining the elastic dynamic response of structures to torsional effects. Typically, design codes specify a static analysis procedure to account for the effects of earthquake induced torsion for relatively uniform or regular structures. Inertia forces are applied at a specified distance from the centre of rigidity, CR, of the floor, defined by two design eccentricity equations. The concept of design eccentricity has been widely adopted by various countries and incorporated into the torsional provisions as a reasonable approach to account for torsional effects. Design codes vary in their definitions of what constitutes regular or irregular structures and in the specified magnitude of the design eccentricity, e_d. Due to the large number of parameters influencing inelastic torsional response, conclusions resulting from elastic and inelastic studies evaluating various code torsional provisions have not always been consistent. As a result revisions and updates to code torsional provisions based on these studies have led to the inconsistencies between major world design codes. Most codes do not incorporate torsional frequency or lateral to torsional frequency ratio into the design equations.

Research indicates that torsional motions of asymmetric buildings lead to non-uniform displacement demand on lateral resisting elements. Studies on seismic responses of asymmetric systems show that flexible-edge elements always experience additional displacements when compared to a similar but torsionally balanced system (Tso & Zhu, 1992). Elements at the stiff-edge may experience a reduction or increase in additional displacement demand depending on the torsional stiffness of the system (Tso & Wong, 1993). Five code provisions are surveyed in this chapter with the focus on the National Building Code of Canada (NBCC), the Uniform Building Code (UBC), and New Zealand Standard (NZS) and a comparison is made with the NEHRP recommendations.

The intention of the serviceability limit state seismic torsional provisions is to restrict the max deflections under low intensity earthquakes, expected to occur several times in the life span of the structure, to less than or equal to the code designed yield deflections. It is assumed that buildings will remain elastic when subjected to low intensity earthquakes. The intent of the ultimate limit state seismic torsional provisions is to limit element ductility demand for the rare but high intensity earthquakes where buildings may be excited well into their inelastic range when subjected to intense ground motions. Most studies examining code torsional provisions focus on the ultimate limit state requirements.

The adequacy of the various code provisions for ultimate limit state is generally judged on their ability to limit the additional ductility demand imposed on edge elements in an asymmetric system due to torsional response, to that of a reference system assumed to have a predominantly translational response (Wong & Tso, 1995; Tso & Wong, 1993; Correnza *et al*, 1996, 1995 & 1992). To limit additional element ductility demand the design codes increase the design strength of lateral resisting elements. There is some controversy over how applicable the studies of elastic response are to inelastic design of ductile structures (Paulay, 1997a).

2.2 Structure and Comparison of Code Torsional Provisions

The building codes examined restrict torsion by defining a pair of design eccentricities, e_d, to account for the increase or decrease in strength demand in each lateral resisting element. The design eccentricities define the distance from the centre of rigidity, CR, or the storey shear centre, CS, (depending on the code) through which forces at each floor are applied to induce the design storey torsional moments. The CR and CS coincide for single storey and uniform multistorey building models. The element design strength is taken as the larger of the two strengths resulting from the load demand imposed by the design eccentricity equations. The equations for design eccentricity, e_d, take the form of:

$$\text{a) } (e_d)_1 = \alpha e_s \pm \beta b \quad \text{and} \quad \text{b) } (e_d)_2 = \delta e_s \pm \beta b \tag{2.1}$$

where $\alpha \geq 1$ and $\delta \leq 1$.

The first term of the equations, αe_s or δe_s, called the dynamic eccentricity (Tso & Wong, 1993) or natural torsion (De La Llera & Chopra, 1995a) accounts for coupling between the lateral and torsional motions of building response due to plan asymmetry. The static stiffness eccentricity, e_s, is inherent in the building form and is defined as the distance between the centre of mass, CM, and CR. Amplification of the static eccentricity, when $\alpha > 1$, and deamplification, when $\delta < 1$, allows for the contribution from higher mode torques and from rotational inertia of the floor slab (Tso & Yao, 1994).

The second term, βb, represents the accidental eccentricity which is to account for discrepancies between estimations of mass, stiffness and strength distributions used in analysis and actual distributions in buildings during an earthquake, for variations of stiffness with time, for additional inelastic action, for torsional vibrations due to base rotational motion, and for other sources of torsion not considered in the analysis.

Studies show that, for an asymmetric structure, the first equation always governs the design strength of the flexible-edge element, whereas the stiff-edge element can be governed by either equation depending on the torsional stiffness and eccentricity of the system (Tso & Wong, 1993). In symmetric buildings the first term is zero and only accidental torsion is considered in the calculations.

The design coefficients for some major building codes are as follows:

Code	α	δ	β	**additional requirements**
NBCC-95	1.5	0.5	0.10	–
UBC-97	1.0	1.0	$0.05A_x$	–
NZS-92	1.0	1.0	0.10	horizontal regularity conditions must be met
EC8-93	$1.0+(e_1/e_s)$	1.0	0.05	minimum regularity conditions must be met
AUS-93	$2.6\text{-}3.6(e_s/b) \geq 1.4$	0.5	0.05	–
NEHRP 94	1.0	1.0	$0.05A_x$	max. horiz. regularity limitation must be checked
NEHRP 97	$1.0A_x$	$1.0A_x$	$0.05A_x$	max. horiz. regularity limitation must be checked

Table 2.1: Code design coefficients for eccentricity equations.

where NBCC-95 represents the National Building Code of Canada, UBC-97 the Uniform Building Code, NZS-92 the New Zealand Code, EC8-93 the European Code, AUS-93 the Australian Building Code, and NEHRP the National Earthquake Hazards Reduction Program.

The variables e_1 and A_x are defined in the following sections.

2.2.1 Static Eccentricity

Traditionally only the building dimension perpendicular to ground motion and static stiffness eccentricity e_s have been taken into consideration as important parameters for determining torsional effects in most existing code provisions. Some of the recently adopted codes now include dependence upon other governing parameters. The design eccentricity equations of the EC8-93 are based on the German DIN 4149. The EC8-93 uniquely incorporates an additional supplementary eccentricity, e_1, in determining the amplification effects of the lateral torsional coupling in the elastic range of response (Correnza *et al*, 1996). The variable e_1 is the lesser of:

$$e_1 = 0.1(a+b)\sqrt{\frac{10e_s}{b}} \le 0.1(a+b) \qquad (2.2a)$$

$$e_1 = \frac{1}{2e_s}\left(r_m^2 - e_s^2 - r_k^2 + \sqrt{r_m^2 + e_s^2 - r_k^2 + 4e_s^2 r_k^2}\right) \qquad (2.2b)$$

where r_m is the mass radius of gyration about the CM, where $r_m = (a^2 + b^2) / 12$ for a rectangular floor plan, and r_k is denoted the "resilience radius" by the EC8-93 which is identical to the stiffness radius of gyration about the CR, with the relationship $r_k^2 = K_{\theta r} / K_y$. $K_{\theta r}$ is the total torsional stiffness about CR and K_y is the total lateral stiffness in the y-direction, the direction of strong motion. The normalized stiffness radius of gyration, $\rho_k = r_k / b$, is regarded as a measure of the structures total torsional stiffness. The ratio $r_k / r_r = \Omega_r$, the uncoupled torsional to lateral frequency ratio about the CR, where r_r is the mass radius of gyration about the CR with the relationship $r_m^2 = r_r^2 - e_s^2$.

The EC8-93 is the only code that considers the important influence of the torsional to lateral frequency ratio and both plan dimensions, a and b, in the code torsional provisions. The variable e_1 particularly influences systems with small to moderate eccentricity. The AUS-93 also has a structural parameter in its definition of the coefficient α as an attempt to incorporate the influence of the magnitude of the e_s on the effects of lateral torsional modal coupling which can be significant in the elastic range (Correnza *et al*, 1996). The maximum value of amplification factor for e_s is $\alpha = 1.4$ for the AUS-93. The NBCC-95 has a constant amplification factor of $\alpha = 1.5$ for the static eccentricity e_s which is the most conservative of all the code provisions for the flexible-edge elements. The UBC-97 and NZS-92 do not amplify the static eccentricity and are the least conservative for the flexible-edge elements. For both of these codes it is not necessary to calculate the location of CR explicitly, thereby simplifying the static analysis procedure.

2.2.2 Accidental Eccentricity

Accidental torsion effects increase structural element deformations predominantly in symmetric systems. Most codes crudely account for the many variables attributing to accidental eccentricity, e_a, by defining a constant value of $\pm\beta b$ where β varies from 5% to 15% of the building dimension, b, perpendicular to the direction of earthquake excitation. The UBC-97 is the only code that does not have a constant value of accidental eccentricity. It introduces an accidental eccentricity amplification factor, A_x, into the coefficient β. The factor A_x is a measure of the torsional to lateral frequency and is expressed as:

$$1.0 \le A_x = \left(\frac{\delta_{max}}{1.2\delta_{avg}}\right)^2 \le 3.0 \tag{2.3}$$

where δ_{max} and δ_{avg} are the maximum and average diaphragm displacements of the structure under applied design lateral forces. Torsional irregularity exists when the factor A_x is greater than one. The provisions for determination of torsional irregularity in the UBC-97 require that δ_{max} and δ_{avg} be computed including accidental eccentricity, however, it does not state what the value of the accidental eccentricity should be used. A_x varies between 1.0 and 3.0 with the effect of increasing the design eccentricity, and therefore, also the increase in stiff-edge element strength. Higher values of A_x apply to torsionally flexible and highly eccentric systems which experience large rotational deformations (Correnza *et al*, 1996).

The NEHRP-94 design eccentricity equations are identical to those of the UBC-97. The NEHRP-97 torsional provisions, however, require that the factor A_x be applied to both the static and the accidental eccentricity portions of the design eccentricity equations where torsional irregularity exists. This implies that when $A_x > 1$ the CR locations are required to be found explicitly. No explanation is given in the provisions as to the reasons for this change. This revision requires more onerous calculations, thereby penalizing even slightly torsionally flexible systems. It is interesting to note that for future design codes the NBCC committee is intending to move away from magnifying the static eccentricity to eliminate the need to determine the CR locations while the NEHRP-97 provisions are moving in the opposite direction.

Although the present state of knowledge could allow for more refinement, the number of parameters influencing accidental torsional effects makes it difficult to establish general conclusions that apply simply to all situations. A recent study by De La Llera and Chopra

(1992) examining the major factors influencing accidental torsion indicates that the increase in response due to all sources of accidental torsion is adequately modelled in a dynamic analysis by shifting the CM by an amount equal to $\pm 0.05b$ from its nominal position and performing a response spectrum analysis for the altered systems. The code static analysis procedure for incorporating accidental torsion was not found to be consistent with their determined *"true"* response due to accidental torsion. A comparison between the static and dynamic methods of incorporating accidental torsion showed substantial differences in the response. The predicted response of systems with small torsional to lateral frequency ratio, Ω, displayed a much greater increase in response for edge elements using the code static method than the dynamic response spectrum analysis. The differences were greater with increasing static stiffness eccentricity, e_s. The variation between response values obtained by code specified static and dynamic analysis to account for accidental torsion can be as much as double the dynamic response values. The magnitude of the discrepancies indicate that the code static procedure should be modified to produce consistent results.

The NBCC-95 does not allow for accidental torsion to be considered by shifting the CM in a dynamic analysis, rather it is obtained by simultaneously applying equivalent static forces at a distance e_a, the specified accidental eccentricity, $\pm\beta b$ from the CM at each floor and combining these results with the dynamic response spectrum analysis results. The UBC-97 allows for accidental eccentricity to be included either dynamically or statically.

The effect of accidental eccentricity on analysis is to modify the magnitude of applied torsional moments in the static approach and to modify the mass matrix in the dynamic approach. Each directional shift of the CM in the dynamic analysis will uniquely modify the vibration period and mode shapes of the system thereby necessitating a new dynamic analysis to compute the maximum system response for each direction. Wong and Tso (1994) found that this can create some irregularity in determining the element strength.

2.2.3 Building Irregularity

Most codes restrict the use of the equivalent static approach to essentially uniform structures. A dynamic analysis is required for buildings with significant vertical and/or horizontal irregularities. The dynamic response spectrum analysis gives a more realistic distribution of seismic forces in the elastic state since it takes into account the elastic dynamic properties of the structure. The codes assume that irregular and asymmetric structures excited into the inelastic range will have a more desirable ductility demand distribution if the design is based on a more realistic load distribution in the elastic range (Wong & Tso, 1994).

The EC8-93 code is the most strict in limiting the application of static torsional provisions by defining minimum regularity conditions to satisfy in lieu of a dynamic modal analysis. Vertical regularity conditions require that the CM and CS of individual floors lie approximately on the same vertical lines. Horizontal regularity conditions require that the static eccentricity at any given storey level should not exceed 15% of the resilience radius, r_k, defined previously. The EC8-93 has been shown to be overly conservative in limiting the application of the static torsional provisions to virtually symmetrical buildings with small eccentricities even if they have moderately high torsional stiffness (Correnza *et al*, 1996).

The equivalent static method of the NZS-92 may only be used when a minimum of one of the following criteria is satisfied: (a) the height between the base and top of the structure does not exceed 15m, (b) the fundamental period determined by the code specified formula (implementing the Rayleigh method) does not exceed 0.45 seconds, (c) the structure satisfies the horizontal and vertical regularity requirements of the code provisions and has a fundamental period less than 2.0 seconds. If none of these criteria are met a dynamic response spectrum or numerical integration time history analysis must be performed. If the horizontal regularity criteria are not met, the analysis must be in 3D (NZS, 1992).

For the horizontal regularity criteria to be met, (a) either (1) the static eccentricity between the shear centre at any level and the CM of all levels is not to exceed $0.3b$, nor may the static eccentricity change sign over the height of the structure, or (2) the ratio of the horizontal edge displacements on the axis perpendicular to the direction of the equivalent static forces, when applied at a distance $e_d = e_s \pm 0.1b$, must be in the range of 3/7 to 7/3, and (b) the diaphragms may not possess abrupt changes in stiffness or major re-entrant corners which could significantly alter the distribution of lateral forces on the structure. For the vertical regularity criteria to be met the lateral displacement at each level must be reasonably proportional to the height of that level above the base (NZS, 1992). The horizontal regularity requirements indirectly limit the acceptable minimum torsional stiffness to a moderate level and minimize the additional ductility demand on the stiff-edge element (Tso & Wong, 1993).

The UBC-97 and NEHRP-94 and -97 provisions explicitly outline acceptable forms of vertical and horizontal building irregularities. Torsional irregularity conditions exist if the ratio between maximum storey drift, computed including accidental torsion, at the building edge and mean storey drift of the two ends of the building is greater than 1.2. Extreme torsional irregularity conditions, defined by both NEHRP provisions, exist when this ratio is greater than 1.4. Buildings possessing extreme torsional irregularities are not permitted by NEHRP when the maximum considered earthquake spectral response acceleration at 1.0 second period is greater than or equal to 0.75g.

The NBCC-95 does not explicitly define irregularities but rather states that the torsional provisions are only applicable to essentially uniform asymmetric structures where the CM and CR of different floors lie approximately on the same vertical lines. The decision of conducting a dynamic analysis is left to the discretion of the design Engineer.

A study examining the contributions of various modes to the response of multistorey asymmetric structures (Tso & Yao, 1994) found that higher mode contributions increase with increased asymmetry of the building. The first two modes are important for a moderately torsionally unbalanced building. The first four modes are significant for a building with eccentric setbacks. Therefore, the static approach of analysis becomes less accurate for increasingly asymmetric buildings since it cannot simulate higher mode contributions. Code provisions which amplify the static stiffness eccentricity, e_s, best estimate shear distributions (Tso & Yao, 1994; Jain & Anniger, 1995). Code provisions are believed to be sufficient in estimating force distribution for most moderate forms of torsionally asymmetric structures, based on comparisons with elastic dynamic analyses, but there is no guarantee. A 3D dynamic analysis is still considered to be the best means of evaluating torsional effects.

2.2.4 Determination of Torsional Moment

The eccentricity concept together with equivalent static loading is most commonly used to determine torsional effects for regular buildings. Although the eccentricity concept is widely accepted, the definition of eccentricity differs between codes (Tso, 1990). For single storey buildings determining torsional moment is a simple process since all the possible definitions for centre of rotation are located at the same point, however, complications arise with multistorey buildings. Building code torsional provisions usually require the torsional moment to be calculated by one of two approaches.

With the first approach, floor torques for each storey are calculated as the product of the resultant lateral load at that floor and the eccentricity at that floor. The floor eccentricity is defined as the distance between the centre of rigidity, CR, and the load resultant at that floor. The torsional moment at any storey is the sum of the floor torques above that storey.

There are many definitions of CR but the one most frequently encountered in this review, developed by Tso (1990), defines CR as "the set of points located at the floor levels such that when the given equivalent static lateral loads are applied through these points, no rotations of any floors will occur" (Tso, 1990). The CR is dependent on the structure and load distribution and differs from the stiffness centre or shear centre, CS, which is solely a property of the structure. Studies show that rigidity centres are extremely sensitive to even very small variations in stiffness between stories causing large shifts in CR location. In asymmetric buildings the CR can jump to both sides of the CM, scattered along the height of the building and may even fall outside of the building walls. This creates positive and negative values of floor eccentricities and complicates interpretation of the code. Buildings with hybrid lateral resisting systems consisting of a combination of walls and frames produce large shifts in CR between floors near the ground and the tops of the buildings when only modestly asymmetric, even when the resisting walls and frames are relatively uniform over the entire height.

During an earthquake, the actual CR would be constantly shifting location due to variations in applied load and yielding of elements. The location used in design is an instantaneous position under the specified static design loads. Since the location of CR is so sensitive to variations in asymmetry, according to the limitations of most code provisions, essentially all multistorey buildings would require a dynamic analysis. To avoid the cumbersome process of determining the location of CR a method for directly determining torsional moments without locating rigidity centres was developed combining the results from three 3D static analyses (Goel & Chopra, 1993).

In the second approach, the torsional moment is calculated as the product of the storey shear and the storey eccentricity at that level. The storey eccentricity is the distance between the storey shear centre, CS, and the resultant of all the lateral forces above the storey being considered. The CS is the location of the resultant of storey frame shears obtained from a free body diagram to satisfy lateral equilibrium assuming only floor translation and ignoring rotations.

Torsional moments and eccentricities may be computed by both methods with the use a plane frame program. A comparison shows that both approaches result in similar storey torsional moments (Tso, 1990). A comparison was made in one study (Cheung & Tso, 1987) between the two discussed approaches and a third method of defining the eccentricity as the distance from the applied resultant floor lateral load and the centre of stiffness of that floor determined by treating each floor as a single storey building. Despite the simplifications, similar results were obtained using this method in comparison with the above methods and a dynamic analysis. Code torsional provisions that do not amplify the static eccentricity in the design eccentricity equations by setting $\alpha = 1.0$ and $\delta = 1.0$ do not require the determination of CR or CS.

2.2.5 Assessment of Current Code Torsional Provisions

The majority of studies examining or comparing design code torsional provisions are based on asymmetric structures with elemental strengths distributed according to the individual code provisions. The increase in torsional and lateral response of the asymmetric structure is compared to that of a reference system assumed to have a predominantly translational response. Past studies have discovered that the static provisions of some codes underestimate the ductility and strength demand on stiff-edge elements and increase associated risk of damage. Other codes have been found to be overly conservative. Code provisions vary in their requirement for element strength increase, allowances for strength reductions, restrictions on building regularity, and point about which to determine torsional moment. Results were surveyed from a number of studies on elastic and inelastic torsional response of single storey structures. Few studies examine multi-storey structures. The large number of parameters governing torsional effects of even simple single storey structures makes it difficult for studies to be all encompassing and to identify common problematic areas. As a result contradictions exist in conclusions drawn between various studies and it is not clear how to consolidate and transform these results into general design guidelines. This would account for the existing discrepancies between major code torsional provisions. (Correnza *et al*, 1996, 1995, 1992; De La Llera & Chopra, 1994e; Humar, 1998; Humar & Kumar, 1999; Paulay, 1997a; Tso & Wong, 1995, 1993; Tso & Zhu, 1992; Wong & Tso, 1995, 1994; Zhu & Tso, 1992).

2.2.5.1 Elemental Strength Distribution:

Flexible-edge Elements. The design eccentricity equation 2.1(a) always governs the design strength of flexible-edge elements in asymmetric structures. For flexible-edge elements the design strength factor, the normalized increase in element design strength due to the individual torsional provisions, increases linearly with stiffness eccentricity, e_s, proportional to α of the design eccentricity equation 2.1(a). The greater α the more rapid the increase in required element strength. This increase becomes more exaggerated for elements further away from the CR and for systems with small torsional stiffness (Tso & Zhu, 1992). For configurations having the same CR location, element strength increases with decrease in torsional stiffness. Greater strength increase is required with large stiffness eccentricity, e_s.

The NZS-92 and UBC-97 do not amplify the static eccentricity, e_s, and overall, impose the lowest strength increase for flexible-edge elements. The EC8-93 and AUS-93 require the greatest increase in strength for the flexible-edge elements of most systems while the NBCC-95 lies somewhere in-between.

Stiff-edge Elements. The design strength of stiff-edge elements is usually controlled by the second design eccentricity equation 2.1(b) except for structures with large static eccentricity where the first equation may govern. In some cases the design eccentricity equations allow reductions in the strength of stiff-edge elements (Correnza *et al*, 1996). This is based on theoretical studies that stiff-edge elements experience a decrease in response depending on the torsional stiffness of the structure (Tso & Zhu, 1992). For a torsionally stiff system the torsional response can decrease stiff-edge displacements, whereas with a torsionally flexible system the torsional response will increase stiff-edge displacements (Wong & Tso, 1994). A higher code coefficient δ leads to a greater possible decrease in element strength. The EC8-93 and NZS-92 allow the greatest strength reductions with significant reductions at high static eccentricity, e_S. The NBCC-95 and AUS-93 allow moderate strength reductions, approximately 50% of the EC8-93 and NZS-92. The UBC-88 contained a clause stating that the beneficial effects of the design eccentricity equations were to be ignored and did not allow strength reductions for elements on the stiff side of the building. This clause has been omitted in the UBC-91 and -97 but Wong & Tso (1995) claim that it is still intended that strength reductions be ignored despite the high value of δ which would otherwise allow similar reductions to NZS-92 and EC8-93.

The UBC-97 is the most conservative for stiff-edge elements if no strength reductions are allowed (Correnza *et al*, 1996). Studies indicate that with the EC8-93 and NZS-92 provisions the stiff-edge element could experience an increase in response due to torsional effects which is contrary to the philosophy on which the provisions are based (Tso & Wong, 1993; Correnza *et al*, 1996).

2.2.5.2 Total Lateral Strength

The total lateral strength is the sum of all element strength in the direction of interest. The increase in total lateral strength among codes ranges from 1.1 to 2.2 times that of a structure without the inclusion of the torsional provisions. Codes that allow a substantial strength reduction for stiff-edge elements compensate for the large increase in strength imposed on flexible-edge elements, resulting in moderate total lateral overstrength values. The NZS-92 and EC8-93 require the lowest increase in total strength for all structures while the UBC-97 and NBCC-95 reach an overstrength above 2.0 at high e_s for torsionally flexible buildings. This large overstrength penalty is to act as a deterrent against construction of torsionally flexible buildings (Correnza *et al*, 1996).

2.2.5.3 Ductility Demand

Studies show that for torsionally unbalanced systems there is always additional displacement demand on flexible-edge elements regardless of code torsional provisions. The displacement is a function of eccentricity and torsional stiffness of structure and the distance of the flexible-edge from the CR, and can impose excessive ductility demands on elements located farthest from the CR. Systems designed without torsional provisions experience large additional ductility demand on flexible-edge elements (Tso & Zhu, 1992).

Some codes allow substantial strength reduction for stiff-edge elements which may lead to considerable additional ductility demand for these elements. Stiff-edge elements designed based on the UBC and, to a lesser extent, the NZS experience large ductility demands for structures with moderate to large eccentricities. The NBCC better controls ductility demand because the torsional provisions better limit the amount of strength reduction permitted (Tso & Zhu, 1992). A possible means of limiting ductility demands would be to restrict strength reductions for stiff-edge elements.

2.2.5.4 Displacement Demand

Code torsional provisions have concentrated mainly on limiting the element ductility demand. Research indicates that displacement demand is relatively independent of the torsional provisions used to distribute element strength and more dependent on the torsional stiffness of a structure (Tso & Wong, 1995). Torsionally stiff buildings are not highly affected by torsional coupling and the maximum inelastic deformations are not significantly different from deformations predicted by an elastic response. Excessive deformations are an important issue for torsional design of torsionally flexible systems where the difference in response between elastic and inelastic systems is much greater. Torsional displacements are magnified when the first mode of vibration is predominantly torsional and when a torsional mechanism forms upon yielding.

Correnza *et al* (1992) expressed concern that certain elements subjected to large displacements due to torsional rotations are found to be below the ductility of the reference system with all codes provisions. Code design should provide guidelines for limitations on inelastic displacements due to both translation and torsion.

2.2.5.5 Discussion

The intent of studies examining the adequacy of code torsional provisions is to develop a set of accepted guidelines for the design of ductile asymmetric structures to be incorporated into building codes. The latest modifications to design code torsional provisions have somewhat narrowed the differences between the design requirements of major countries, however, they are still far from establishing a unanimously accepted treatment of torsion in building design. The fact that most code provisions treat all buildings the same independent of torsional and lateral vibration periods and torsional stiffness is perhaps too simplistic of an approach, overlooking large variations in response dependent upon these parameters.

The eccentricity concept adopted by most code torsional provisions is applicable to buildings that are absolutely symmetrical about both principal axes and are assembled from plane frames all of which have geometrically similar lateral deflection patterns. These assumptions, in general, deviate from reality and real structures rarely fall into this category. Despite its limitations, the eccentricity concept is accepted as a viable means of determining design forces for the limited classes of buildings that qualify for use of the static design methods.

The direction of many recent codes is to explicitly define irregularity conditions which limit the use of the equivalent static method by imposing restrictions on allowable torsional displacement under statically applied loads in the form of a displacement ratio. If the specified displacement ratio is exceeded a 3D elastic dynamic modal or time history analysis must be performed.

3 Input Ground Motions

3.1 Original Earthquake Records

The input ground motions from three earthquake records with similar properties were used in the time history analyses. The first two records are separate near field recordings from the San Fernando crustal earthquake and the third is a subduction earthquake recorded in Japan. Table 3.1 summarizes the original earthquake properties.

File Name	Event	Mag^n	Epi-central dist. (km)	peak ground accln a(g)	peak velocity v(m/s)	a/v ratio	Station	Soil Cond
Van51	San Fernando California 1971 crustal	6.4	39	0.165	0.166	0.99	3407 W. 6th Street	soil site
Van35	San Fernando California 1971 crustal	6.4	37	0.185	0.163	1.13	Millikan Lib. CTT	alluvium
Miyans	Japan 1978 Miyagiken-Oku subduction	7.7	116	0.26	0.38	0.68	unknown	unknown

Table 3.1: Original recorded input ground motion records

Obtaining compatible time histories of past earthquakes to match the desired seismic region "target" spectrum is not a trivial feat particularly for the Canadian seismic environment. There are virtually no applicable records available for the magnitude-distance combinations and local faulting mechanisms identified as representative of the 1/475 year target design spectra since no large earthquakes have occurred in this region since earthquakes have been recorded. The direct use of California or other records to represent local Canadian events is not appropriate because there are primary differences in source and site characteristics between California earthquakes and Canadian earthquakes that directly affect the amplitude and frequency content of potential ground motions (Atkinson & Beresnev, 1998). For this reason it was decided to use strong motion records modified to fit the NBCC tripartite 5% damped response spectrum.

The original earthquake time histories should possess characteristics and properties that best represent the desired magnitude, epicentral distance, duration, and faulting mechanisms that contribute most to the hazard of the desired target spectrum in order to minimize the degree of alteration required for spectral compatibility. The two crustal earthquakes were chosen to represent the hazard on the west coast of British Columbia from near field crustal source earthquakes. The site conditions of the two crustal earthquakes are different, however, the remaining properties are similar. The subduction earthquake was selected to represent the hazard from the Cascadia subduction zone and to observe the variation in response due to a modified subduction earthquake compared to the modified crustal earthquakes. All three earthquake are similar in duration.

3.2 Modified Earthquake Records

The earthquake records were modified to be compatible with the NBCC tripartite 5% damped response spectrum using the program SYNTH (Naumoski, 1985). SYNTH modifies the original acceleration record by iteratively amplifying or suppressing the Fourier amplitude coefficients based on the ratio of the target spectrum to the original time history response spectrum while maintaining the phase of the original record. The peak acceleration of the generated record was selected as 0.2g. The computed spectrum was adjusted to fit "around" the target spectrum rather than be enveloped by it. A total of five iterations were used to best preserve the original character of the earthquake while providing a reasonable match to the desired spectral properties.

Although this approach of fitting the target spectrum is relatively straightforward there are some drawbacks. The dynamic characteristics or the non-stationary character of the original reference time history may be significantly altered if too many iterations are performed due to excessive modifications to the shape of the Fourier amplitude spectrum. Also, it has been found to have relatively poor convergence properties (Preumont, 1984).

Other approaches for spectral matching have been developed such as adjusting the time history in the time domain by adding wavelets to the reference time history. However, a reasonable match to the target spectrum was achieved using SYNTH, therefore, other techniques were not pursued.

To find the peak velocity of the record, the scaled acceleration record was integrated using Newmark's average acceleration technique. A base line correction of the scaled acceleration and velocity records were necessary to correct the linear trend off the baseline of the resulting velocity and displacement records. The records were then corrected using linear regression. The equation of the best fit line using the method of least squares was found for the velocity record. The acceleration record was corrected for the slope of the best fit line of the velocity record by dividing the magnitude of the rise at the end of the record by the total time and then subtracting this constant value from each point of the acceleration record. The adjusted acceleration record was re-integrated to give a new velocity record. The value of the y-intercept of the best fit line of the initial velocity record was then subtracted from each point to give an adjusted velocity record. This was then integrated to produce the displacement record. The peak velocity values were read off the adjusted velocity plots. The resulting values of peak acceleration and velocity are shown in Table 3.2. Figures 3.1, 3.2, and 3.3 display plots of the acceleration, velocity and displacement histories for the three modified earthquake records.

File Name	peak ground accln a(g)	peak velocity v(m/s)	a/v ratio	Δ t	duration (s)
Van51	0.2	0.301	0.664	0.02	40.96
Van35	0.2	0.283	0.707	0.02	40.96
Miyans	0.2	0.27	0.741	0.02	40.00

Table 3.2: Modified input ground motion properties

The peak ground acceleration is identical for each modified record at 0.2g. The peak velocities of the modified records are all within close range indicating a reasonable fit to the NBCC spectrum. The values of peak ground acceleration and peak velocity and the a/v ratio are somewhat academic for the modified records since the records are modified to fit the desired spectrum rather than scaled to specific values of spectral velocity or acceleration. They will vary from the original record depending on how the spectral content is modified. Typically records with large spectral values in the long period, velocity dominated range, will result in a somewhat smaller a/v ratio than ones with small values in the long period range. This is not evident in the modified records since all the records are altered to fit the same spectrum and possess very similar spectral values. Figure 3.4 displays the acceleration spectra of the three earthquakes plotted with the NBCC acceleration spectrum.

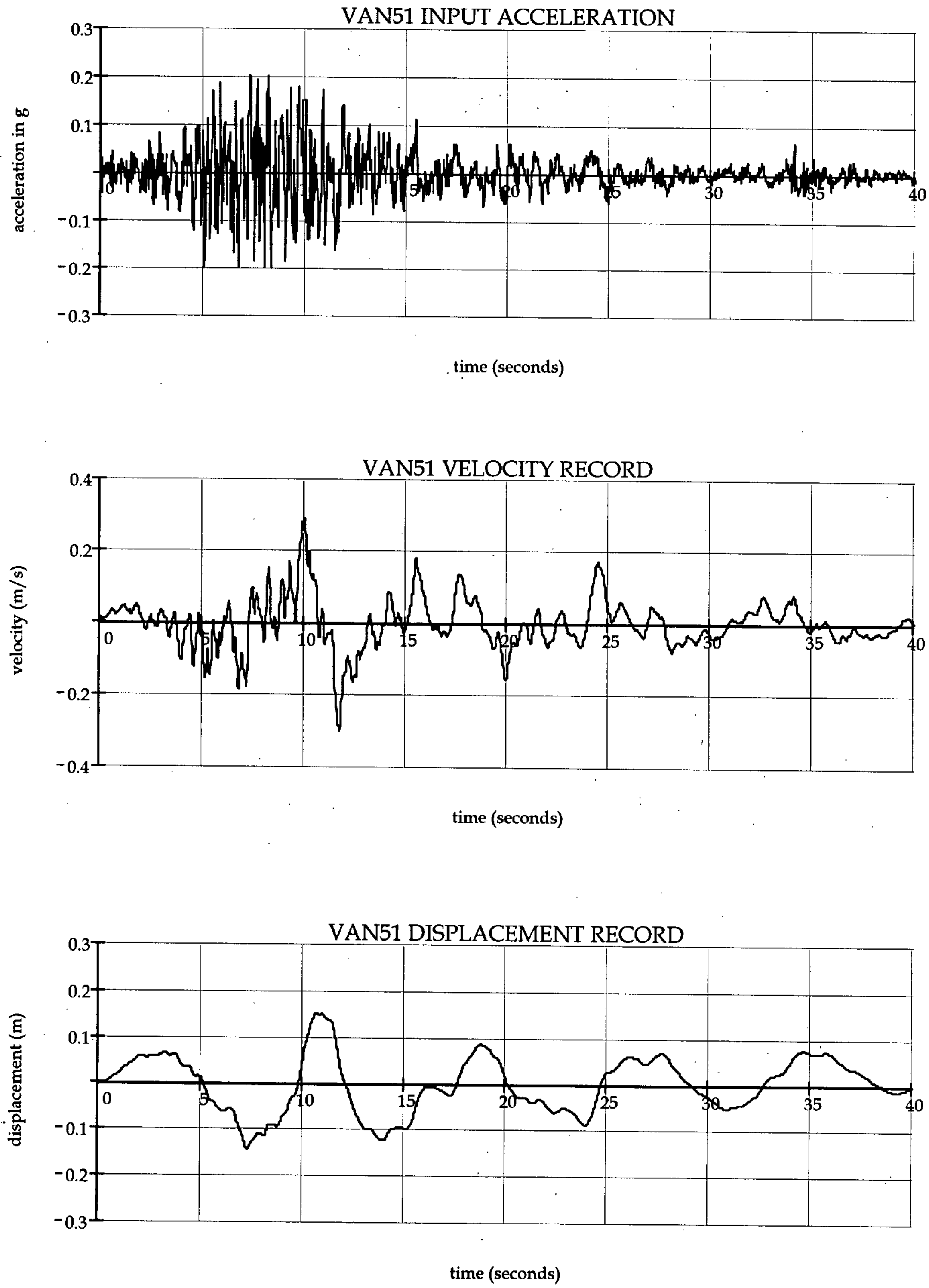

Figure 3.1 Van51 modified input ground motion - EQ1

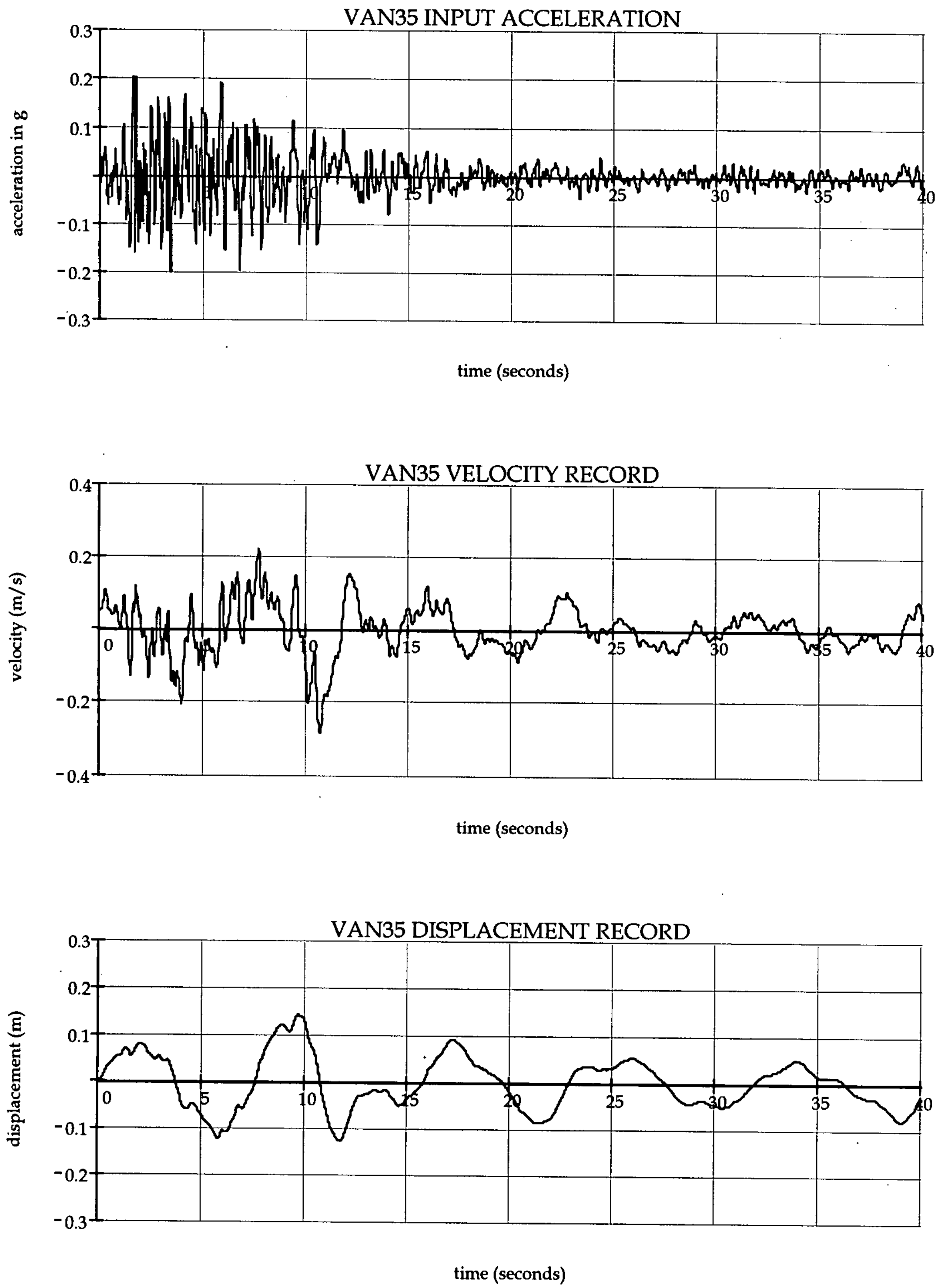

Figure 3.2 Van35 modified input ground motion - EQ2

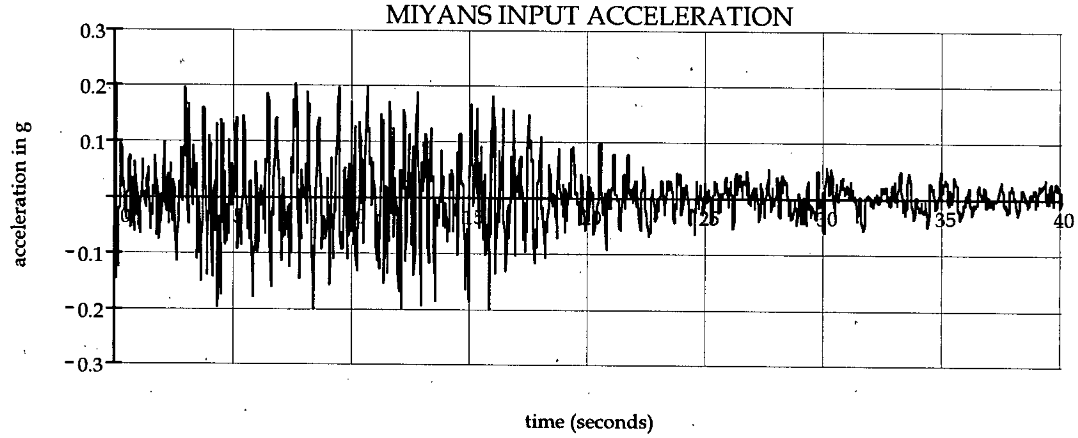

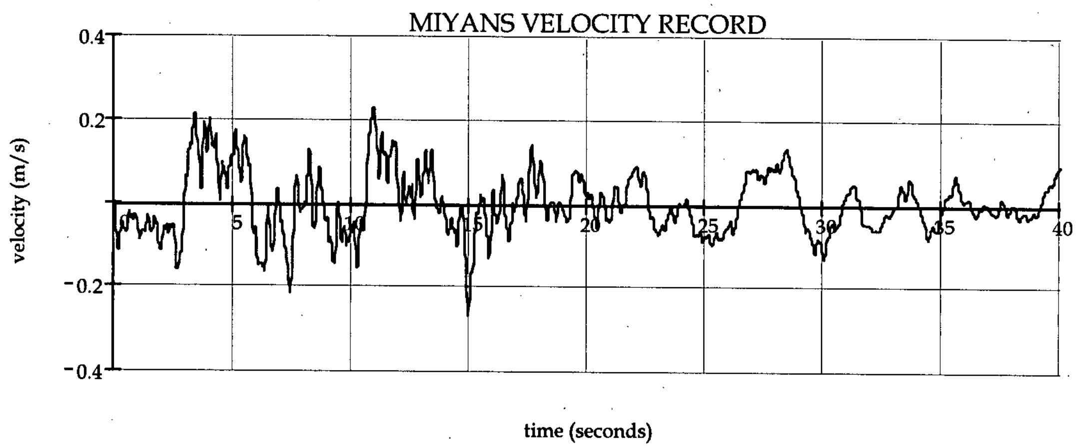

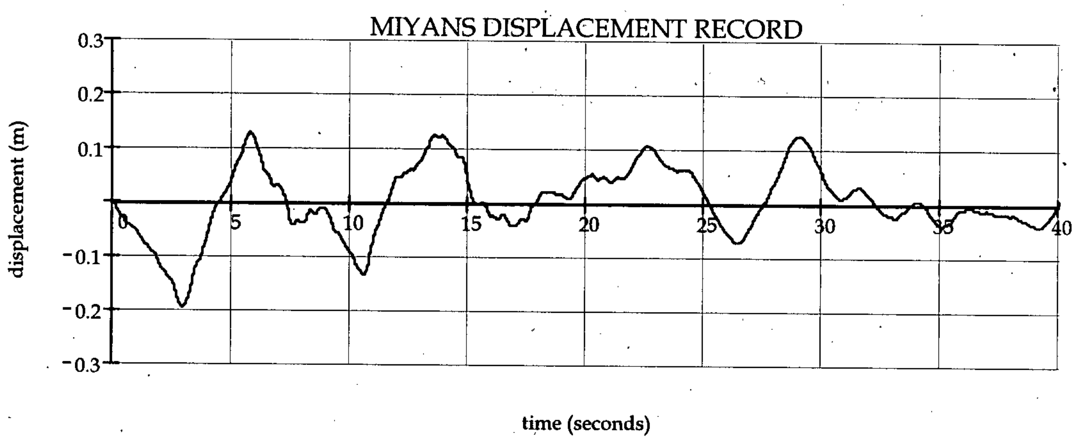

Figure 3.3 Miyans modified input ground motion - EQ3

The acceleration spectra of the earthquakes fit well to the NBCC spectrum above a period of 0.1 seconds. In the short period range, the spectral acceleration values of the modified records all fall below that of the NBCC spectrum which is characteristic of a true earthquake acceleration spectrum. The NBCC spectrum is kept artificially high and flat in the short period range at the level of the peak spectral acceleration to guard against an increased response of short period structures due to period elongation when excited into the inelastic range.

The power spectral density plots (PSD) of the three earthquakes are shown in Figure 3.5. The Miyagiken earthquake has somewhat higher peaks in the frequency range of 5 to 7 Hz. indicating that it contains more energy than the other two crustal earthquakes in this range.

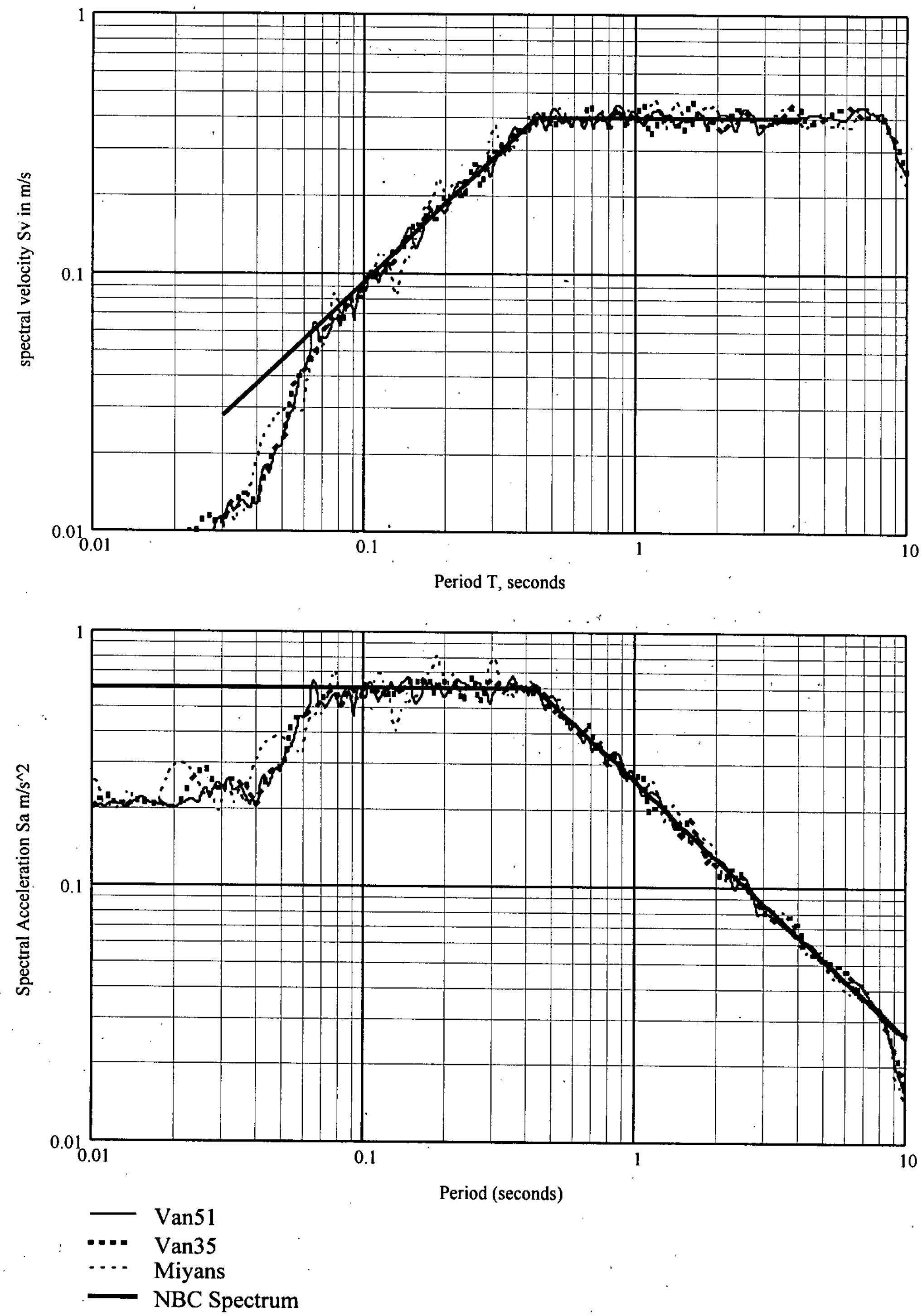

Figure 3.4 Velocity and acceleration spectra - 5% damping

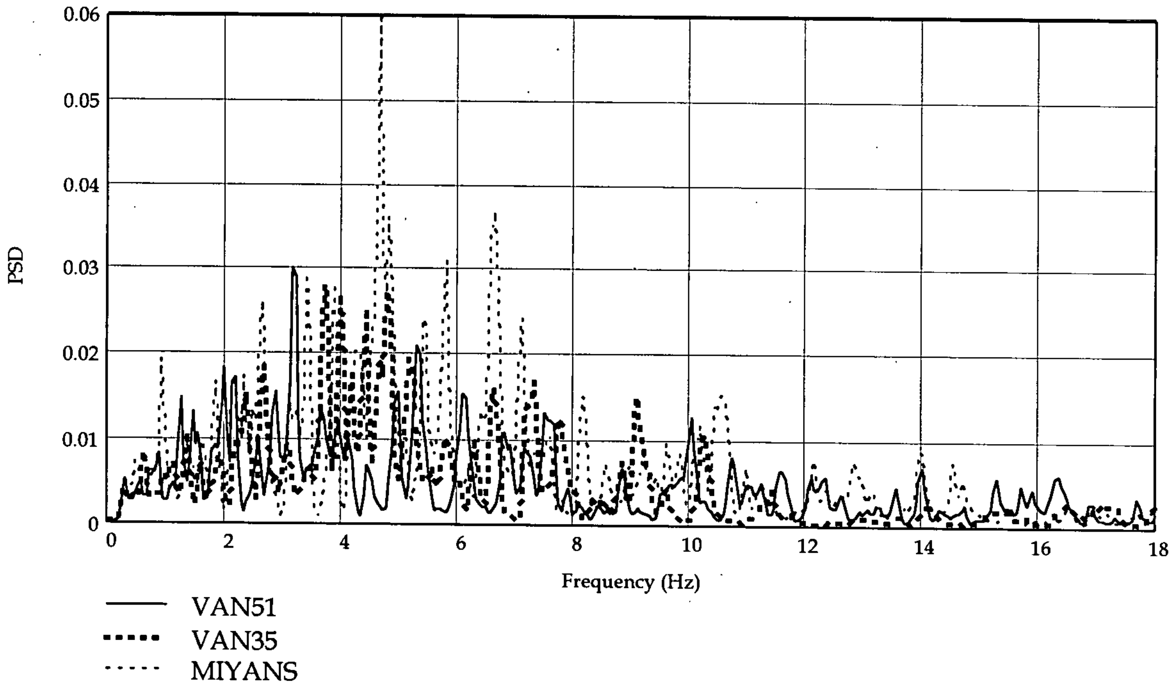

Figure 3.5 Power spectral densities

4 Building Models

Exhaustive studies have been conducted previously by researchers on single storey asymmetric models of various configurations. Studies on multistorey buildings usually focus on frame structures where the floor structures are assumed to be perfectly rigid both axially and in flexure (Correnza *et al*, 1992). Therefore, the building response would be essentially as for a shear frame. Very few multistorey models incorporate or examine the response of wall elements. In the Vancouver region and other west coast cities of Canada, high rise buildings are primarily reinforced concrete shear core structures with the main lateral resisting elements consisting of a combination of coupled and uncoupled walls concentrated near the centre core of the building.

This study focuses on simple multi-storey building models with the lateral resisting system composed of individual walls. Although the models are idealized in form, they possess the key dynamic characteristics of properties of actual buildings.

4.1 General Multistorey Elastic Models

The building systems analyzed in the study can be categorized as a "special class of multistorey buildings" (Newmark & Rosenblueth, 1971) possessing the following properties:

- The centres of mass (CM) of all floors lie on a vertical line.
- The resisting elements are positioned orthogonal to the *x*- and *y*-axis and the centres of rigidity (CR) of all stories lie on a vertical line.
- The floors diaphragms are infinitely rigid in their own plane.
- The building is symmetric in the *x*-direction.

In this study, the CR is defined as the set of points at each floor level through which a particular distribution of lateral forces, when statically applied, result in a purely translational response of the complete structure (Tso, 1990). The typical building floor plan shown in Figure 4.1 is rectangular in shape with an aspect ratio *a*/*b* equal to 0.5 where *a* measures 18m in the *y*-direction and *b* 36m in the *x*-direction. The floor to floor height is constant at 3.7m. The floor mass, *m*, was kept constant for all models and is uniformly distributed across each floor so that the centre of mass, CM, and the geometric centre of the floor, GC, coincide. The lateral resisting planes consist of individual walls for all models. Three resisting planes or walls are positioned in the y-direction, parallel to the direction of earthquake motion. A three element model in the direction of ground motion was chosen over the two element model used in some early studies because it is more representative of a real structure. The three element model is statically indeterminate and torsional frequency changes are due to varying the element stiffness distribution rather than merely the torsional moment of inertia of the floor slab as with the two element model (Tso & Sadek, 1985).

Eccentricity is introduced into the systems of this study by varying the distribution of element stiffness in the *y*-direction. A typical floor plan is displayed in Figure 4.1. One wall element is fixed at the centre of the building (y_2 referred to as w_{mid}) and is allocated a constant elastic stiffness used in all models considered in this study. The two outer wall elements (y_1 and y_3 referred to as w_{flex} and w_{stiff}, respectively) may possess different stiffness properties and are located asymmetrically about the *y*-axis. Their stiffness is varied to give the desired static eccentricity. For a given eccentricity, the stiffness distribution is kept constant and the location of the outer walls is shifted as required to achieve the desired range of torsional frequency.

One wall is positioned at the centre of the building in the x-direction (x_I), orthogonal to the direction of ground motion. This ensures that the torsional stiffness is provided solely from the walls in planes parallel to the direction of earthquake excitation. The mass of the walls and columns is ignored. The fundamental lateral period and total lateral stiffness in both directions is identical. The building can be divided into stiff (right) and flexible (left) side as shown in Figure 4.1. The associated walls on each side are designated as the stiff wall and flexible wall, respectively and will be referred to as such for the rest of this study.

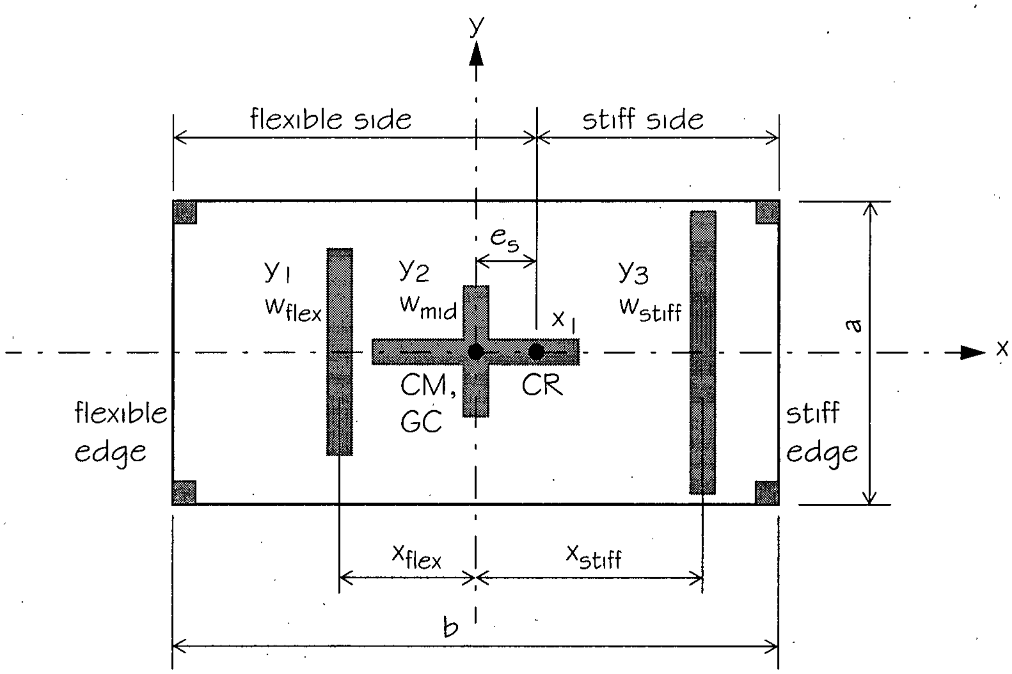

Figure 4.1 Plan of generalized torsionally unbalanced model with asymmetric stiffness

Four columns are fixed at the extreme corners of the building to represent a perimeter gravity load carrying frame. Their contribution to lateral and torsional restraint is negligible. These corners are used as the common reference points between all models since the stiff and flexible walls shift position from model to model. These corners and are referred to as the stiff and flexible corners, corresponding to the stiff- and flexible-edges of the structure. The buildings possess no vertical irregularities (every storey is taken to be identical in layout, stiffness, strength). For this special class of buildings the static stiffness eccentricity, e_s, defined as the distance between the CM and CR, is the same for each floor since the CR and CS coincide.

4.1.1 Stiffness Distribution

The total storey stiffness was chosen to attain the desired fundamental lateral period. The location and stiffness was allocated to the walls so as to create the desired static stiffness eccentricities, e_s, and torsional frequencies examined in this study. The values were selected to enable torsional frequencies over the selected range of study while maintaining the desired stiffness eccentricity and valid wall positions i.e. located within the boundaries of the building footprint. These values were kept constant up the height of the building. For uniform wall structures, yielding of the lateral resisting elements occurs at the base of the wall. In a real structure, the stiffness and strength of the lateral resisting walls usually decreases with building height since the demand on these elements decreases with building height. However, nonlinear response and analysis is a function of many variables, and varying or decreasing the wall stiffness would add additional variables to the problem that would further complicate the analysis. For this study it was desired to limit the number of dependent variables, therefore, the walls properties were kept constant up the height of the building. The plastic hinge was isolated at the building base to enable relatively straightforward comparisons of response values.

For each eccentricity examined, the stiffness distribution was kept constant over the range of torsional frequencies. The stiffness values for each wall element of the models are given in

Table 4.1 as a fraction of total storey stiffness.

eccentricity	0.2*b	0.1*b	0.0*b
k_1 flexible wall stiffness	0.25*K_y	0.3125*K_y	0.4375*K_y
k_2 centre wall stiffness	0.125*K_y	0.125*K_y	0.125*K_y
k_3 centre wall stiffness	0.625*K_y	0.5625*K_y	0.4375*K_y
K_x	K_y	K_y	K_y

Table 4.1: Stiffness distribution for general elastic models

K_y is the total storey stiffness in the y-direction and K_x is the total storey stiffness in the x-direction. For this study the total storey stiffness in the x-direction was made identical to that in the y-direction, therefore, the uncoupled fundamental lateral period for both directions is identical. For a given value of e_s the same stiffness distribution was used for all values of uncoupled lateral period, T_y, examined in this study. The value of modulus of elasticity, E, of the walls was the variable altered to produce the overall storey stiffness resulting in the desired fundamental lateral period for each model.

4.2 Reference Models

To quantify the effects of torsion induced by structural asymmetry, the response of an eccentric or torsionally unbalanced (TU) system is generally compared or normalized to the response of a similar reference model which does not respond torsionally. Two types of reference models have been commonly employed in past studies, (1) the symmetric reference model, and (2) the torsionally balanced (TB) reference model. With both reference models, the normalized results indicate the increase in response of an asymmetric system above that of a similar system exhibiting no torsional response. Although these comparisons can be useful in calibrating the increase in response due to torsion, some information is lost with the normalization process. The results of the investigation both quantitatively and qualitatively may vary depending on the choice of reference model (Correnza *et al*, 1992).

Since the results and conclusions of an investigation of inelastic torsional effects are dependent on the choice of reference model, the response results of the eccentric models, in most cases in this study, are not normalized to the results of a reference model. Instead, the results of both the eccentric and reference models are displayed in a single plot to demonstrate the variations between models caused by inherent eccentricity and torsional flexibility of the structure. In this way, the actual magnitudes of the response of each system examined are evident and a direct comparison can be made with the reference model results. Also, it is then clear which responses fall within an acceptable range of values.

Both the symmetric and torsionally balanced models were examined in this study. The symmetric model, however, was treated in the same manner as the eccentric models for the inelastic analysis with $e_s = 0$. The wall strengths were increased to account for torsional effects, including accidental torsion, and accidental torsion was introduced during the time history analyses in the same manner as for the asymmetric models. Since torsional effects are included in the strength distribution of the symmetric model, the TB model is the true reference model of this study.

4.2.2 Symmetric Reference Models

In early studies examining the effects of torsion, the response of eccentric structures were compared with symmetric reference models (Goel & Chopra, 1990, 1991; Sadek and Tso, 1989; Tso & Ying, 1992; Tso and Sadek, 1985). Traditionally symmetric models have three walls oriented parallel to the direction of strong ground motion all possessing the same stiffness and strength properties. The storey mass is uniformly distributed throughout the floor so that the CM, CS and CR all coincide with the geometric centre, GC, of the building. Therefore, the building does not exhibit any torsional response in both the elastic and inelastic ranges of dynamic response.

For the symmetric models of this study, the centre wall maintains the same stiffness properties as for the TU models and is fixed at the GC of the building. The remaining storey stiffness (and strength) is distributed equally to the outer walls to maintain symmetry. The stiffness (and strength) of the outer walls differs from that of the centre wall. This was done to maintain a constant fraction of total stiffness distributed to the outer two walls between all models in an attempt to produce reasonably similar combined lengths of lever arms from the centre of rotation to the location of the outer walls. The outer walls are located equal distance from the GC of the building and their positions are varied to achieve the desired lateral to torsional frequency ratio.

The symmetric model is the most simplistic system that displays a pure translational response in both the elastic and inelastic ranges. However, there are some issues that need to be addressed that limit the usefulness of the symmetric model as a reference model. A direct evaluation of the torsional effects on a particular perimeter wall is not possible. To maintain symmetry, the individual stiffness of the outside walls of the symmetric model differs from that of the stiff and flexible walls of the TU models. Only the sum of total stiffness distributed to the two outside walls remains constant between all models. Also, the position of the outer walls is varied to achieve the same torsional frequency as the TU models being examined and will not match the location of the TU models. Therefore, the length of the individual lever arms, which is a measure of the contribution of the wall to torsional stiffness, is not consistent between the TU and symmetric models. Because of these factors, the influence of torsion on a particular wall element of the TU model is not directly comparable to an element of the symmetric system. For this reason, the extreme corners of the buildings were chosen as the main point for comparison for peak displacement and storey drift. The location of the walls in plan and the distance from the CR is considered in the evaluation of the wall element ductility results.

A further issue is that eccentricity is introduced into the asymmetric systems either by varying the stiffness distribution to the wall elements or the mass distribution in the floors. These models are referred to as stiffness eccentric systems, SES, or mass eccentric systems, MES, respectively. A SES and MES with a given eccentricity, displaying the same results in the elastic range may respond quite differently when excited into the inelastic range. Also the ductility demand on lateral resisting elements differs for SES and MES. It has been found that elements on the flexible side of the building are most vulnerable to additional ductility demand for SES (Tso and Ying, 1992) and elements on the stiff side are most susceptible for MES (Goel and Chopra, 1990). The ductility demand on the elements of the symmetric and TU systems would also not be directly comparable since the stiffness distribution, mass distribution, and lever arms from the CR to the wall elements the vary between the models.

4.2.3 Torsionally Balanced Reference Model

Because of the limitations with the symmetric reference model, Tso and Zhu (1992) developed a more generalized reference model derived directly from the asymmetric models to identify the increase in response due to torsion in asymmetric buildings. The model is constructed with the same stiffness distribution properties as the associated asymmetric model but with the mass distribution such that the CM is shifted to coincide with the CR without changing the torsional inertia of the floor used to get Ω. In effect the system becomes *torsionally balanced* and all torsional effects are eliminated from the response. Hence, the reference model is called a *torsionally balanced* (TB) reference model.

Torsionally balanced models have been adopted by other researchers in recent studies assessing the effects of torsion (De La Llera & Chopra, 1994a-e; Kumar, 1998; Humar & Kumar, 1999). The response of the asymmetric or torsionally unbalanced building (TU) is usually normalized to the response of the balanced building. The increase in response can be attributed to the presence of torsion due to asymmetry or irregularities in the structure. The eccentricity in the asymmetric model is due to varying the mass distribution from the reference model. Defined this way, the comparison incorporates variations in both stiffness and mass distribution, thereby eliminating the need to specify whether an asymmetric system is a SES or MES. Also, a direct comparison of the ductility and displacement demand can be made between the individual lateral resisting elements of the TB and TU models since the TB model retains the exact stiffness distribution and element lever arm length from the CR as the asymmetric TU model under investigation while exhibiting a purely translational response under dynamic loading.

The response values in this study are not normalized to the TB system because it was desired to see the actual magnitude of the response values for both configurations. In many cases the TB responses are plotted in the same graphs for the purpose of comparison.

4.3 System Parameters

Researchers have conducted many studies on the effects of inelastic torsion on asymmetric structures in an attempt to understand the relationship between structural parameters inherent in an eccentric building structure and excessive torsional response during a seismic event. Due to the large number of parameters that affect torsional response in the inelastic range for even single storey structures, it has not been an easy task to identify clear relationships. Early studies often produced conflicting conclusions resulting from the various assumptions made in the chosen analytical models. After further investigations (Goel & Chopra, 1990; Zhu & Tso, 1992; Tso & Zhu, 1992), some of the conclusions were recognized to be restricted to the particular model under consideration. In more recent studies, researchers appear to agree that the main factors affecting inelastic torsional response are the static stiffness eccentricity, the ratio of torsional to lateral frequencies, distribution of torsional resisting elements, and element strength and strength eccentricity (De La Llera & Chopra, 1994a, 1994e, 1995, 1996; Kumar, 1998; Humar, 1998; Paulay 1997b).

4.3.4 Stiffness Eccentricity

The static stiffness eccentricity, e_s, is the geometric distance between the CM and CR. For the special class of multistorey buildings analyzed in this study the CR and centre of stiffness, CS, coincide. The building floor plan is symmetric about the x-axis and asymmetric about the y-axis. The CS is located on the x-axis at a distance e_s from the CM, where e_s is given by

$$e_s = \frac{\sum_{i=1}^{n} k_{yi} \cdot x_i}{\sum_{i=1}^{n} k_{yi}} \tag{4.1}$$

k_{yi} is the lateral stiffness of the i^{th} element in the y-direction, x_i is the distance to the i^{th} element, and n is the number of resisting planes in the y-direction.

Determining the locations of the CR at each floor for a regular multistorey building can be an onerous procedure. The current torsional provisions of the NBCC require the CR to be determined for the calculation of the design eccentricities since the coefficient applied to the static eccentricity in the design eccentricity equations is either 0.5 or 1.5. The current UBC does not apply a factor to the stiffness eccentricity, and therefore, the CR does not need to be explicitly determined for buildings.

The stiffness eccentricities, e_s, examined in this study are $e_s = 0.2b$; $0.1b$ and zero eccentricity (the symmetric model).

4.3.5 Uncoupled Torsional to Lateral Frequency Ratio

The uncoupled fundamental torsional to lateral frequency ratio is one of the most significant system parameters that influences a building's torsional response (De la Llera & Chopra, 1995). The uncoupled frequency ratio, Ω, is defined as the ratio between the uncoupled fundamental torsional frequency, ω_θ, and the uncoupled fundamental lateral frequency, ω_y (or ω_x), in the direction of interest. The torsional and lateral frequencies are defined by the lateral and torsional stiffness matrices, K_y & $K_{\theta r}$, and the mass matrix, m, of the structure under consideration. For single storey structures or a special class of uniform multistorey structures, where the location of the CR is easily established, the fundamental frequencies can be resolved by the standard procedure for solving eigenvalue problems (Chopra, 1995). For irregular multistorey structures, where the CR locations are not inherently obvious, the frequencies can be estimated to reasonable accuracy by the Rayleigh method discussed in section 4.3.5.1 (De La Llera & Chopra, 1994a).

In past studies, two definitions of torsional to lateral frequency ratio for single storey structures have been employed:

$$\Omega = \omega_\theta / \omega_y = \frac{\sqrt{K_{\theta r}/m r_m^2}}{\sqrt{K_y/m}} = \sqrt{\frac{K_{\theta r}}{K_y}} \cdot \frac{1}{r_m} \tag{4.2a}$$

$$\Omega_r = \omega_{\theta r} / \omega_y = \frac{\sqrt{K_{\theta r}/m r_r^2}}{\sqrt{K_y/m}} = \sqrt{\frac{K_{\theta r}}{K_y}} \cdot \frac{1}{r_r} \tag{4.2b}$$

where $\omega_{\theta r}$ and ω_θ are the uncoupled torsional frequencies calculated about the CR and CM, respectively, and ω_y is the uncoupled translational frequency in the y-direction. The difference between the two definitions lies in the determination of the rotational moment of inertia of the floor diaphragm, whether it is calculated about the CM, as for r_m, or about the CR, as for r_r. $K_{\theta r}$ is the torsional stiffness calculated about the CR which is given for a single storey building by

$$K_{\theta r} = \sum_{i=1}^{n} k_{yi} \cdot (x_i - e_s)^2 + \sum_{i=1}^{n} k_{xi} \cdot y_i^2 \tag{4.3}$$

where x_i or y_i is the distance from the CR to the i^{th} element in the y- and x-directions, respectively. For the analytical models used in this study, the second term is dropped since the walls in the x-direction do not contribute to torsional stiffness. The definitions of frequency ratio are related by

$$r_m^2 = r_r^2 - e_s^2 \tag{4.4}$$

and therefore, Ω_r is always less than Ω for all values of e_s greater than zero. The approach employing Ω_r has the advantage in that all the terms are defined about the same point, the CR, however, r_r varies with the value of e_s. On the other hand, for a system with uniformly distributed mass, r_m is only a function of the plan aspect ratio and remains constant with variations in eccentricity and CR location. For this reason, and for continuity with the method of estimating the fundamental frequencies for irregular multistorey buildings, Ω was adopted as the method of determining the uncoupled torsional to lateral frequency ratio for this study. The mass radius of gyration for a floor slabs modelled as a rectangular thin plate is $r_m = \sqrt{(a^2 + b^2)/12}$.

The value of $\Omega = 1$ has been adopted as the transition point between torsionally flexible and torsionally stiff systems as has been established in previous studies. A system with $\Omega < 1$ is considered torsionally flexible representing a building with most of the lateral and torsional resisting elements concentrated in a stiff central core with a flexible perimeter. A system with $\Omega > 1$ is deemed torsionally stiff with most of the resisting elements positioned close to the building perimeter.

The uncoupled torsional to lateral frequency ratios, Ω, examined in this study are 0.5, 0.75, 1.0 and 1.25. Values of Ω up to approximately 1.5 are common for buildings with low e_s, however, reasonable wall configurations were not possible to achieve for buildings with this magnitude of frequency ratio and eccentricities of $0.2b$, and therefore, the cutoff was made at $\Omega = 1.25$.

4.3.5.1 Estimating Uncoupled Frequencies by the Rayleigh Method for General Multistorey Buildings

Recent studies indicate that the frequency ratio Ω is an important factor influencing the effects of torsion in building response. Current design code torsional provisions are a function of static eccentricity only and do not the incorporate torsional flexibility of the system. New design equations proposed by Humar and Kumar (1998) require the estimation of Ω which is not clearly identifiable for a multistorey building with any irregularities or with combination of frames and shear walls. De La Llera and Chopra (1994a) suggest the use of the Rayleigh method to obtain an approximation of the uncoupled frequencies. This method has also been endorsed by Kumar and Humar (1998) and recommended by the NZS-92.

The Rayleigh method requires a static analysis of the building subjected to two loading states which approximate the first lateral and first torsional vibration modes. To estimate the lateral vibration mode a reasonable set of horizontal storey forces, F_i, are applied to the model with the floor rotations restrained. For example, the lateral forces may be taken as being proportional to the equivalent static code forces. The resulting floor displacements δ_i are recorded. The estimate of lateral frequency, ω_y, is then calculated using the following expression:

$$\omega_y \approx \sqrt{\frac{\sum_i F_i \cdot \delta_i}{\sum_i m_i \cdot \delta_i^2}} \tag{4.5}$$

To estimate the torsional mode, a reasonable height-wise distribution of storey torques, T_i, proportional to the lateral floor forces, such as F_i*e, where e is an arbitrary value of eccentricity, are applied. The building will rotate about the CR's and the resulting floor rotations, θ_i are recorded. I_{cm_i} is the polar moment of inertia about the CM. The following expression is then used calculate the uncoupled torsional frequency:

$$\omega_\theta \approx \sqrt{\frac{\sum_i T_i \cdot \theta_i}{\sum_i I_{cm_i} \cdot \theta_i^2}} \tag{4.6}$$

Finally Ω is taken as the ratio of ω_θ/ω_y. Statistically, the resulting estimate of Ω is thought to be more accurate than the individual estimations of ω_θ and ω_y since the errors inherent in their computation will tend to cancel out through the division process.

4.3.5.1 Uncoupled Lateral Period

Previous studies on single storey buildings indicate that while actual edge displacement varies with lateral period, normalized displacement to a TB model or normalized ductility demand on elements due to torsional effects are not highly dependent upon lateral period (Tso & Wong, 1995; Humar & Kumar, 1998). Correnza et al. (1995) believes that additional deformation and ductility demand are highly period dependent, however, the reference model used in his study was different from that of previous studies in that accidental eccentricity was included in determining the wall strengths of the TB model. This lead to a perceived increased ductility demand for the TU models when normalized to the TB ductility response and would account for the conflicting conclusions drawn. Because of the apparent independence of normalized response to variation in lateral period, studies examining elastic and nonlinear response of multistorey analytical models frequently focus on buildings with a lateral period around 0.5 to 1 second (De La Llera & Chopra, 1994; Kumar, 1998; Tso & Wong, 1995; Wong & Tso 1994; Tso & Zhu, 1992).

To examine the effects of uncoupled lateral period on torsional response of asymmetric buildings, two values of uncoupled lateral period, T_y, of 1 and 2 seconds were examined in this study. The buildings were considered to be 10 and 20 stories in building height, respectively.

4.3.6 Torsional Restraint

Paulay hypothesizes that distribution of torsional resisting elements to all four sides of a building is imperative to providing adequate torsional resistance (Paulay, 1997b). He emphasizes that a system is only truly torsionally restrained as long as walls are positioned in the orthogonal planes which possess sufficient stiffness to remain elastic when subjected to strong ground motion in the *y*-direction. Paulay's studies are based on the formation of a failure mechanism in single storey models by means of static nonlinear analyses. Another study examining Paulay's hypothesis found his results conservative compared to a nonlinear dynamic analysis due to the fact that Paulay does not account for rotational inertia of the floor diaphragm or dynamic effects (Farah, 1998).

Recent studies have shown that it is the overall torsional restraint which is the important parameter influencing torsional response. It makes little difference if torsional restraint is provided solely by resisting elements located parallel to the direction of earthquake motion rather than by a combination of elements placed both parallel and orthogonal to the direction of earthquake motion (Tso & Wong, 1995; Kumar, 1998; Humar, 1999). Humar and Kumar found that the torsional effects were at most 20 percent greater for structures with no contribution to torsional restraint from orthogonal walls. In this study, the orthogonal walls do not contribute to the torsional restraint of the system to represent the most extreme conditions of torsional response. The torsional restraint defined in this study is the ratio of the torsional to lateral frequency, Ω, as described previously.

4.3.7 Strength Distribution and Eccentricity

Strength eccentricity is also an important parameter influencing inelastic torsional response. Previous research has shown that when the strength distribution varies significantly from the stiffness distribution, excessive ductility demand can result primarily in the stiff-edge element. If the strength eccentricity is small (generally it is smaller than the stiffness eccentricity), torsional response is reduced in the inelastic range, which can result in the reduced ductility values for flexible-edge elements (Tso & Ying, 1990). However, excessive ductility demand may arise in stiff-edge elements. When the effects of torsion are excluded, as in the TB model, the stiffness and strength eccentricities are equal since the element strengths are distributed in proportion to the element stiffness (NBCC, 1995; NEHRP, 1997). With torsion included, the strength distribution is dependent upon how torsion is accounted for in the design codes.

In this study the element strengths are distributed according to various code or proposed code methods of accounting for torsional effects and correlated with the resulting displacements or ductility demands on the walls.

5 Elastic Dynamic Response Spectrum and Static Analyses

5.1 General

The structural analysis program SAP2000 was used to conduct all the static and elastic dynamic response spectrum analyses. A response spectrum analysis (RSA) was conducted initially on a stick model with identical total storey stiffness and mass properties to that of the 3D models examined in the study to determine the total base shear, base overturning moment, and lateral distribution of dynamic forces for both uncoupled lateral periods, T_y = 1 and 2 seconds. These forces were used for determining the static storey torsional moments to account for accidental torsional effects when determining the element design strengths.

There are differing opinions on what method should be employed to determine torsional effects and resulting wall element design strengths. The current approaches implemented in design practice, either by static analysis or dynamic response spectrum analysis, vary significantly and can result in quite different element design strengths, particularly for torsionally flexible buildings (De la Llera & Chopra, 1994e; Wong & Tso, 1994). There is also no consensus on whether the effects of accidental torsion should be included in the determination of strength distribution of the reference models (Correnza et al. 1992; Tso 1993).

5.2 Lateral Distribution of Forces

The lateral distribution of forces used to determine the static storey torsional moments may be either the triangular distribution of forces as suggested by the NBCC (1995) or that determined from a dynamic response spectrum analysis. Many codes, such as the NBCC and UBC (1997), recommend dynamic analysis to analyze buildings with significant irregularities in plan or elevation. It is believed that a dynamic analysis will lead to a more realistic distribution of forces on the structure in the elastic range since the elastic dynamic properties of the particular structure are taken into account. When excited into the inelastic range the primary parameters of concern are the magnitude and distribution of displacement and ductility demand. It was assumed that a structure's design based on a more realistic seismic load distribution in the elastic range will display a more favourable displacement and ductility demand distribution when excited into the inelastic range.

In this study, the seismic distribution of storey forces was found through conducting a dynamic response spectrum analysis, using the 5% damped NBCC code design acceleration spectrum scaled to 0.2g, shown in Figure 3.4, for an equivalent stick, lumped mass model, possessing identical properties to the 3D building under study. This is equivalent to finding the storey forces from a response spectrum analysis of the 3D model with the floors rotations restrained. The intent was to find the lateral floor forces of an equivalent torsionally balanced or uncoupled system, excluding the effects of torsion. The maximum storey forces were scaled to sum to the maximum base shear and are distributed as displayed in Figure 5.1. The influence of higher modes is evident in the shape of the force distribution up the height of the building.

5.3 Strength Distribution

When torsional effects are ignored, the seismic design strength is determined by dividing the resulting elastic forces by the force reduction factor, R, and is distributed to the various vertical

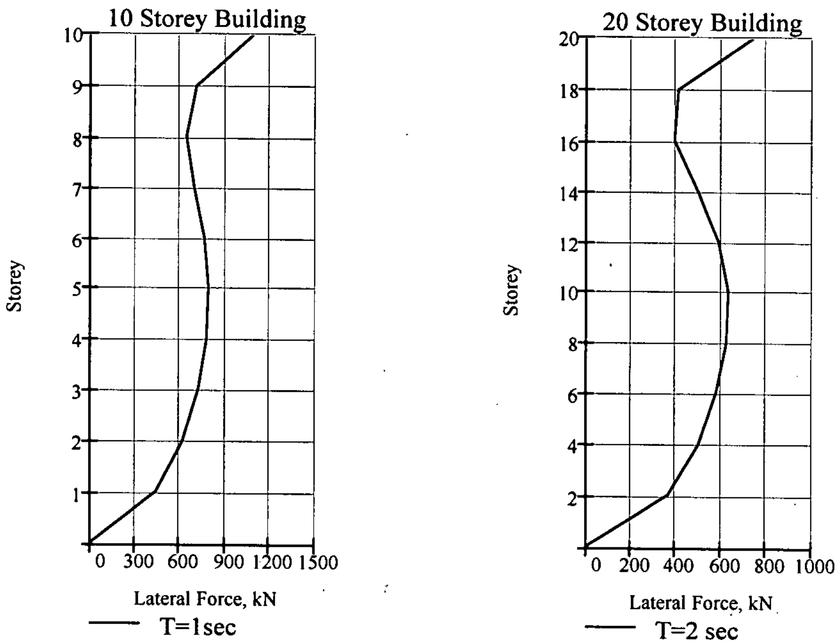

Figure 5.1 Lateral distribution of storey forces

elements of the seismic force resisting system based on their relative lateral stiffness (NBCC, 1995; NEHRP, 1997). Alternatively, the forces could be determined from the RSA of a torsionally balanced model where the CM is shifted to coincide with the CR or where the floor slabs are restrained against rotation.

The discrepancy in determining the magnitude and distribution of strength for asymmetric structures between countries stems from the differences in the various major code static torsional provisions in the amplification and deamplification of the inherent plan eccentricity, e_s, and the adopted magnitude of accidental eccentricity discussed in Chapter 2. Another factor contributing to the differences is the broad range of opinions on how to treat accidental torsion in a dynamic analysis and in the reference models used to evaluate code torsional provisions. Also, recent research by Humar (1998) and Kumar (1998) suggests changes to the current code torsional provisions.

5.3.1 Incorporation of Accidental Torsion:

All codes require the inclusion of accidental torsion in the determination of design strengths of lateral resisting elements. However, there are differing opinions on how it should be effectively incorporated into models evaluating torsional provisions. There also remains some controversy between researchers as to whether or not accidental torsion provisions should be incorporated into determining the strength distribution of the elements in the reference model. (Correnza et al. 1992; Tso 1993).

Accidental eccentricity is incorporated into a static analysis by amplifying or deamplifying the stiffness eccentricity by an amount $\pm\beta b$, where β varies from 5% to 15% of the building dimension, b, perpendicular to the direction of earthquake excitation as discussed in Chapter 2. De la Llera and Chopra (1994e) found that the discrepancies between the predicted increase in response due to accidental eccentricity by static and dynamic analysis can be in the same order of magnitude as the actual increase in response. The magnitude of the difference increases for torsionally flexible buildings with static eccentricity, $e_s > 0.15b$. They concluded that the static method needs to be modified to give more consistent results with the dynamic analysis.

In subsequent studies De La Llera and Chopra (1995, 1994a, b, c, d) investigated the increase in building response due to several sources of accidental torsion including base rotational excitation, stiffness uncertainty, uncertainty in the location of CM, and uncertainty in element stiffness and mass distribution in the orthogonal direction. They concluded that the effects of accidental torsion due to the combined effects of all sources examined can be adequately represented in a dynamic analysis by displacing the CM a distance $\pm 0.05b$ from its nominal position corresponding to an exceedance probability of approximately 30%. They also showed that the increase in displacement response determined from the dynamic analysis followed similar trends as the simulated "true" increase in response due to the combination of all examined sources of accidental torsion. The static analysis procedure for representing the effects of accidental torsion results were not consistent with the "true" response particularly for torsionally flexible structures.

For a dynamic analysis most building codes require that the effects of accidental torsion be considered by applying an equivalent distribution of forces at a specified distance from the CR, usually given as a percentage of the building dimension b perpendicular to the direction of interest. The resulting element shears and bending moments due to the storey torques are added to the shears and bending moments found by a dynamic analysis. The NEHRP 94 and 97 guidelines suggests that one of the two following approaches below may be used.

1. By taking the envelope of the combination of results from dynamic response spectrum analysis with the results of statically applied torsional moments.

2. By taking the envelope of the results from two dynamic response spectrum analysis where the CM is displaced to the right and to the left of its original position respectively, in our model from the geometric centre, by the amount βb. The value of β, which dictates the amount of

displacement required, varies between codes.

The current NBCC (1995) allows only the first of the NEHRP approaches for incorporating accidental torsion into a dynamic analysis. Earlier editions had allowed both approaches and required the CM to be shifted ±0.1b. A study by Wong and Tso (1994) examining single storey buildings found that the first approach was the most consistent and computationally simpler of the two methods for determining design strengths. In the second approach, the dynamic properties of the building are altered due to shifting the CM from its original position causing irregularities in the level of strength margin which, under some conditions, results in smaller design strengths for stiff-edge elements than if no torsional provisions were included.

The first approach suggested by NEHRP for incorporating accidental torsion into the dynamic modal analysis was chosen for this study to determine the wall strengths for the inelastic analysis. The envelope of a dynamic response spectrum analysis, using the design response spectrum, was combined with statically applied storey torques of ±0.1b as required by the NBCC. For some models statically applied storey torques of ±0.05b were examined for comparison. Also, in the preliminary investigation of these models, the peak elastic displacements were determined for three dynamic and two static conditions: (1) the RSA plus statically applied storey torques of $\pm 0.1b$, (2) the RSA plus statically applied storey torques of $\pm 0.05b$, (3) the RSA with the CM shifted $\pm 0.05b$, (4) NBCC static approach, and (5) Humar/ Kumar proposed static method. Typically the shifting the CM $\pm 0.05b$ produced smaller displacements than all other methods examined.

Since the NBCC considers $\pm 0.1b$ for contribution due to accidental torsion, this value was used for determining the moment capacity when applying the static torques to be added to the results of the dynamic response spectrum analysis. In the elastic and nonlinear time history analyses accidental torsion effects were represented by displacing the mass by the amount $\pm 0.05b$ from its nominal position as suggested by Chopra (1994e). Accidental torsion effects were not included in the analyses of the TB reference models.

5.3.2 Methods of Determining Wall Element Strengths

Three different methods were examined for determining design wall strengths. The first is a dynamic response spectrum analysis, RSA, with statically applied storey torsional moments of $\pm F_i \cdot 0.1b$ denoted as *Dyn+T1*. The second is the static approach suggested by the NBCC referred to as *NBC* and the third is a new method proposed by Humar and Kumar (1998), abbreviated *H/K*, that attempts to eliminate the requirement to find the CR for most building configurations. All approaches were conducted using the storey forces as shown in Figure 5.1. A constant value of force reduction factor, R, of 4 was adopted for this study.

5.3.2.1 Dynamic Response Spectrum Analyses

For the dynamic response spectrum analyses, *Dyn+T1* and *Dyn+T05*, the torsional moments, equal to $\pm F_i \cdot 0.1b$ and $\pm F_i \cdot 0.05b$, respectively, were applied statically at each floor level. The maximum shears and moments in each wall from the two analyses were combined with the results of the 3D dynamic response spectrum analysis for each element.. The resulting maximum moment at the base of each wall was divided by R to give the design moment capacity of the walls to be used in nonlinear time history analyses.

The moment capacity in the x-direction was taken directly as the base moment, M_b, divided by R. No increase was made for accidental torsion since there is no contribution to torsional resistance from this direction.

5.3.2.2 Static Analyses

The design strengths or moment capacities resulting from two different static analyses were examined. First, the NBCC 1995 static approach, referred to as *NBC,* of the applying the storey forces at a distance equal to:

$$1.5e_s \pm 0.1b \quad \text{and} \tag{5.1}$$

$$0.5e_s \pm 0.1b \tag{5.2}$$

The second static approach, abbreviated *H/K*, proposed by Kumar (1998) and Humar (1998), applies the storey forces at a distance equal to:

$$e_s \pm 0.1b \quad \text{for} \quad \Omega > 1.0 \tag{5.3}$$

$$\pm 0.1b \quad \text{for} \quad \Omega < 1.0 \tag{5.4}$$

Kumar (1998) reasoned that half of the amount $\pm 0.1b$ can be assumed to account for natural torsion or dynamic amplification due to coupling between the lateral and torsional motions of the building, while the remaining $\pm 0.05b$ is to account for accidental torsion. The maximum values of base moment were divided by R to give the static design moment for each lateral resisting element. The total base moment and element moment capacity will be different for each model dependent upon the analysis method implemented for including torsional effects. Also, the element design shear and storey shear, including torsional effects, will vary between models at each floor level.

5.3.3 Comparison of Methods for Determining Wall Element Strength

A comparison of the required stiff and flexible wall design base moment capacity determined by each method described above are shown in the Figures 5.2 to 5.6 for the flexible and the stiff walls for buildings with T_y of 1 and 2 seconds and eccentricity range of $e_s = 0.2b$, $0.1b$ and 0, over the range of torsional to lateral frequency ratio, $\Omega = 0.5$, 0.75 1.0, 1.25. Also shown are the required torsionally balanced, TB, moment capacities. The second plot in each figure shows the ratio of the TU/TB magnitudes to express the increase in strength required due to the combination of natural and accidental torsion for each method and model.

Since the TB building does not exhibit any torsional response in the elastic range, the wall design strengths were taken as directly proportional to the individual wall stiffness. Their sum is equal to the base moment found in the RSA divided by the force reduction factor, R. To show the worst case scenario the effects of accidental torsion were not accounted for in the TB models. In Figure 5.2 only, (with $T_y = 1$ sec. and $e_s = 0.2b$), the strengths for a dynamic analysis combined with a statically applied torsional moment of $\pm F_i \cdot 0.05b$ were also computed.

The wall strengths determined by the static and dynamic RSA methods vary significantly, especially for the flexible wall with high eccentricity, confirming the results found by De La Llera and Chopra (1995). The strengths determined by the dynamic analysis are considerably less than those by the static analysis for the flexible wall at low frequency ratio Ω, however, they fall below the static values for the stiff wall at high Ω. In some cases the design moment decreases to values below that of the TB building for both the *Dyn+T1* and *H/K* methods of analysis. Although this would reduce the strength eccentricity it could lead to a large ductility

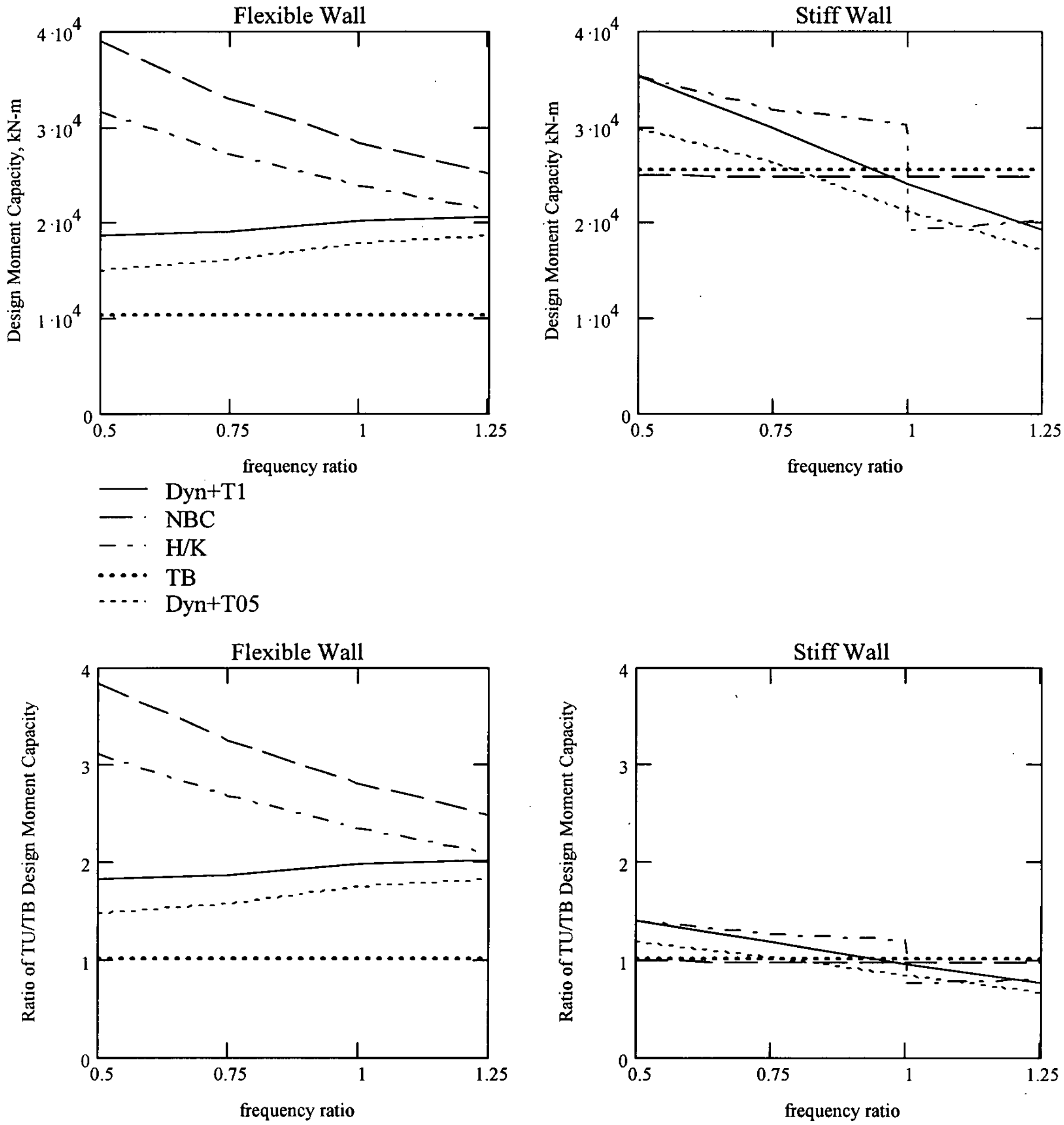

Figure 5.2 Design moment capacity vs. frequency ratio, Ω, for $T_y = 1$ sec. $e_s = 0.2b$

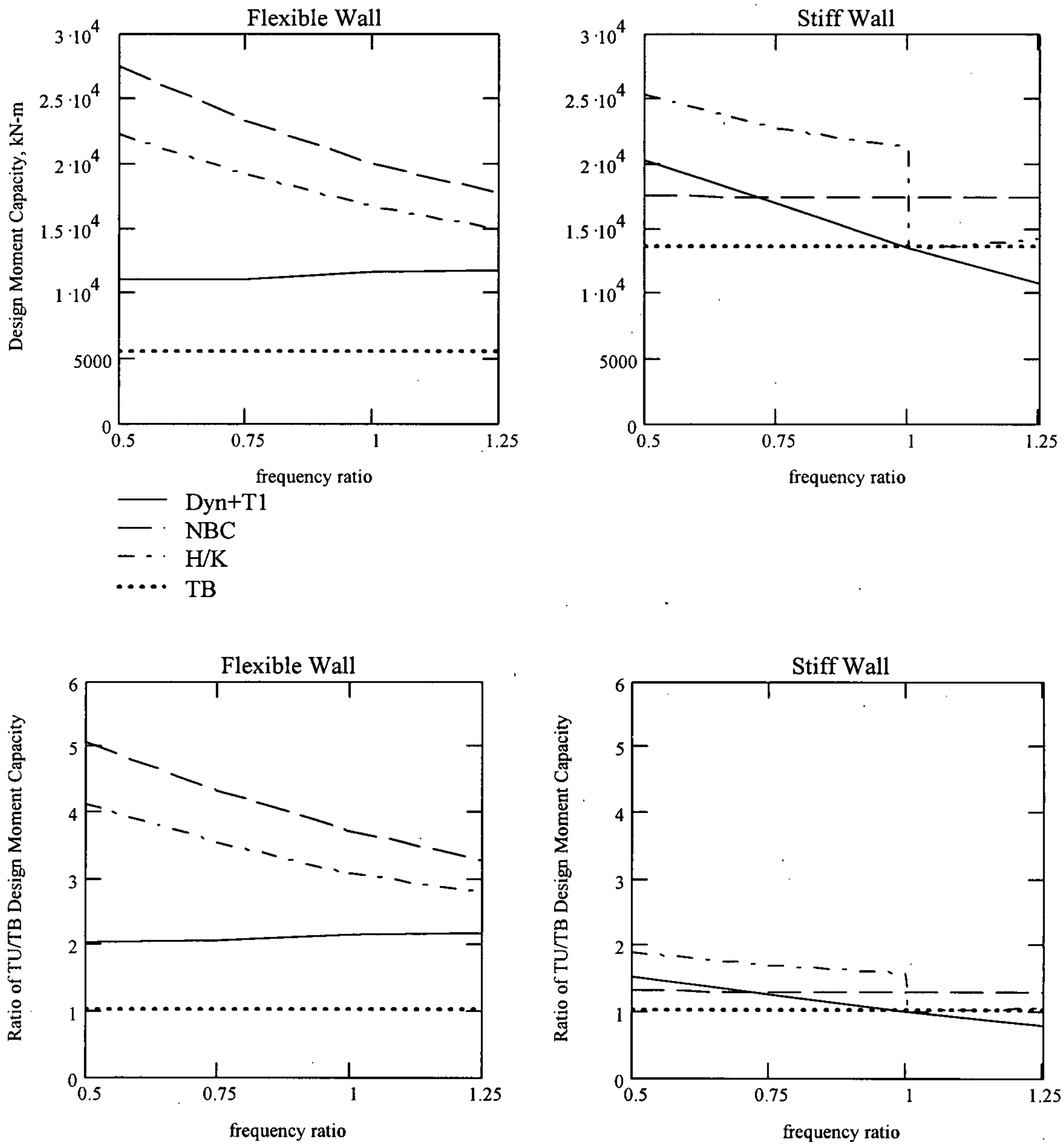

Figure 5.3 Design moment capacity vs. frequency ratio, Ω, for $T_y = 2$ sec. $e_s = 0.2b$

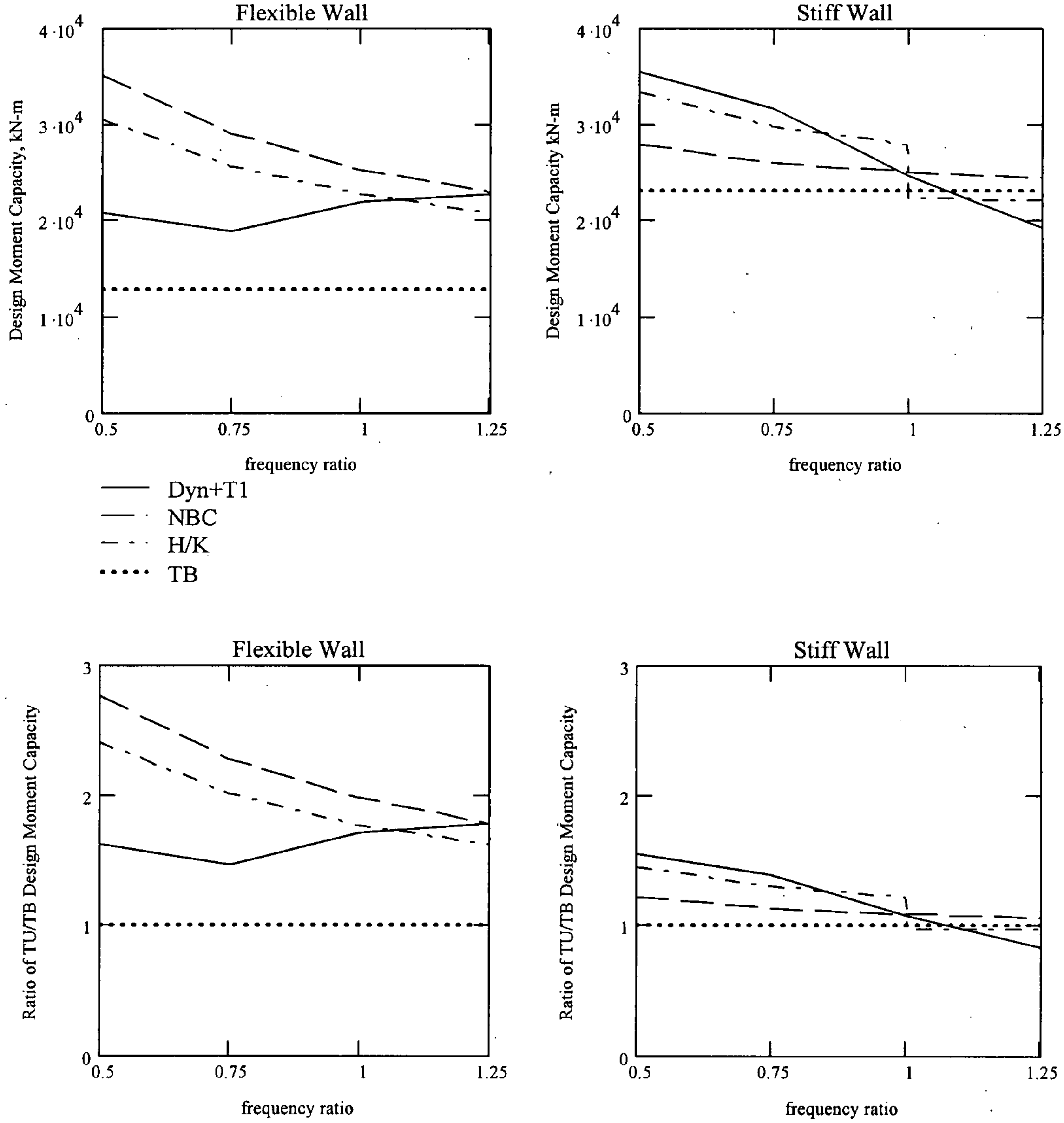

Figure 5.4 Design moment capacity vs. frequency ratio, Ω, for $T_y = 1$ sec. $e_s = 0.1b$

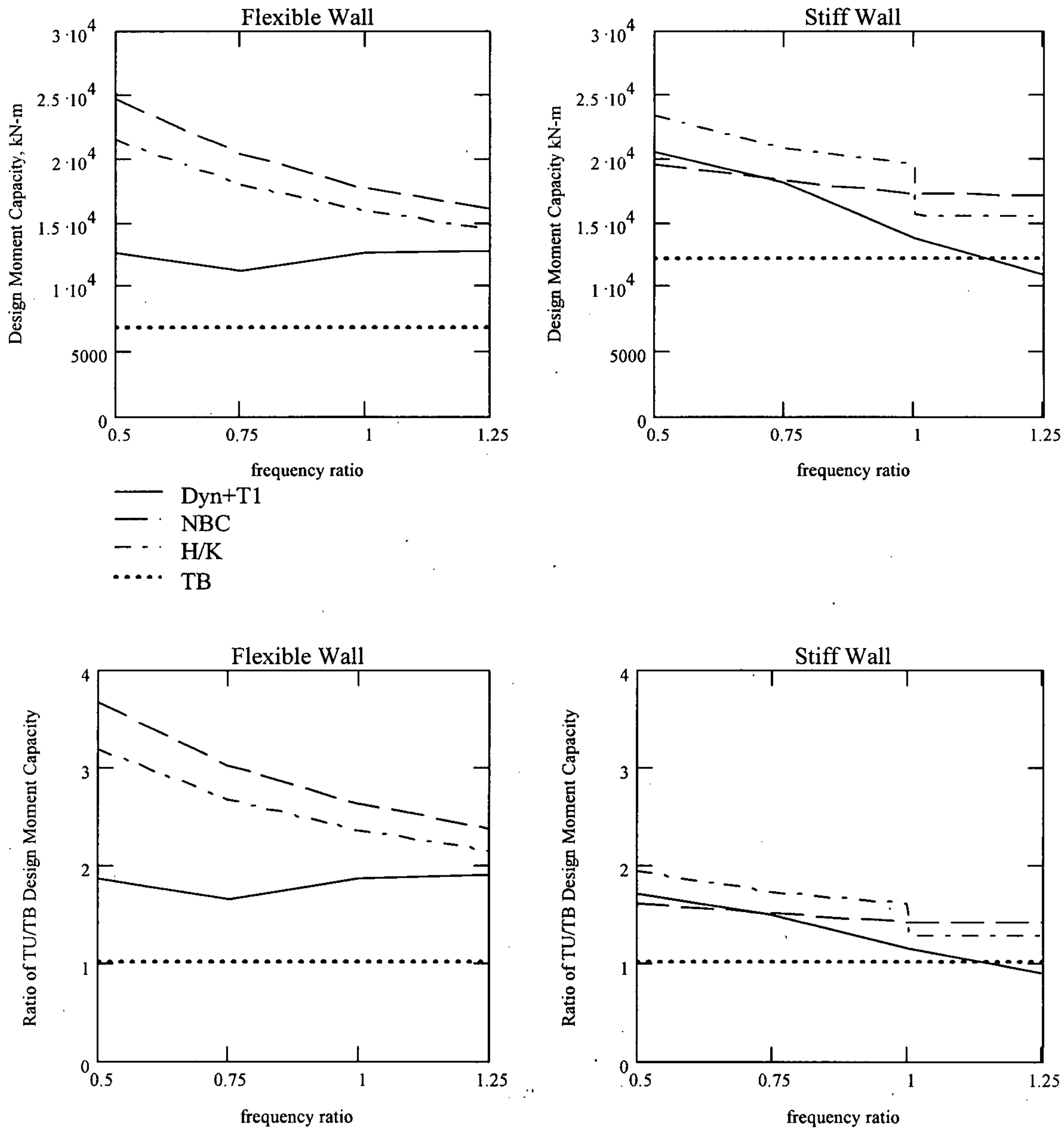

Figure 5.5 Design moment capacity vs. frequency ratio, Ω, for $T_y = 2$ sec. $e_s = 0.1b$

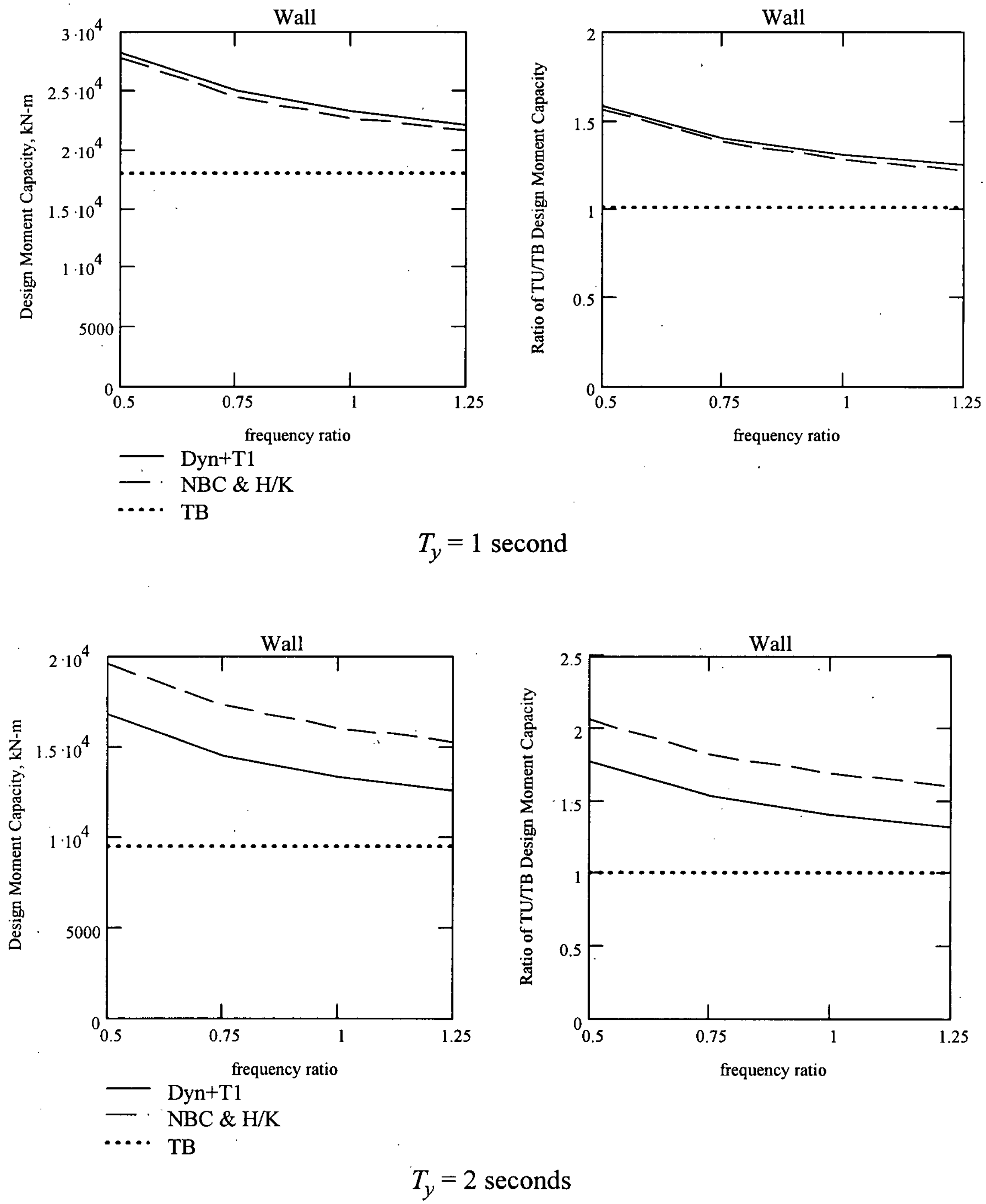

Figure 5.6 Design moment capacity of both walls 1 and 3 vs. frequency ratio, Ω, for symmetric buildings

demand for the stiff-edge element.

The values computed for the symmetrical buildings are due to accidental torsion only since the static eccentricity is zero. Therefore, the *NBC* and *H/K* design equations become identical. The static response is very close to that of the *Dyn+T1* method for the $T_y = 1$ second building and follows the same trend but is somewhat greater than the dynamic response for the $T_y = 2$ second building. This difference in design moment could be due to the second mode effects in the modal analysis. The *NBC* and *H/K* design moments were not reduced by the J factor.

The *H/K* proposed equations follow the trend of the *Dyn+T1* response more closely than the *NBC* static response for both the flexible and stiff-edge elements, however, there is a large step in the *H/K* response at $\Omega = 1$ for the stiff-edge element. This step is undesirable since the estimate for frequency ratio is not precise and discrepancies could arise as to which is the valid design value for structures that lie in the vicinity of $\Omega = 1$. A more gradual transition between the two proposed equations would be an improvement.

Generally the *NBC* static torsion design equations give conservative results for design strength. Also, flexible buildings with $\Omega < 1$ are penalized by the static methods since the required strength increase for the flexible-edge element is up to five times that of the equivalent TB building or two and a half times that of the *Dyn+T1* method. This is to deter designers from constructing buildings that fall in this range, however, if the dynamic analysis does more accurately predict the "true" response of the building as suggested by De La Llera and Chopra (1992), the *NBC* and *H/K* methods are overly conservative for the flexible-edge. Since both static and dynamic methods are currently allowed by the NBCC as valid techniques for determining design moment capacity then the static method should be altered to be consistent with the *Dyn+T1* method for moderately eccentric buildings.

Plots showing the variation in strength eccentricity with the various design methods are shown in Figure 5.7. Strength eccentricity is the distance between the CM and centre of element strength at each floor level. The strength eccentricity is identical for each storey of the models used in this study since the strength of the elements is kept constant up the height of the buildings. The strength eccentricity is the greatest for the *Dyn+T1* models and the smallest for the *NBC* static approach, except at high frequency ratios where the *H/K* approach drops slightly below that of the *NBC*. Also, the strength eccentricity values are consistently less than the stiffness eccentricity.

5.4 Elastic Response Quantities

The elastic response quantities of interest from the dynamic RSA and static analyses in this study are:

- the elastic peak base shear force of the stiff and flexible wall elements and shear distribution envelope up the individual walls and,
- the elastic moment distribution envelope up the individual stiff and flexible walls

These values were recorded to be compared with the nonlinear time history response values. The elastically predicted peak displacements from the dynamic RSA combined with the three different methods of incorporating accidental torsion described in section 5.3.1 (1) the RSA plus statically applied storey torques of $\pm 0.1b$, (2) the RSA plus statically applied storey torques of $\pm 0.05b$, and (3) the RSA with the CM shifted $\pm 0.05b$ for some of the models were

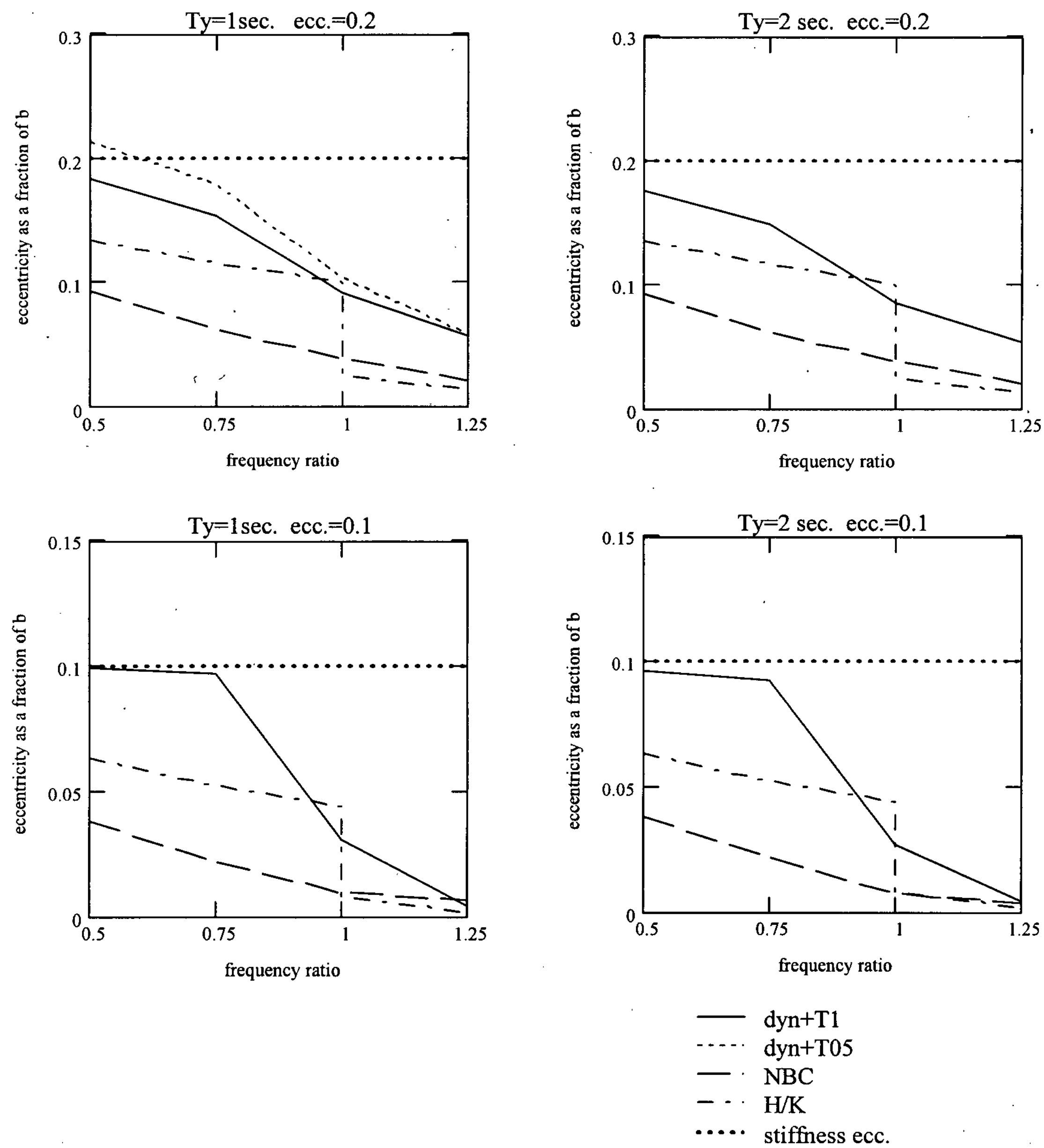

Figure 5.7 A comparison of stiffness and strength eccentricity with frequency ratio.

recorded to examine the ability of the elastic dynamic methods to accurately predict peak nonlinear displacements of asymmetric structures.

6 Time History Analyses

6.1 General

Time history (TH) analyses were conducted for the three earthquakes described in Chapter 4. Both elastic and nonlinear time history analysis were performed. Accidental eccentricity was accounted for in the time history analyses by shifting the CM $\pm 0.05b$ from its nominal position in all models as suggested by De La Llera and Chopra (1995). The peak response values for moment, shear, displacement, interstorey drift and plastic rotation were recorded for each of the three lateral resisting walls in the y-direction. The peak displacement and interstorey drift were also recorded for the corner columns on both the flexible and stiff edges.

6.2 Nonlinear Analysis

Nonlinear time history analyses were performed for the following three models:

- *Dyn+T1*: Wall strengths determined from the combination of a dynamic response spectrum analysis and statically applied storey torsional moments equal to $\pm F_i \cdot 0.1b$
- *NBC*: wall strengths determined from statically applied storey forces according to the requirements of the NBCC (1995) given by equations 5.4 and 5.1.
- *H/K*: wall strengths determined from statically applied storey forces according to the newly proposed method by Humar and Kumar (1999) given by equations 5.2 and 5.3.

These three methods produce quite different element strength and distribution requirements, therefore, it is of interest to investigate the significance of their effect on the response parameters in the nonlinear range.

6.2.1 Nonlinear Analysis Program

Most existing nonlinear computer programs developed for building structures are either incapable of managing 3D non-linear reinforced concrete wall structures or produce questionable results in the inelastic range. ANSYS (1998), a sophisticated general commercial finite element program, was considered, however, it is computationally demanding and for the system under investigation was determined not to be feasible. SAP2000 (1997) was also explored as a possible program for the nonlinear analysis. SAP2000 uses the Fast Nonlinear Analysis technique for solving nonlinear equations which relies on reducing the analysis to dynamic modes and nonlinear deformation modes using load dependent Ritz-vector analysis. The results of simple nonlinear models using the available nonlinear bending element, NLINK, were inconsistent. It was concluded that the nonlinear bending element adopted by SAP2000 for nonlinear time history analysis is not suitable for the type of analysis explored in this study. The program CANNY-E (1996b) was finally chosen for the nonlinear analysis portion of this study because of its 3D nonlinear capabilities and wide library of hysteresis elements to represent the nonlinear behaviour of various materials. CANNY-E was also used to conduct the elastic time history analyses to give the most consistent TH response results between the elastic and nonlinear models.

CANNY-E is a 3D nonlinear analysis program developed specifically for reinforced concrete frame and shear wall structures. It is applicable for buildings, towers, truss structures and any other type of structure that can be represented by linear elements and slabs. It is also suitable for steel structures or steel reinforced concrete structures. The elements available in CANNY-E are the 2D and 3D beam bending and shear elements, column elements capable of modeling biaxial axial torsion, bending, shear, and axial deformation, a tension/compression truss or cable element, a shear panel element and a support element. Single component or multi-spring models can be used to describe each material property of the element. Multi-spring models are capable of simulating axial load-bending moment and biaxial shear interaction nonlinearities. For the single component models, the response in each direction is examined independently and biaxial interaction is not accounted for. CANNY-E has gone through many stages of development and improvement and is constantly being updated. The latest version has been written for a Windows based PC but the visual portion was not complete at the time of this analysis, therefore, the November 1996 version of CANNY-E program was used in this study.

CANNY-E is capable of performing nonlinear dynamic time history analysis subjected to up to four components of ground motion (x-, y-, & z-directions, and rotation), elastic frequency analysis, static pushover analysis for a gradually increasing load or cyclic loads, and Japanese or Chinese static code analysis. Various boundary conditions and soil-structure interaction can be accounted for by proper modelling of the support conditions. The individual elements are considered massless and are located by their centroidal axis. Both rigid and flexible floor diaphragms can be modelled. Inertial masses are either lumped at the nodes or concentrated at the centre of gravity of each floor if a rigid floor slab is assumed.

The analysis is limited to small deformations due to material nonlinearities with the option of including P-delta effects. Geometric nonlinearities or large deformations are not included. The solution of the nonlinear time history analysis is based on the following relationships:

1. a nonlinear relationship between forces and the resultant displacements,
2. compatibility of displacements at the structural nodes,
3. equilibrium of forces at structural nodes (inertial, damping, resisting, and external forces) and,
4. the dynamic response of the structure to an external excitation can be described by a system of differential equations defined by the time response functions of acceleration, velocity and displacement.

The equations of motion of the time history analysis are solved by one of the two available numerical procedures, the Newmark Beta-Method (linear acceleration method) or the Wilson Theta-Method assuming a piece-wise linear force-displacement relationship over a small time interval. The duration of the time interval is selected based on the characteristics of the input motion and is recommended to be maximum 0.01 seconds. The Newmark Beta-Method with a time interval of 0.005 seconds was used for this study. The damping was selected to give 5% of critical damping in the first two vibrational modes. The force imbalance resulting from the change in stiffness for nonlinear elements is calculated at the end of the time step to fit the specified force-displacement relationship and is then added as an external force to the following time step.

The program CANNY is executed in three separate phases: (1) The preprocessor PRECANNY reads the freeformat data input file, performs memory allocation, auto-renumbering, and initialization of data and structural and element matrices, and creates a binary-format data file to be read by the analysis program. An example input file is shown in Appendix A.1. (2) The main analysis program CANNY reads the binary-format data file, performs the necessary numerical computation, and writes the results to an output file in binary format. (3) The postprocessor PSCANNY transforms the results from binary format to text format.

A utility program VCANNY is also included which can be used to graphically check the contents of the input and output files, animate mode shapes and view time histories. It is possible to animate overall storey shear, moment, displacement, and interstorey displacement envelope histories for the duration of the input ground motion.

When using a rigid floor diaphragm in CANNY-E, the displacement and inter-storey displacement history output is given at the geometric centre of the diaphragm only. In order to get displacement output at the corner nodes and wall nodes of each floor, dummy nodes were introduced. These nodes were offset 2 mm from the wall or column node at each floor level in the plane of the floor attached by a rigid horizontal beam column element. CANNY-E will output displacements and interstorey displacements for individual nodes not part of a diaphragm.

6.2.1.1 Elements and Hysteresis Properties.

In this study, the walls and corner columns were modeled as linear column elements. Separate one component hysteresis models were used to represent axial deformation, bending, and shear deformation in both directions. The floors were considered to be rigid in their own plane. The walls were designed to remain elastic in shear and out of plane bending. Axial deformations were also considered to remain elastic. All of the properties of the corner columns were taken to be elastic since their stiffness contribution is negligible compared to the wall elements and only the deformations at the corners were of interest. The CANNY linear elastic element model EL1 was selected to represent the elastic properties of the columns and walls shown in Figure 6.1 (Canny 1996a).

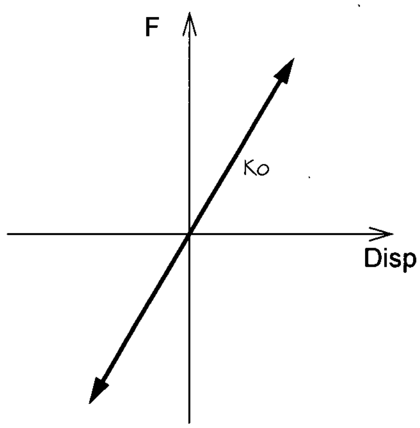

Figure 6.1 Linear-elastic model EL1

The hysteresis model selected to represent the flexural nonlinearities in the plane of the wall elements was the CANNY simple bilinear/trilinear model CA3 shown in Figure 6.2 (Canny, 1996a). This model has relatively simple rules for load reversals with the capability of modeling stiffness degradation and strength deterioration. For this study a bilinear curve was used by setting α to 1 in order to maintain the traditional method of determining rotational ductility. Only a very small strain hardening was considered with β equal to 0.001. The stiffness degradation was defined as $Ku = 0.66Ko$ by setting the first hysteresis parameter γ = 0.3. A strength degradation of 4% was chosen by setting the third hysteresis parameter λ_u = 0.053. These values were approximated through examination of actual hysteresis curves for individual reinforced concrete walls under cyclic loading (Paulay & Priestley, 1992).

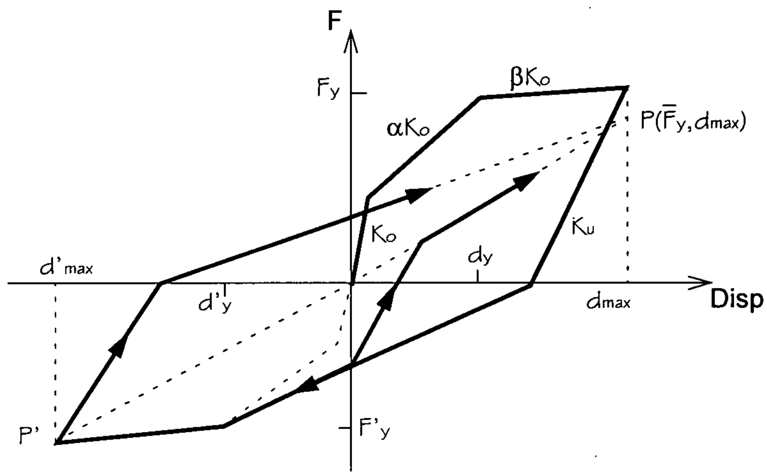

(a) Outside loop

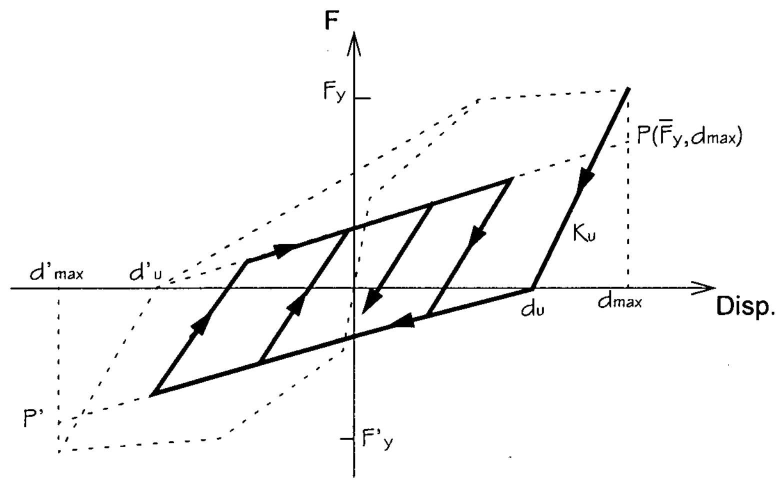

(b) Bi-linear rule for smaller loop

Figure 6.2 CANNY CA3 bilinear/trilinear hysteresis model

Shear deformations were included in the analysis, however, P-delta effects were neglected. Since we are modelling individual walls not coupled to other elements variation in axial load was not considered to be significant. Axial loads of the approximate proportional tributary dead load of the floors were applied to the walls.

6.3 Dynamic Shear Magnification

For the buildings of this study, the wall elements are designed to yield primarily in flexure and the wall strength is defined as the flexural moment capacity. However, the walls need to possess sufficient strength in shear to sustain the maximum shear forces resulting from strong ground motion. Dynamic magnification of shear forces increase the shear demand on individual cantilevered walls above what is estimated by dividing the elastic forces by the strength reduction factor, R. At some instances during an earthquake, the response may be strongly influenced by second and third modes of vibration. At higher modes the centre of inertia forces is lower than for the fundamental mode (Keintzel, 1990). Also, the shape of the higher modes do not vary significantly when the base fixity is changed from fixed to hinged indicating that the higher modes may not be largely affected by the formation of a plastic hinge at the base of the wall (Paulay & Priestley, 1992). The contribution of higher modes increases with the increased lateral period of the building (Keintzel, 1992).

The inelastic shear forces are not expected to reduce by the same factor as the value of the force reduction factor, R, used to determine the design moment capacity. The NBCC 1995 merely states that dynamic magnification of shear is to be considered but. The concrete material code suggests that the NZS provisions for dynamic shear amplification be adopted as a guideline. The NZS provisions are based on the Eurocode 8 (EC8) provisions for dynamic shear amplification. The EC8 (1988) adopted equations proposed in earlier studies by Keintzel (1990) that magnify shear by up to 1.8 times depending on the number of stories and is given by:

$$\omega_v = 0.9 + 0.1 \cdot n \tag{6.1}$$

for number of stories, n ≤ 5

$$\omega_v = 1.2 + 0.04 \cdot n \le 1.8 \tag{6.2}$$

for number of stories, n > 5, where ω_v is the magnification factor to account for the dynamic inelastic behaviour of the wall. Paulay and Priestley (1992) show $\omega_v = h_1/h_2$ where the ratio represents the height to the centre of the inertia forces in an elastic analysis, h_1, divided the lower height to the centre of the inertia forces in an inelastic analysis, h_2. The 1982 New Zealand Standard Code of Practice for the Design of Concrete Structures (NZS) has adopted similar equations to those proposed by Keintzel. The first equation for n ≤ 6 stories is identical to equation 6.1 but second equation for n > 6 stories differs slightly and is taken as

$$\omega_v = 1.3 + n/30 \le 1.8 \tag{6.3}$$

A parametric investigation by Keintzel (1992) indicates that dynamic shear magnification is also a function of ground accelerations and building period rather than only building height. Dynamic shear magnification has been shown to be larger for higher levels of seismic input acceleration and larger ductility or force reduction factors which are not accounted for in the proposed equations. Shear also does not necessarily increase proportionally with the designated yield moment of the walls as suggested by current design techniques and has been found to be more a function of lateral period, *T*, than number of stories, *n*. Further research in this area is being conducted to develop equations applicable to the Canadian design codes (CPCA, 1995) and to improve upon the existing equations to incorporate variables for spectral acceleration and lateral period. Keintzel (1992) proposed a new equation for the EC8 incorporating these variables. The seismic base shear force is approximated as $Q = \omega Q_I$ where

$$\omega = q\gamma_c\sqrt{(M_y/qM_I)^2 + 0.1(Sad_{max}/Sad(T_1))^2} \leq q \tag{6.4}$$

ω is the dynamic magnification factor for shear, Q_I is the design value for shear force, q is the behaviour factor ranging from 1 to 12 (similar to the force reduction factor of the NBC), γ_c is a correction factor taken as 1 for code design, M_y is the yield moment, M_I is the design value of bending moment, Sad_{max} is the peak value of the design acceleration spectrum, and $Sad(T_I)$ is the spectral acceleration corresponding to the fundamental lateral period. The fact that q appears in the denominator of the first part of the equation under the root sign indicates that only the contribution from the fundamental mode is considered to be reduced by yielding. The second term under the root corresponds to the contribution of higher modes and is not reduced by yielding. Only flexural cracking and degradation were taken into consideration in the development of these equations. Since diagonal shear cracking is not accounted for, the estimations of shear force imposed upon the resisting wall elements should be conservative.

The Canadian CSA Standard A23.3-94 (CPCA, 1995) for design of reinforced concrete clause 21.7.2.3 states that "Allowance for dynamic magnification of shear forces shall be made where applicable." The standard does not prescribe any means to account for the dynamic magnification of shear forces except in the commentary where it suggests to follow the recommendations of the New Zealand code reduced by the J factor, since the NZS does not apply a J factor, and reduced again by 1/1.25, since the NZS uses the nominal resistance for reinforcing steel rather than the probable capacity required by the CSA Standard. This increase in shear would be in addition to the increase to account for the shear corresponding to the development of the probable moment capacity at the base of the wall, however, the total need not be greater than that corresponding to an elastic system with R = 1. One of the factors of interest in this study is to find the extend of shear magnification in the lateral resisting walls when limiting the wall's bending moment capacity by the factor of R for multistorey torsionally unbalanced buildings from the nonlinear time history analyses.

6.4 Response Parameters

The response parameters of interest for this investigation are:

- a comparison of the peak elastic and nonlinear displacement of the stiff and flexible edges, Δ_f and Δ_s, at the extremes of the building for the time history analyses,
- the displacement ductility, μ_Δ, at the extremes of the building's stiff and flexible edges from the peak displacement response of the elastic and nonlinear time history analyses,
- the peak plastic rotation, θ_p, at the base of the stiff and flexible wall elements from the peak response of the elastic and nonlinear time history analyses,
- the rotational ductility, μ_θ, of the stiff and flexible wall elements from the peak rotation response of the elastic and nonlinear time history analyses,
- a comparison between the elastically predicted and nonlinear average peak base shear force of the stiff and flexible wall elements from the nonlinear time history analyses,
- a comparison between the elastically predicted and the nonlinear time history analyses shear distribution envelopes up the individual walls,
- a comparison between the elastically predicted and the nonlinear time history

analyses moment distribution envelopes up the individual stiff and flexible walls.

The results of the elastic time history analyses were conducted for the purpose of comparing the elastic and nonlinear displacements and for computing the desired ductilities. The time history results were used rather than comparing with either the elastic dynamic response spectrum analysis or the *NBC* or *H/K* static analyses because they would give response values more consistent with the nonlinear time histories since both models are subjected to the same ground motions.

Combining the results of the elastic and nonlinear time history analyses, the peak displacement ductility, μ_Δ, at the extremes of the building stiff and flexible edges were computed as:

$$\mu_\Delta = \frac{\Delta_u}{\Delta_y} \tag{6.5}$$

where Δ_u is the ultimate or peak displacement experienced during strong motion of the inelastic system and Δ_y is the displacement at yield. The yield displacement is defined as the maximum displacement recorded for an equivalent elastic system, Δ_{max}, divided by the R value as given by:

$$\Delta_y = \frac{\Delta_{max}}{R} \tag{6.6}$$

The rotational ductility, μ_θ, was determined by comparing the elastic rotation at yield, θ_y, defined in equation 6.8, to the plastic rotation, θ_p, and is defined as:

$$\mu_\theta = 1 + \frac{\theta_p}{\theta_y} \tag{6.7}$$

where

$$\theta_y = \frac{\Delta_y}{L} \tag{6.8}$$

and L is the vertical length/height of the wall element. Curvature ductility was not determined for this study since it is a section property and the wall reinforcement and details were not specifically defined.

7 Results & Discussion

7.1 Peak Displacement & Interstorey Displacement

The maximum displacement relative to ground of a shear wall building subjected to seismic ground motion will occur at the uppermost storey or roof of the building. For torsionally balanced structures (TB), which do not exhibit any torsional response, the peak displacement will be identical at any point along the roof. However, for an asymmetric building the peak displacement will occur on the flexible-edge at the extreme corner for an elastic model and at either the flexible or stiff-edge corner for a nonlinear model depending on the strength distribution to the lateral resisting wall elements. The peak interstorey displacement will occur in the top storey in all cases for a shear wall structure. The NBCC requires that the maximum displacement of a building relative to ground and the maximum interstorey displacement relative to the floor below be determined at critical locations in the structure for deflections due to translation and torsion. (NBCC, 1995; Supplement to NBCC, 1995). Both the NBCC 1995 and the UBC 1997 limit the maximum allowable interstorey drift to 2% of the storey height for the buildings of this study.

7.1.1 Peak Displacements

Figures 7.1 and 7.2 show the average peak displacement for the three input ground motions, at the roof level for the flexible- and stiff-edge corners, of the elastic time history analysis (*TU elast*) and the nonlinear TH analysis for the three design approaches for determining element strength (*Dyn+T1, NBC & H/K*), all with the mass shifted $\pm 0.05b$, over the range of frequency ratio, Ω. Also plotted are the results for the elastic and nonlinear torsionally balanced models

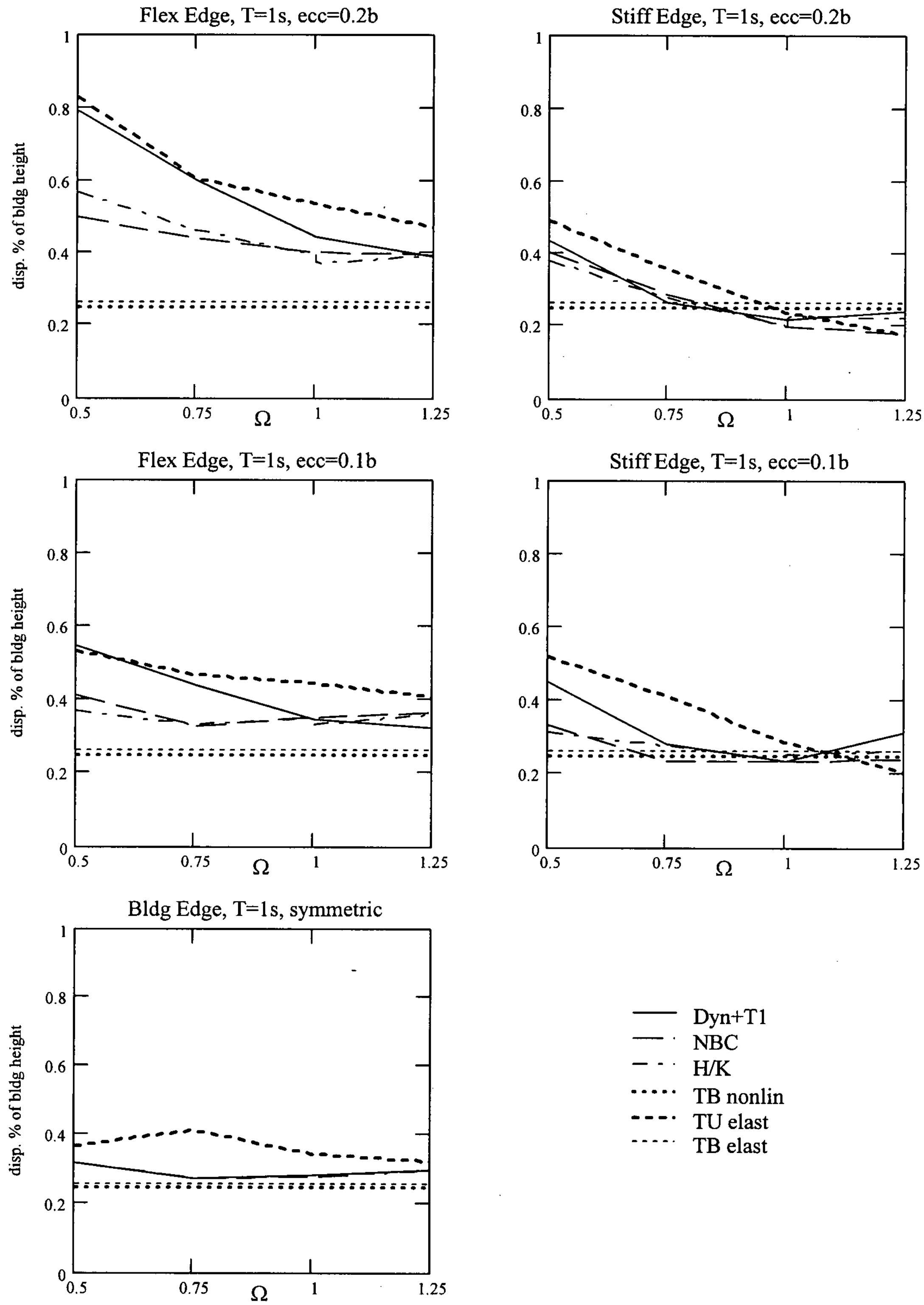

Figure 7.1 Avg. peak displacement of top of building in % of height vs. freq. ratio, Ω, $T_y = 1$s for TH analyses.

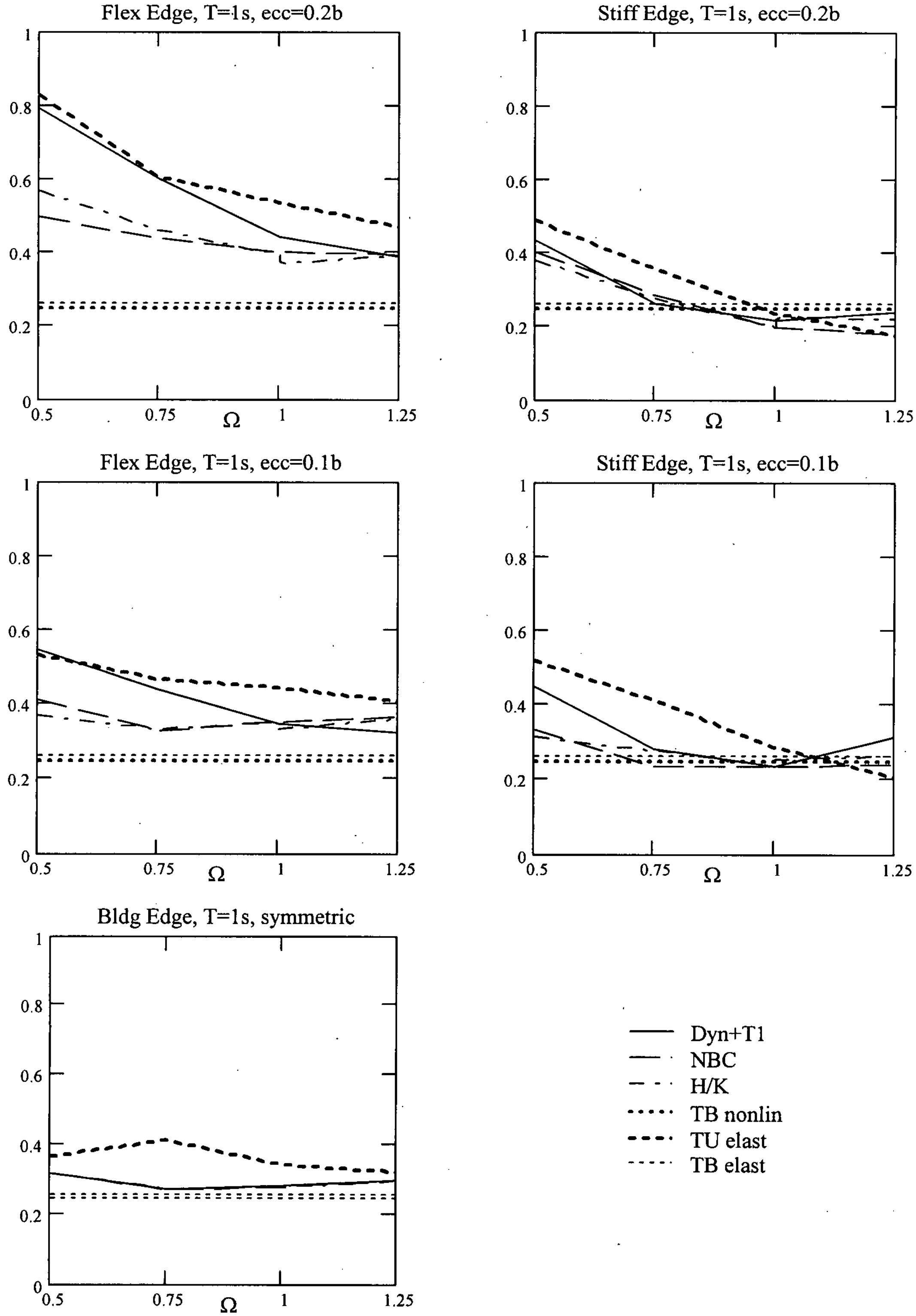

Figure 7.2 Avg. peak displacement of top of building in % of height vs. freq. ratio, Ω, $T_y = 2$s for TH analyses.

(*TB elast* and *TB nonlin*) which are independent of Ω.

Compared to the TB response the peak displacements generally increase with torsional flexibility, or decreasing torsional to lateral frequency ratio, Ω, for all asymmetric systems with $\Omega < 1$. In many cases, for $\Omega > 1$ the displacements of the stiff-edge element increase for the *Dyn+T1* and *H/K* systems. The increase, or decrease, in displacement due to torsion is evident by comparing the elastic and nonlinear TB model curves to those of the TU models. For the symmetric model, comparing the TB and TU curves depicts the effects of pure accidental torsion since there is no inherent plan eccentricity and the torsional effects are induced by the shift of the CM away from the GC. It is interesting to note that the symmetric curves do not follow the same trend as the asymmetric TU models.

For the symmetric system with $T_y = 2$ seconds, the effects of accidental torsion are greatest for high Ω, and despite the element strengths being greater than those of the equivalent TB model, the displacements including accidental torsion are greater than the TB response at high Ω. The TU elastic analysis also under-estimates peak displacement for $\Omega \geq 1$. For the symmetric system with $T_y = 1$ second the effects of accidental torsion are relatively uniform for all frequency ratios and are independent of the design method used to determine element strength.

The variation in results between the symmetric systems with $T_y = 1$ and 2 seconds contradict findings by De La Llera and Chopra (1994a & c, 1995) where they showed that the normalized response of a nominally symmetric single storey buildings to accidental torsion effects caused by uncertainty in stiffness and mass distribution, were essentially insensitive to changes in the value of the uncoupled fundamental lateral period T_y of the building. The sources of accidental eccentricity included in their study are rotational motion of the building foundations, uncertainty in stiffness of structural elements, uncertainty in location of CM, stiffness uncertainty in elements perpendicular to the direction of ground motion, and uncertainty in stiffness and mass distributions on other stories than the one analyzed. They found that, of all the sources of accidental eccentricity examined in their studies, the uncertainty in stiffness and mass distribution accounted for over 70% of the total increase in response due to accidental eccentricity. They modelled both uncertainty in stiffness and CM location as perturbations of the static eccentricity of the system. This is the same method adopted in the TH analyses of this study to model accidental eccentricity by shifting the CM a distance of $\pm 0.05b$ from its nominal position. Because of the apparent insensitivity to change in T_y, De La Llera and Chopra considered only structures with an uncoupled vibration period of $T_y = 1$ second for the remainder of their analysis.

The results found in this study for systems with $T_y = 1$ second are consistent with the trends of the studies by De La Llera and Chopra. The response of equivalent single storey symmetric structures to the effects of accidental torsion were also examined and the results were similar to those found for the multistorey structures. It is possible that De La Llera and Chopra did not consider this variation in response between the 1 and 2 second systems significant, and therefore, concluded that the normalized displacement ductility is essentially insensitive to variations in uncoupled lateral period. The variation between the displacement response of 1 and 2 second systems found in this study could possibly be due to the effect of the distributed mass up the height of the multistorey building and the contribution of higher modes to the vibration response. The response of long period buildings is generally more greatly affected by higher modes.

The elastic TU time history analysis usually estimates a greater peak displacement than seen by the nonlinear analysis, except for the stiff-edge element at large Ω and the symmetric model with $T_y = 2$ seconds, where the elastic predictions, in many cases, fall below the nonlinear values. For the asymmetric models, if the strength of the stiff-edge element is kept above that of the equivalent TB model, the influence of torsion typically decreases the response on the stiff side below the TB response as Ω increases, following the trend of the TU elastic predictions. The variation from the TU elastic response at $\Omega = 1.25$, however, could be partially due to the fact that strength reduction is allowed for the stiff-edge element, below that of a TB model, with the largest reduction allowed for the *Dyn+T1* models. The strength reductions allowed in the *H/K* method for the stiff-edge element are not as significant as for *Dyn+T1*, but the stiff-edge element strengths often still fall below that of the TB system. For the system with $T_y = 2$ seconds and $e_s = 0.1b$, the elastic analysis under-estimates the deflections of the stiff wall elements for all methods despite that the stiff wall strengths are all greater than for the equivalent TB system. This discrepancy between the TU elastic and nonlinear time history displacements at high Ω could also be influenced by the large variation between the stiffness and strength eccentricities, as indicated by Tso & Ying (1992).

If the strength distribution varies significantly from the stiffness distribution, then for stiff-edge elements with strength reductions, the measured plastic displacements will be larger than for an equivalent TB system, with strengths distributed proportional to element stiffness. The greater inelastic displacements indicate that the elastic analysis is incapable of giving accurate predictions of the inelastic systems where the strength and stiffness eccentricity vary substantially and where significant strength reductions are allowed. The elastic analysis needs to be modified at high Ω to give the designer meaningful information for the displacement demand on the stiff-edge.

Despite the large variation in strength allocated to the flexible-edge between the various design approaches at low Ω, the resulting flexible-edge displacements of the 2 second models are all quite similar. In fact, the *Dyn+T1* method requires the lowest strength increase for the flexible element in all cases and frequently produced the lowest displacements on the flexible-edge. Displacement demand, in particular for the 2 second systems, is relatively insensitive to the design method implemented for determining strength distribution.

The nonlinear response of the symmetric TB models for the systems with $T_y = 2$ seconds is consistently greater than that of the TB elastic models. This implies that the equal displacement rule may not hold for asymmetric structures with high lateral periods. Further study is required to expand upon this for structures with lateral periods greater than 2 seconds.

To assess the ability of the various elastic design approaches to conservatively estimate inelastic displacements, Figures 7.3, 7.4 and 7.5 display the predicted elastic displacements by the Humar/Kumar method (*H/K elast*), the NBCC quasi static method (*NBC elast*), the dynamic response spectrum analysis combined with statically applied torsional moments of $0.1b$ (*Dyn+T1 elast*), and $0.05b$ (*Dyn+T05 elast*), and the dynamic response spectrum analysis with CM shifted $0.05b$ (*DynCM±0.05b elast*), with the elastic and nonlinear time history analysis average peak displacements for the three methods of determining element strengths

(*Dyn+T1 THnonlin, NBC THnonlin,* and *H/K THnonlin*). The TB results are omitted for clarity.

The dynamic response spectrum analysis with shifted CM (*DynCM0.05b elast*) most accurately predicts the nonlinear displacements for the flexible-edge elements of the asymmetric buildings over the range of frequency ratios examined. Also the *DynCM0.05b elast* closely follows the trend of the TU elastic time history (*THelast*) analysis results. All elastic methods excessively overestimate flexible-edge average peak displacements for torsionally flexible buildings with the *NBC* and *H/K* method being the most conservative. The dynamic response spectrum analyses results, with statically applied torsional moments of $0.1b$ and $0.05b$, generally lie in-between the results from the static methods and dynamic response spectrum analyses with shifted CM. At high frequency ratio the response results are much closer together.

For the stiff-edge elements, again the elastic static methods give the highest predictions for peak displacement for the case when the eccentricity $e_s = 0.2b$. For an eccentricity of $e_s = 0.1b$, the *Dyn+T1 elast* results surpass those of the static methods except at high frequency ratio, Ω. Also for high Ω, most methods underestimate nonlinear stiff-edge element displacement. Only the *NBC* static method gives consistently conservative estimates of inelastic displacement at high frequency ratio, Ω.

Based on the results of this study, the elastic methods do not provide a good method of adequately predicting nonlinear displacement response for stiff-edge elements. The stiff-edge element displacements would not govern the structure's drift limitations, therefore, this may

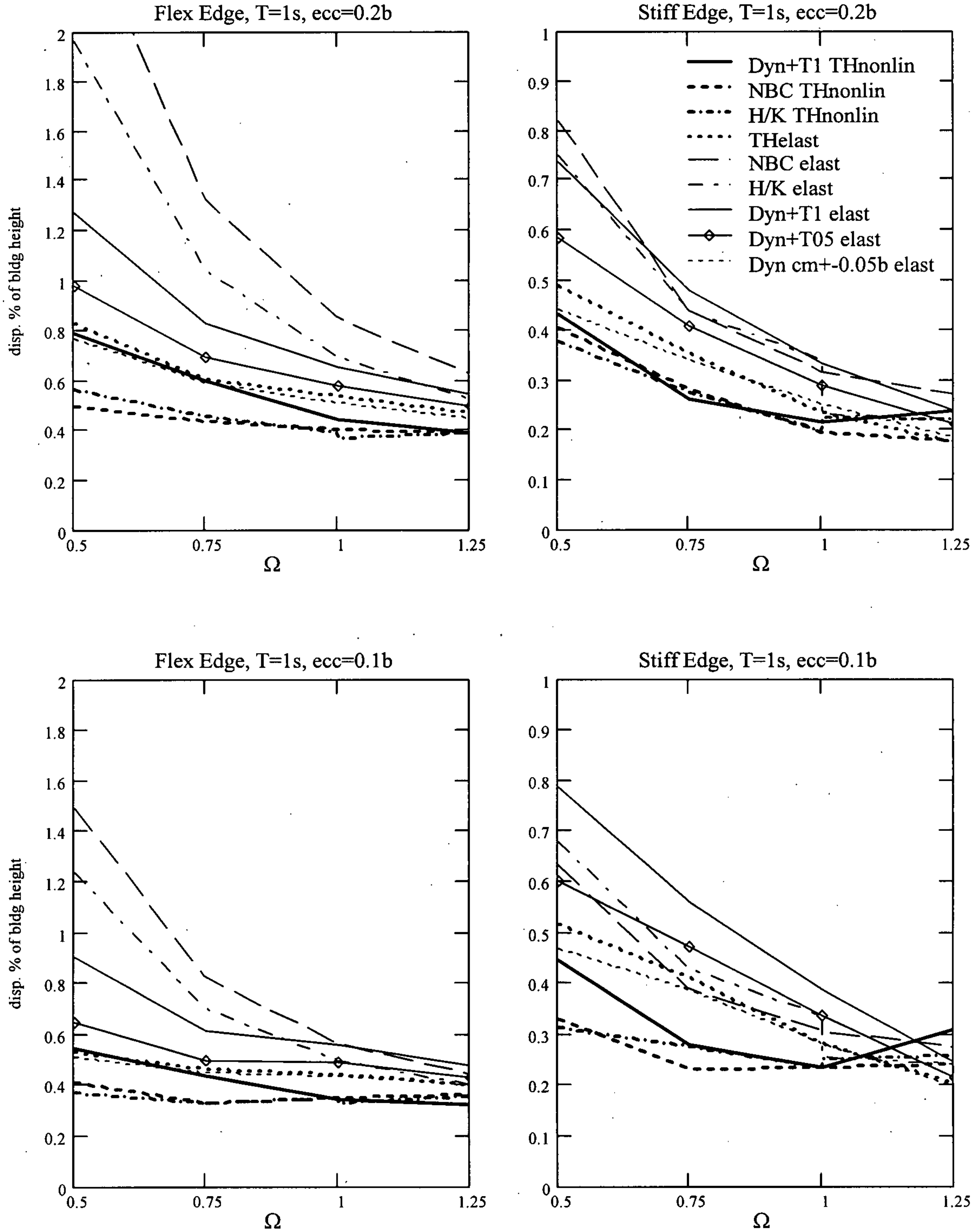

Figure 7.3 Nonlinear TH analyses and elastically predicted displacements, T_y = 1s

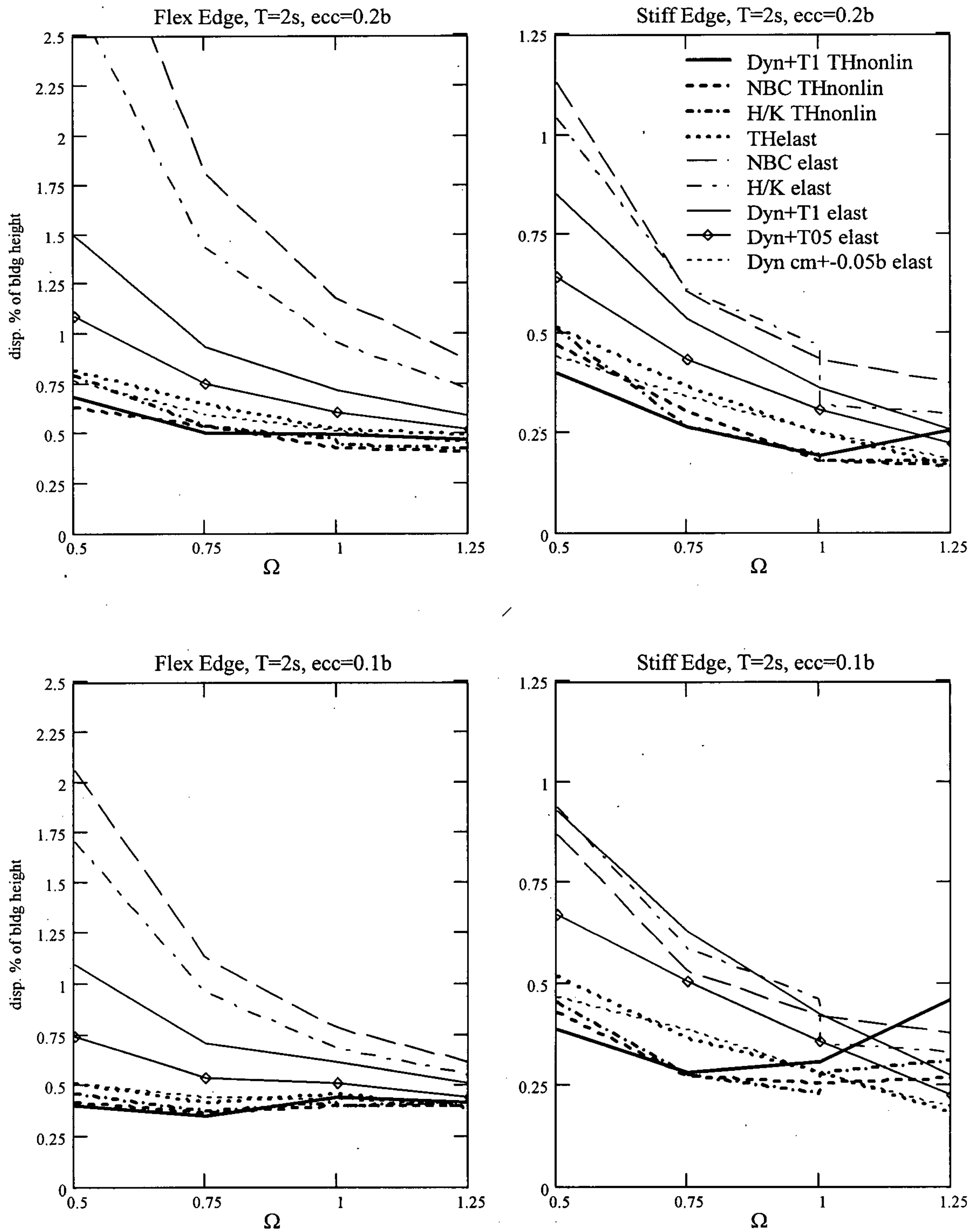

Figure 7.4 Nonlinear TH analyses and elastically predicted displacements, $T_y = 2$s

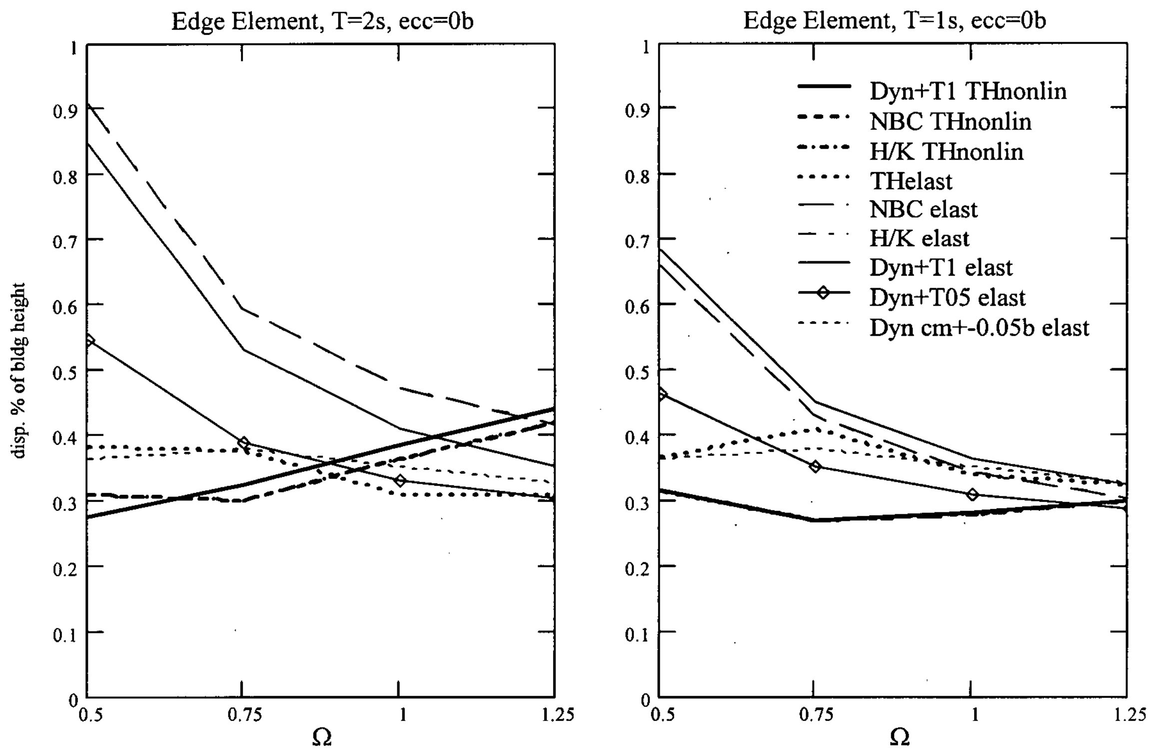

Figure 7.5 Nonlinear TH analyses and elastically predicted displacements - symmetric buildings.

not be critical. However, it is important to realize that the predicted elastic displacements are erroneous.

7.1.2 Peak Interstorey Displacements

The average peak interstorey displacements are shown in Figures 7.6 and 7.7. As found with peak displacements, the peak interstorey displacements generally increase as Ω decreases except for the nonlinear response of the symmetric systems with a lateral period, T_y of 2 seconds, where the interstorey displacements increase with increasing Ω. With these models the effects of accidental eccentricity are greater at large Ω, which is contrary to the TU elastic

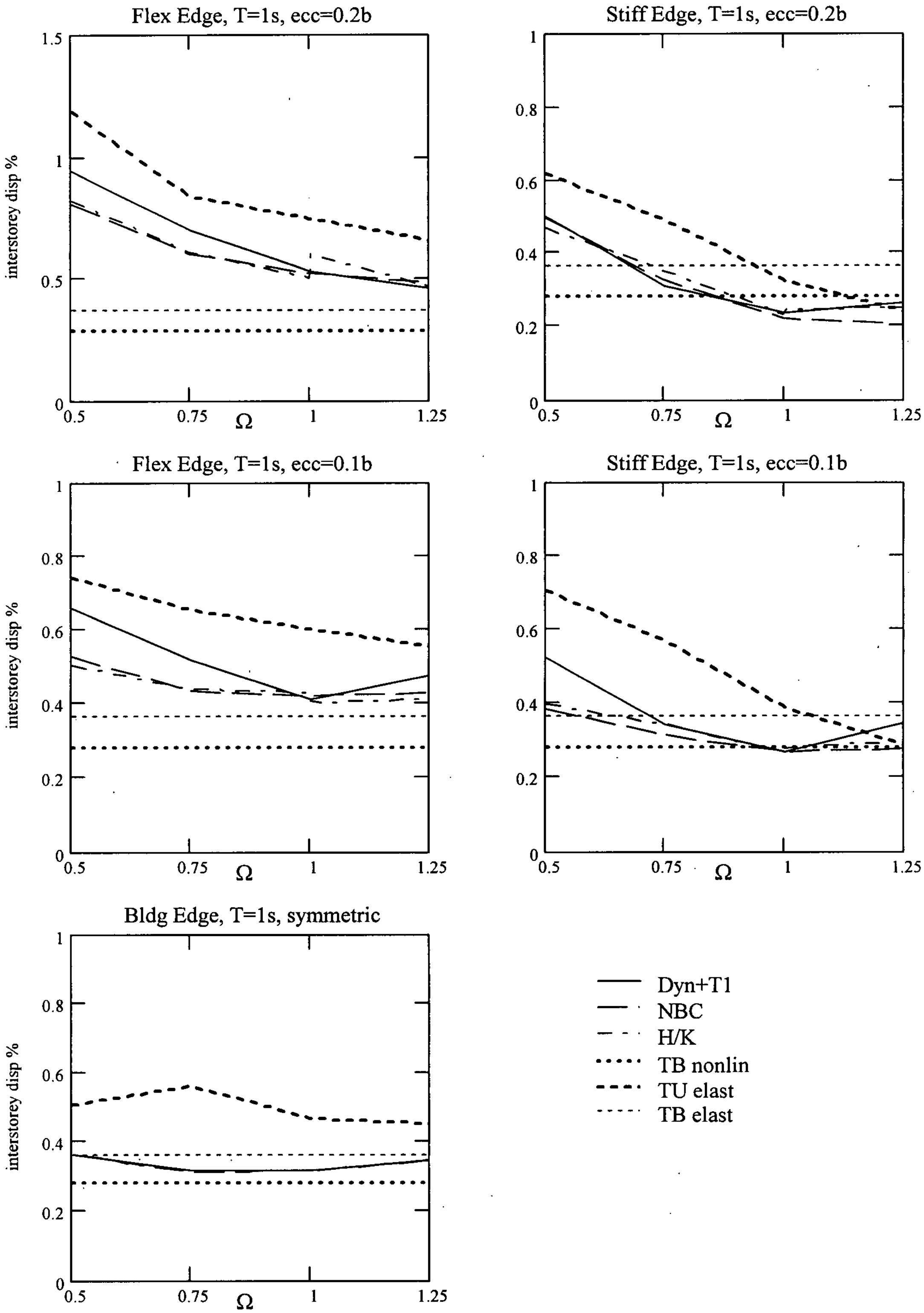

Figure 7.6 Avg. peak interstorey displacement in % vs. freq. ratio, Ω, T_y = 1s, for TH analyses.

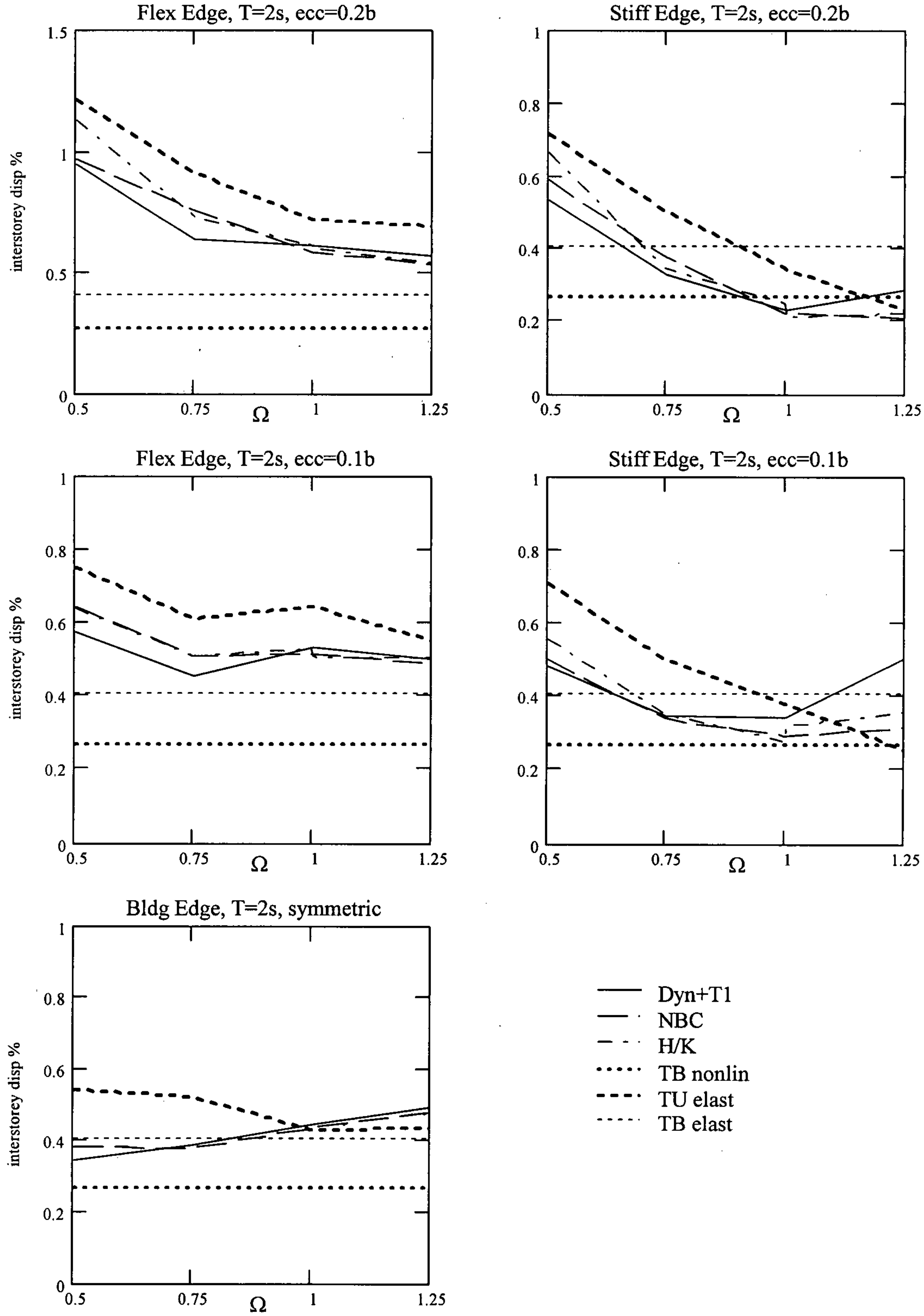

Figure 7.7 Avg. peak interstorey displacement in % vs. freq. ratio, Ω, $T_y = 2\text{s}$, for TH analyses.

time history predictions. The symmetric system with a lateral period of 1 second exhibits a relatively constant response over the range of Ω studied.

The elastic TU response values for interstorey displacement are generally greater than those of the nonlinear with the exception of the stiff-edge element for $e_s = 0.1b$ at $\Omega = 1.25$ for both lateral periods and $e_s = 0.2b$ at $\Omega = 1.25$ for $T_y = 2$ seconds. The *Dyn+T1* systems typically exhibit the largest response at $\Omega = 1.25$. As described for peak displacements, this could be partially due to the fact that the strength of the stiff wall element for *Dyn+T1* systems falls below that of the TB system, and all other systems, at this frequency ratio.

The inelastic response of the *Dyn+T1* systems for a lateral period of 1 second is generally greater than for the other design methods especially for the flexible wall at low Ω. This does not hold when the lateral period increases to 2 seconds which indicates that the increased strength allocated to the flexible walls for low Ω by both static methods, *NBC* and *H/K*, does not guarantee decreased interstorey displacements with higher periods. This indicates that the interstorey displacement at higher periods is relatively independent of the design method implemented to determine element strength. At low Ω, the variation in strength allocated to the stiff wall elements between the various design methods is not as great as it is for the flexible wall elements and, in suit, the response results for the flexible wall elements are more widely spaced than for the stiff wall elements. The strength of the stiff wall element is the lowest for the *Dyn+T1* systems at $\Omega = 1.25$ and the nonlinear response of the stiff-edge is consistently the greatest for these systems. The interstorey displacements all fall below the maximum allowable 2% of the storey height. Only on the flexible-edge, for an eccentricity of $0.2b$, do the response values surpass 1% of the storey height. Typically the flexible-edge interstorey displacements are greater than those of the stiff-edge.

Although the elastic estimates are mostly conservative for the peak interstorey displacements which occur in the top storey of the building, the interstorey displacement distribution response up the height of the building is not as consistent. For the lower storeys the elastic predictions may fall far below those exhibited in the nonlinear analysis. An example of a typical distribution of interstorey displacements up the height a 10 storey building is shown in Figure 7.8 for $T_y = 1$ second, $e_s = 0.2b$, $\Omega = 1.0$, and the *Dyn+T1* strength distribution. The

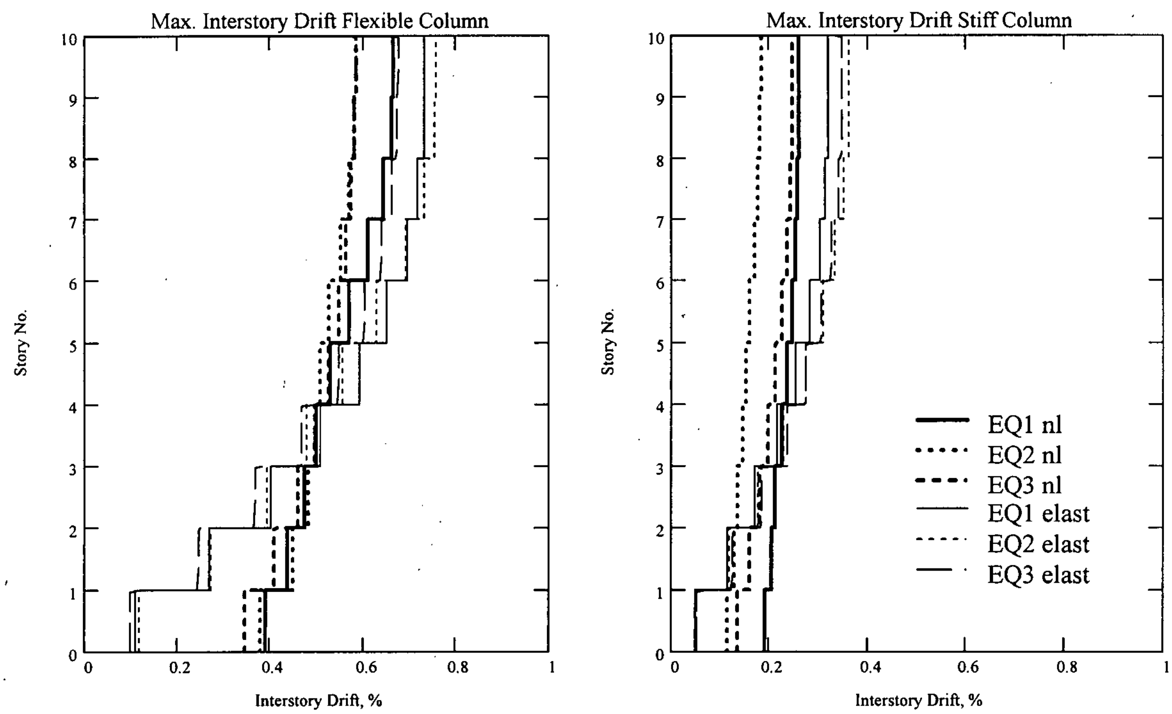

Figure 7.8 Interstorey displacement distribution $T_y = 1$s, $e_s = 0.2b$, $\Omega = 1.0$ for *Dyn+T1*, elastic and nonlinear time history analyses

elastic predictions substantially under-estimate the interstorey displacement experienced in the lower stories of the flexible wall. This was seen typically for all systems of this study and is to be expected since no rotation occurs at the base of the walls for the elastic systems. An example of the spread between the time history response to the three earthquake records can also be seen in this plot for both the elastic and nonlinear response. There is reasonable spread between the responses and it is interesting to note that the earthquake that induced the greatest response for the inelastic system is not the same as that for the elastic system.

7.2 Displacement Ductility

In many of the previous studies, the displacement ductility ratio at the building stiff- and flexible-edges has been utilized as one of the primary means of quantifying the effects of torsion. Typically the ratio of the TU to TB displacement ductility is used to measure the increase in response due to the effects of torsion of a TU system over an equivalent but TB system. The ability to limit ductility demand has also been adopted as a means of evaluating the effectiveness of current code torsional provisions. In this study the displacement ductility response values are displayed in one plot together with the TB values to observe which systems are critical. Since a force reduction factor of R = 4 was used consistently for this study, a displacement ductility $\mu_\Delta > 4$ would be considered excessive. The method of calculating displacement ductility used in this study is discussed in Section 6.4.

Plots of the peak average displacement ductility response, μ_Δ, of the systems subjected to the three earthquakes are displayed in Figures 7.9 and 7.10. For buildings with a lateral period T_y = 1 second the displacement ductility is less than 4 for all but the stiff-edge at $\Omega = 1.25$, where μ_Δ is a high as 6 for the *Dyn+T1* system and near 5 for both the *H/K* and *NBC* systems. The

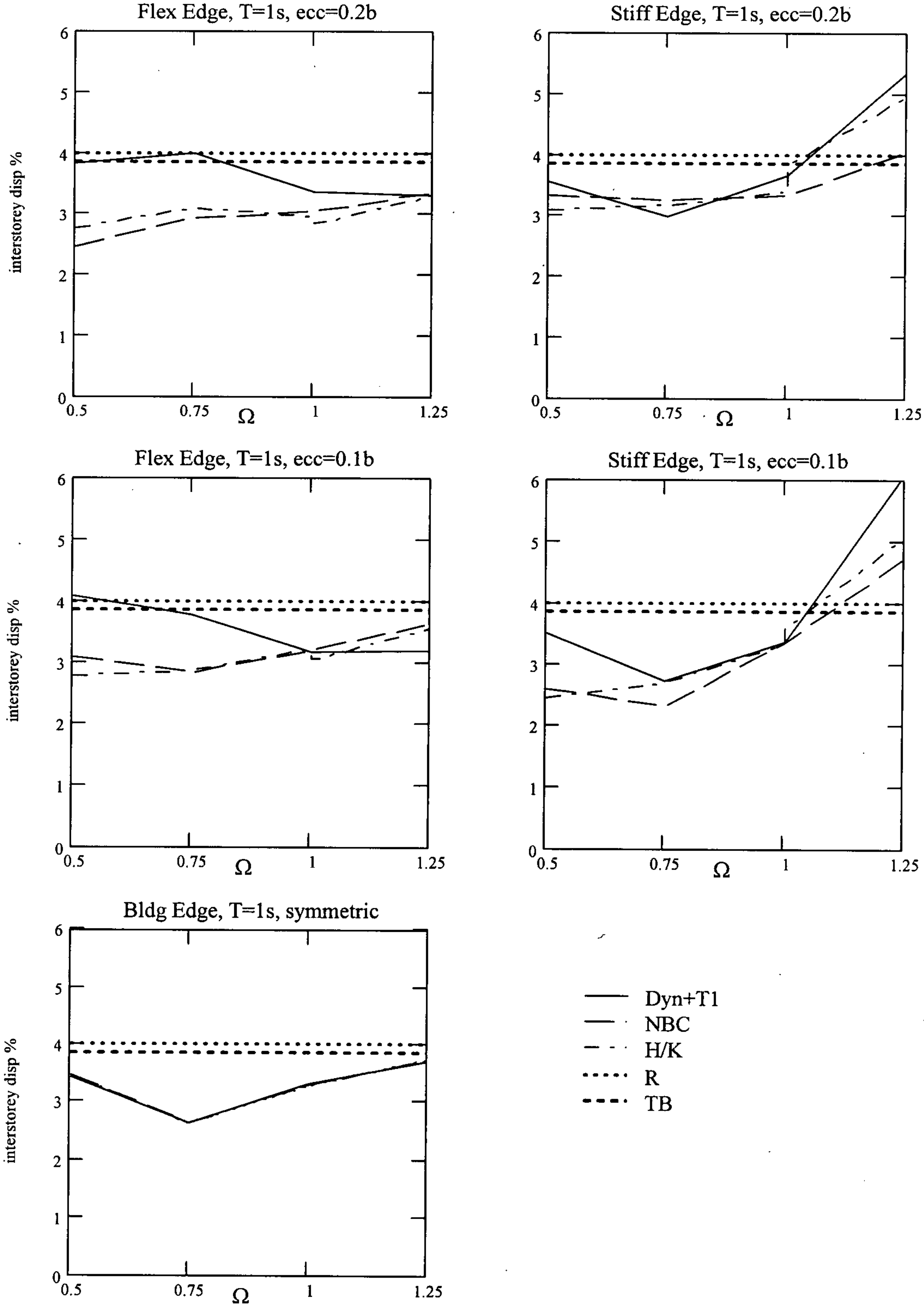

Figure 7.9 Peak average displacement ductility, $T_y = 1$ second

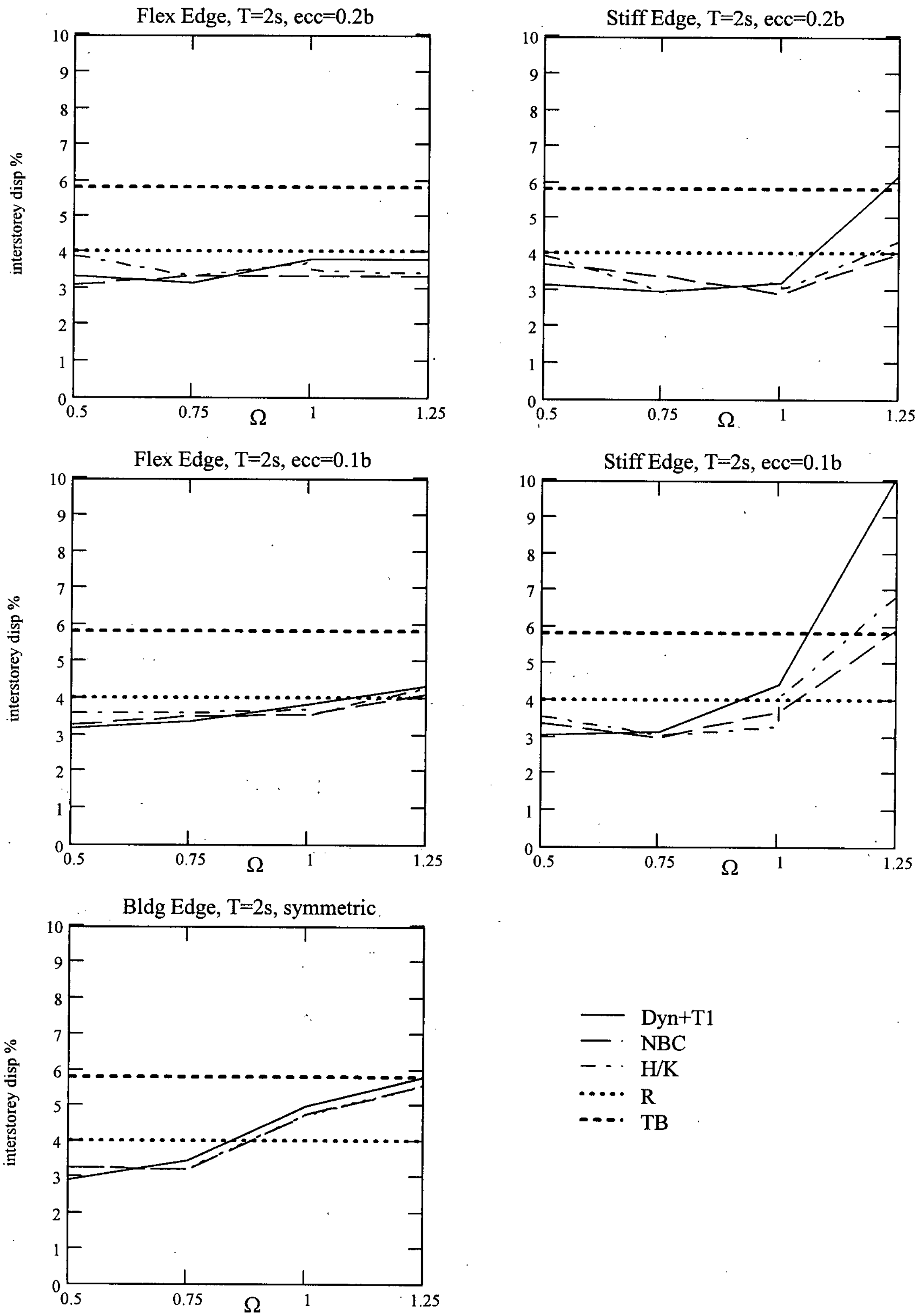

Figure 7.10 Peak average displacement ductility, $T_y = 2$ seconds

TB systems exhibit a displacement ductility very close to the design target R = 4. The *Dyn+T1* system, for $T_y = 1$ second, typically exhibits the largest displacement ductility at low frequency ratio Ω for the flexible-edge and at high Ω for the stiff-edge of all systems.

The buildings with a lateral period of $T_y = 2$ seconds exhibit an average peak displacement ductility values near to the target design value of 4 for all but the stiff-edge and the symmetric system in the high frequency ratio range. The maximum value of displacement ductility of the stiff-edge at $\Omega = 1.25$ reaches as high as 10 for $e_s = 0.1b$ for the *Dyn+T1* system, and approximately 6 for the *H/K* and *NBC* systems. Displacement ductilities of 6 are also exhibited for $e_s = 0.2b$ and the symmetric system for all design methods. The TB systems produce a displacement ductility of just below 6 which is 50% greater than the target value of 4. In the $T_y = 2$ sec. buildings, the ratio of torsionally unbalanced to torsionally balanced displacement ductility, $\mu_{\Delta TU}/\mu_{\Delta TB}$, would give deceptively good values except where $\mu_{\Delta TU}$ exceeds 6. For this reason the actual values of displacement ductility were displayed rather than the ratio which is typical of previous studies (Humar, 1998; Wong & Tso, 1995; De La Llera & Chopra, 1994a-e).

Contrary to what is expected, the stiff-edge exhibits the largest values of displacement ductility. Similar results were found in a study by Kumar (1998) for slightly irregular multistorey frame buildings. The large values of μ_Δ for $\Omega = 1.25$ could be partially due to the large variation between the stiffness and strength eccentricities of the elastic and inelastic models as discussed earlier for displacement response (Tso & Ying, 1992). The largest difference between stiffness and strength eccentricity at $\Omega = 1.25$ occurs for the $T_y = 2$ second system with a stiffness eccentricity $e_s = 0.1b$. This system also exhibits the largest displacement ductility response. Some contribution could be due to the large reduction in strength allowed for the stiff-edge elements at high Ω, below that of an equivalent TB system, especially for the *Dyn+T1* design method. If the strength reduction of the stiff-edge elements was limited to that of an equivalent TB system the difference between the stiffness and strength eccentricity would also decrease. However, this would not provide a solution for a symmetric system where only accidental eccentricity induces torsional response.

Again, as found for displacement and interstorey displacement response, the displacement ductility response of the symmetric systems is not consistent with results of previous studies by De La Llera and Chopra (1994a & c, 1995) where they found that the normalized response of nominally symmetric, single storey buildings to accidental torsion were essentially insensitive to variations in uncoupled lateral period. As found for inelastic displacements, the displacement ductility response for the systems with a lateral period of 1 second gives results similar to those found by De La Llera and Chopra, however, for the systems with a lateral period of 2 seconds, the nonlinear response increases with increasing Ω.

Structures exhibiting large displacement ductility could undergo significantly higher displacements than would be predicted by an elastic analysis and could possibly experience major damage during strong motion excitation if not accounted for in the design. For these systems, the existing elastic analysis techniques do not adequately restrict the nonlinear displacement ductility response. In order to limit displacement ductility demand for a symmetric system with a lateral period $T_y > 1$ second, additional element strength is required for $\Omega > 1$ or an appropriate scaling factor needs to be applied to the results of the elastic analysis to better estimate the nonlinear response.

7.3 Rotational Ductility

The most desirable source of inelastic deformation is rotation in the designated potential plastic hinge regions. Rotational ductility, μ_θ, is an elemental property which gives a good indication of the amount of rotational demand on an element when subjected to intense ground motion. Prior to yielding, the base of the wall element does not rotate since it is considered to be fixed at the base. The yield rotation is determined empirically from the peak recorded elastic displacement. When the wall element yields, a plastic hinge forms at the base about which the wall begins to rotate. The intent of design is to limit the ductility demand on the elements so as not to exceed the ductility capacity. The rotational ductility, μ_θ, was determined as described in section 6.4 Response Parameters. The program CANNY-E outputs the total plastic rotation for each end of the elements enabling simple determination of this parameter. Plots of the peak average rotational ductility experienced by the systems of this study subjected to the three earthquakes are displayed in Figures 7.11 and 7.12.

The rotational ductility demand is below the target design ductility of 4 for all but the stiff wall element of the torsionally stiff systems in the high frequency ratio range ($\Omega > 1$). The response follows the same trend as seen for displacement ductility demand as expected. Again the rotational ductility is largest for the $T_y = 2$ second system with an static stiffness eccentricity of $e_s = 0.1b$, reaching a magnitude of just over 8. As described previously, this is possibly due to the difference between the stiffness and strength eccentricity, which is also the greatest for

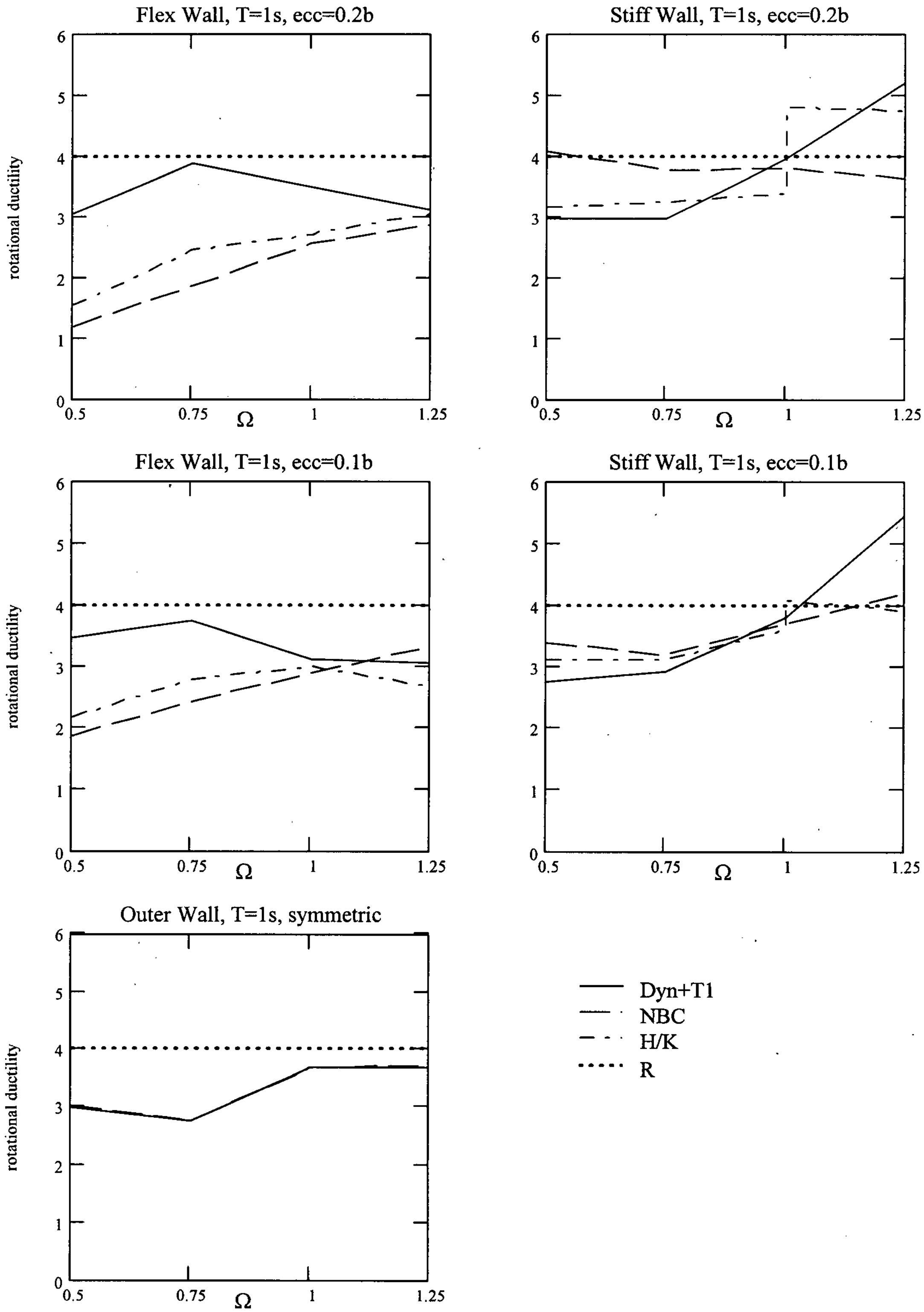

Figure 7.11 Rotational ductility, $T_y = 1$ second.

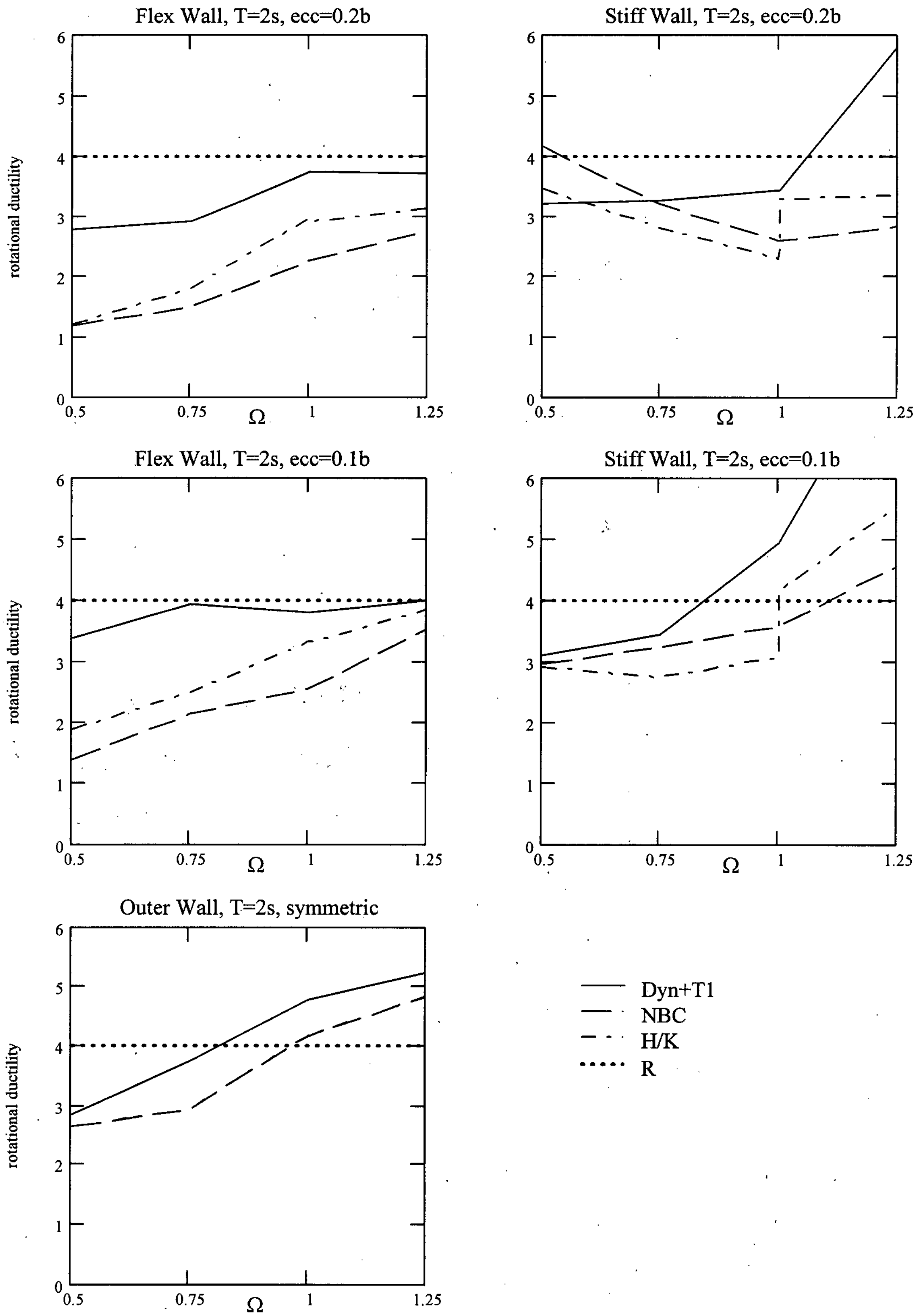

Figure 7.12 Rotational ductility, $T_y = 2$ seconds.

this system, and the inability of the elastic analysis to account for this variation. The strength eccentricity approaches zero at $\Omega = 1.25$ for all examined methods of determining element strength.

The strength reduction of the stiff-edge element for the *Dyn+T1* method falls below that of the equivalent TB system for $\Omega = 1.25$. Because of this, the *Dyn+T1* systems could yield earlier and undergo larger rotations than would predicted by the elastic analysis causing the ductility values to increase above the desired target value of 4. The calculated elastic rotation would be very small for the stiff wall element based on the stiffness distribution. If the strength distribution varies significantly from the stiffness distribution and the stiff-edge element strength is substantially reduced, then the measured inelastic rotations will be larger than for a TB system with strengths distributed proportional to element stiffness. The resulting large ductility values do not necessarily indicate that the plastic rotations would be excessively large, but rather that the elastic TU analysis is incapable of giving accurate predictions of the plastic rotations for systems where the strength and stiffness eccentricity vary substantially, and where the stiff-edge element strength is reduced below that of an equivalent TB system. For these systems an elastic analysis would not give the designer meaningful information for the rotational ductility demand of the stiff wall element.

For the symmetric systems, which are influenced only by the effects of accidental eccentricity, the rotational ductility is below the target ductility for the 1 second systems, but exceeds it for the 2 second systems with large Ω. The static eccentricity is zero in a symmetric system, therefore, both walls will maintain the same strength and the strength eccentricity will also be zero. The wall strengths are increased to account only for accidental eccentricity with the increase in strength being the largest for small Ω. Figure 7.2 shows that edge displacements are small for the $\Omega = 0.5$ symmetric model, thus the wall displacements are small and when combined with stronger walls gives a lower ductility demand. For $\Omega = 1.25$ the walls are not as strong and the displacements are greater, resulting in a larger ductility demand. Referring back to Figure 5.6 for $T_y = 2$ seconds, it is clear that the *Dyn+T1* symmetric system requires the lowest strength increase over the range of Ω studied. The displacements of the wall in the symmetric case are all very close and so it is the smaller strength that and smaller yield rotation that accounts for the larger rotational ductility displayed in the bottom graph of Figure 7.12. Again these results for the two periods studied contradict those found by De La Llera and Chopra (1994a & c, 1995).

The apparent control of rotational ductility for the flexible wall is due to the large increase in element strength on the flexible side, to the extent where in some cases the walls remain essentially elastic and undergo minimal plastic rotation. As seen in Figures 7.13, and 7.14 at low frequency ratio, the stiff wall could experience much larger plastic rotations than the flexible wall, dependent upon the allocation of strength or flexural capacity. It is evident that the flexible walls for both the *H/K* and *NBC* methods of design undergo much lower plastic rotations than for the *Dyn+T1* method and remain virtually elastic at low frequency ratio for high eccentricity. In comparison the stiff walls experience much larger plastic rotations at low frequency for the *H/K* and *NBC* methods. For the *Dyn+T1* method the flexible and stiff walls experience similar plastic rotation at low frequency ratio, but in general, the rotation increases with increase in frequency ratio. A desirable condition would be to maintain a similar

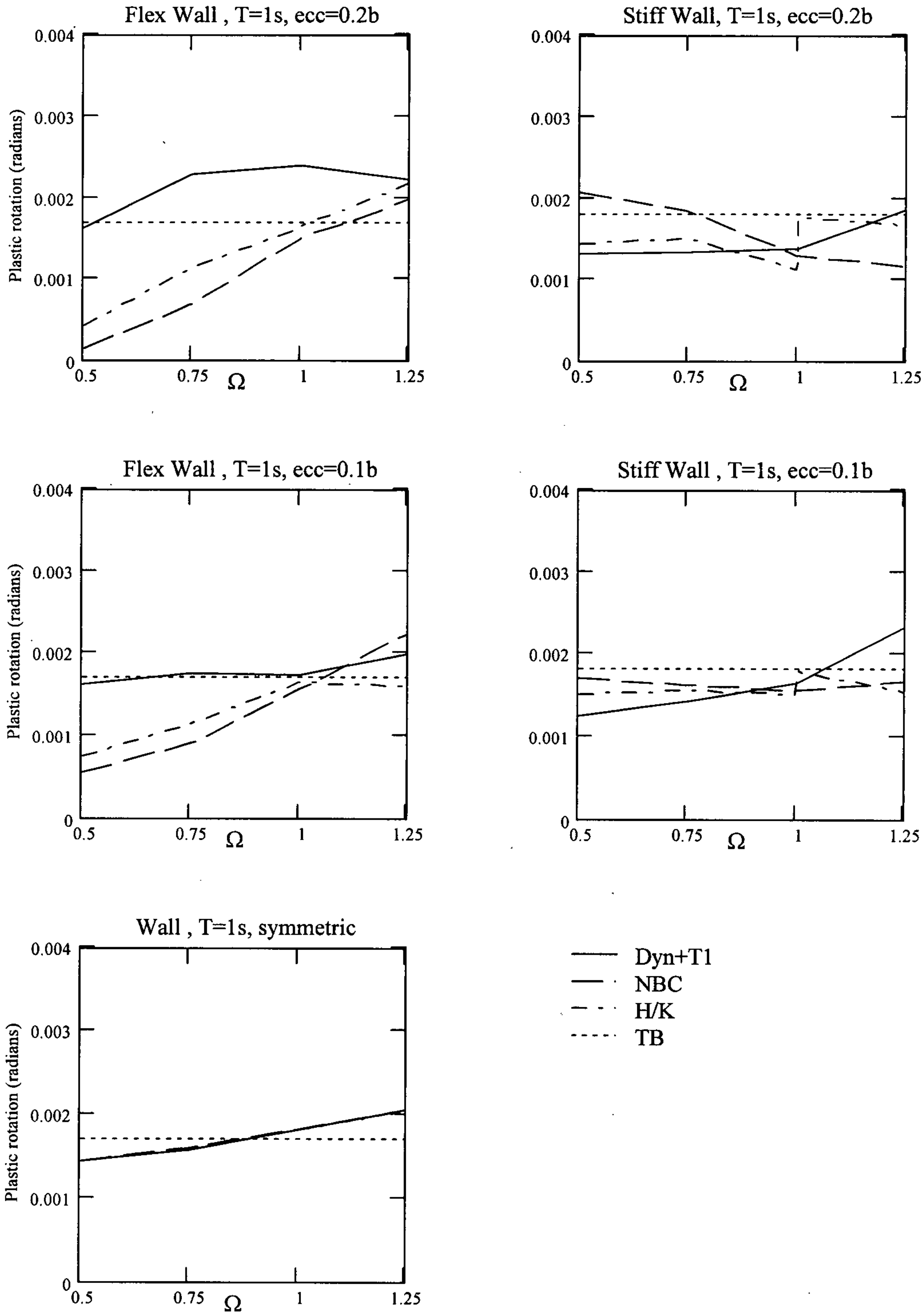

Figure 7.13 Plastic rotation in radians of lateral resisting wall elements, $T_y = 1$ second

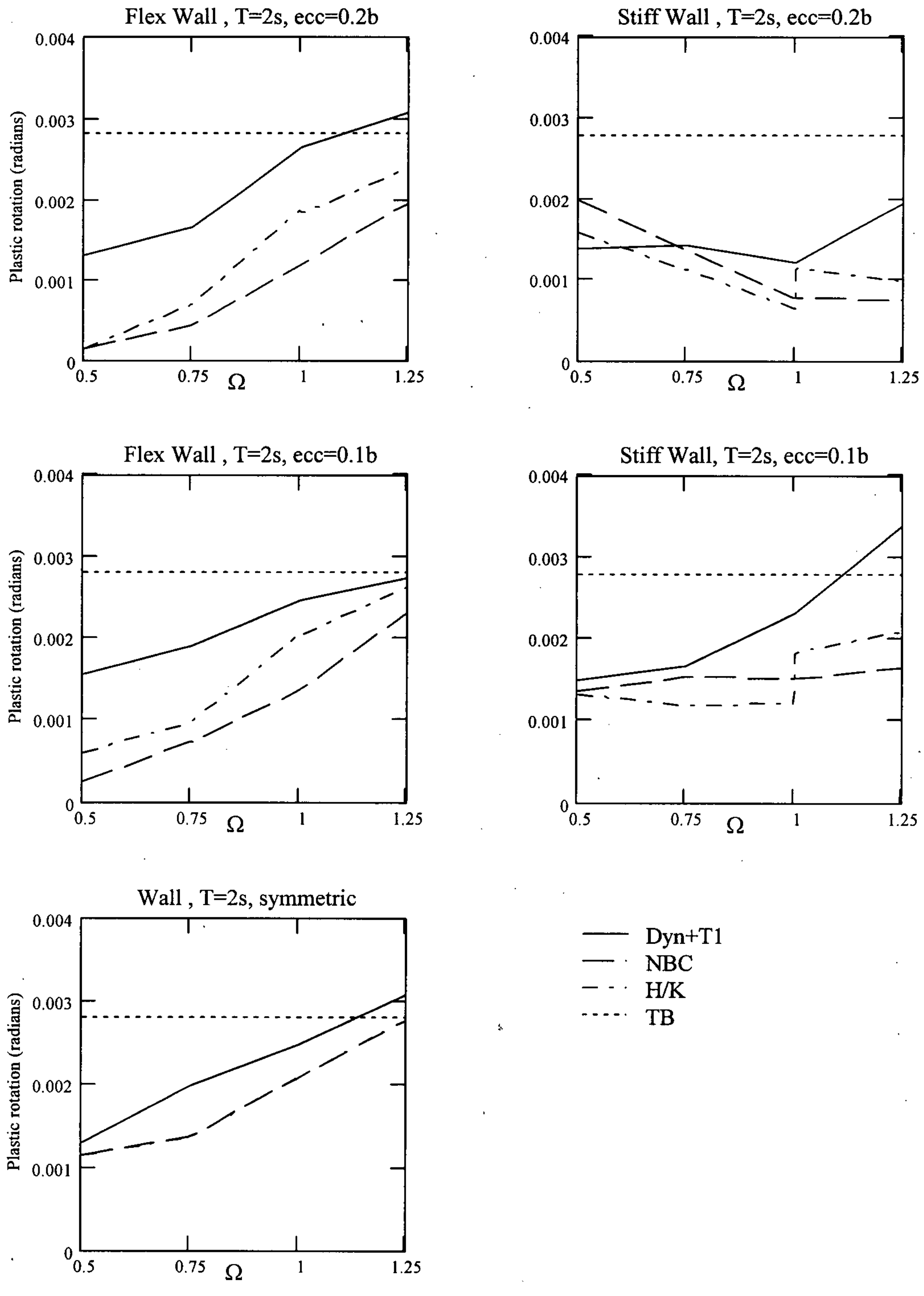

Figure 7.14 Plastic rotation in radians of lateral resisting wall elements, $T_y = 2$ seconds

rotational ductility for both walls over the range of frequency ratios.

In previous research it has been established and generally accepted that adequate torsional design provisions should limit the displacement and rotational ductility response of asymmetric structures to that of an equivalent TB structure. This is essentially attained for the 2 second buildings except for some cases at high frequency ratio for the *Dyn+T1* method. For the flexible wall of the 1 second buildings the TB rotations are exceeded at high frequency ratio for all methods studied but the TB rotational ductility is not exceeded. Curvature ductility and strains also need to be checked to ensure that they are within the acceptable limitations for each wall element. These are properties of the element section, however, and must be checked for each individual wall configuration which was considered beyond the scope of this project.

To get meaningful estimations of ductility for the stiff wall elements, either a nonlinear analysis would be required to more accurately depict the true behaviour, or the strength reduction of the stiff element should be limited, perhaps to that of an equivalent TB system. It is desirable, however, to achieve a low value of strength eccentricity to limit the torsional coupling. This could be achieved by further increasing the flexible element strength, however, for flexible structures the flexible wall strength is already highly conservative and a further strength increase would not be desirable.

7.4 Moment Distribution

The typical bending moment distribution envelopes obtained from the nonlinear time history (TH) analyses vary significantly from those predicted by the elastic analyses, either the elastic

TH analysis, the dynamic RSA, *Dyn+T1*, or *NBC* and *H/K* elastic static analysis. The actual variation of moment demand is more linear or convex in form than that predicted by the elastic analyses. For this reason Paulay and Priestley (1992) recommend that the flexural moment resistance of cantilevered walls be not less than a linear variation from the base moment to zero up the height of the building. Examples of the moment envelopes found from the nonlinear TH analysis for the stiff and flexible walls are shown in Figures 7.16 and 7.16 for the *Dyn+T1* method, Figures 7.18 and 7.17 for the *NBC* method, and Figures 7.19 and 7.20 for the *H/K* method. They are normalized to the elastic element base moment found by the respective design method divided by the factor R.

The bending moment envelopes resulting from the nonlinear response to the 3 earthquakes often exceed even the linear variation of moment recommended by Paulay and Priestley (PP), indicated by the dash-dot line in the figures. Second mode effects are evident in the envelopes of the flexible walls mainly for EQ1 and EQ3 and in some cases for all three earthquakes, and are more pronounced for the buildings with $T_y = 2$ seconds. The flexible wall does not yield for the $\Omega = 0.5$ system designed using the *NBC* method for any of the earthquake records and for the $\Omega = 0.5$ system designed using the *H/K* method for EQ1 for $T_y = 2$ seconds, and for the $\Omega = 0.5$ system designed using the *NBC* method for EQ3 for $T_y = 1$ second. This is due to the large increase in flexible wall element strength required using these design approaches as indicated in Section 5.3 Strength Distribution.

To ensure that the plastic hinges develop only in the predetermined locations at the base of the walls, it is necessary to provide flexural strength over the remainder of the wall that is in excess

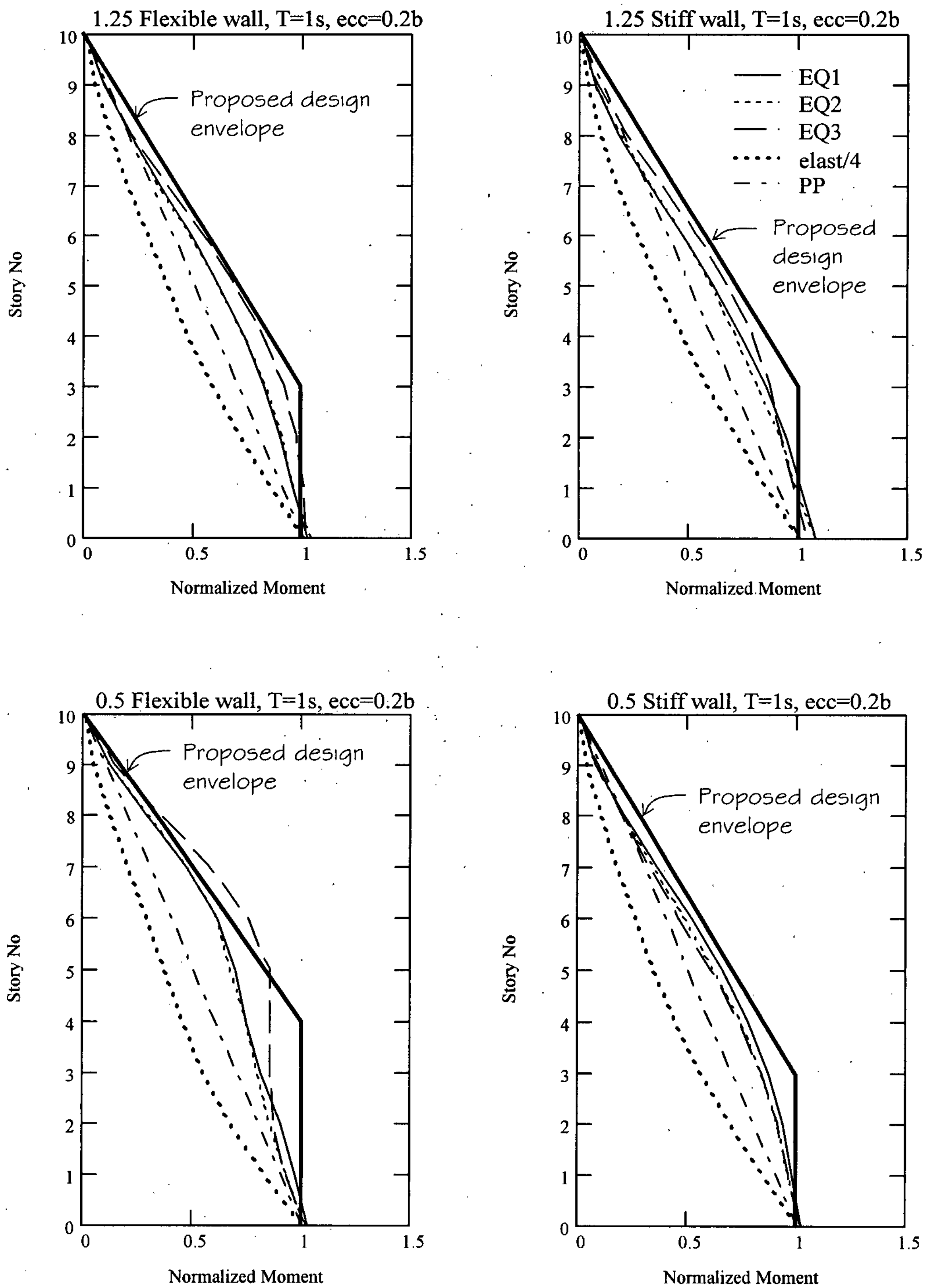

Figure 7.15 Normalized moment envelope of nonlinear TH analyses for *Dyn+T1* design method for $\Omega = 1.25$ (top) and $\Omega = 0.5$ (bottom) for $T_y = 1$ second and $e_s = 0.2b$

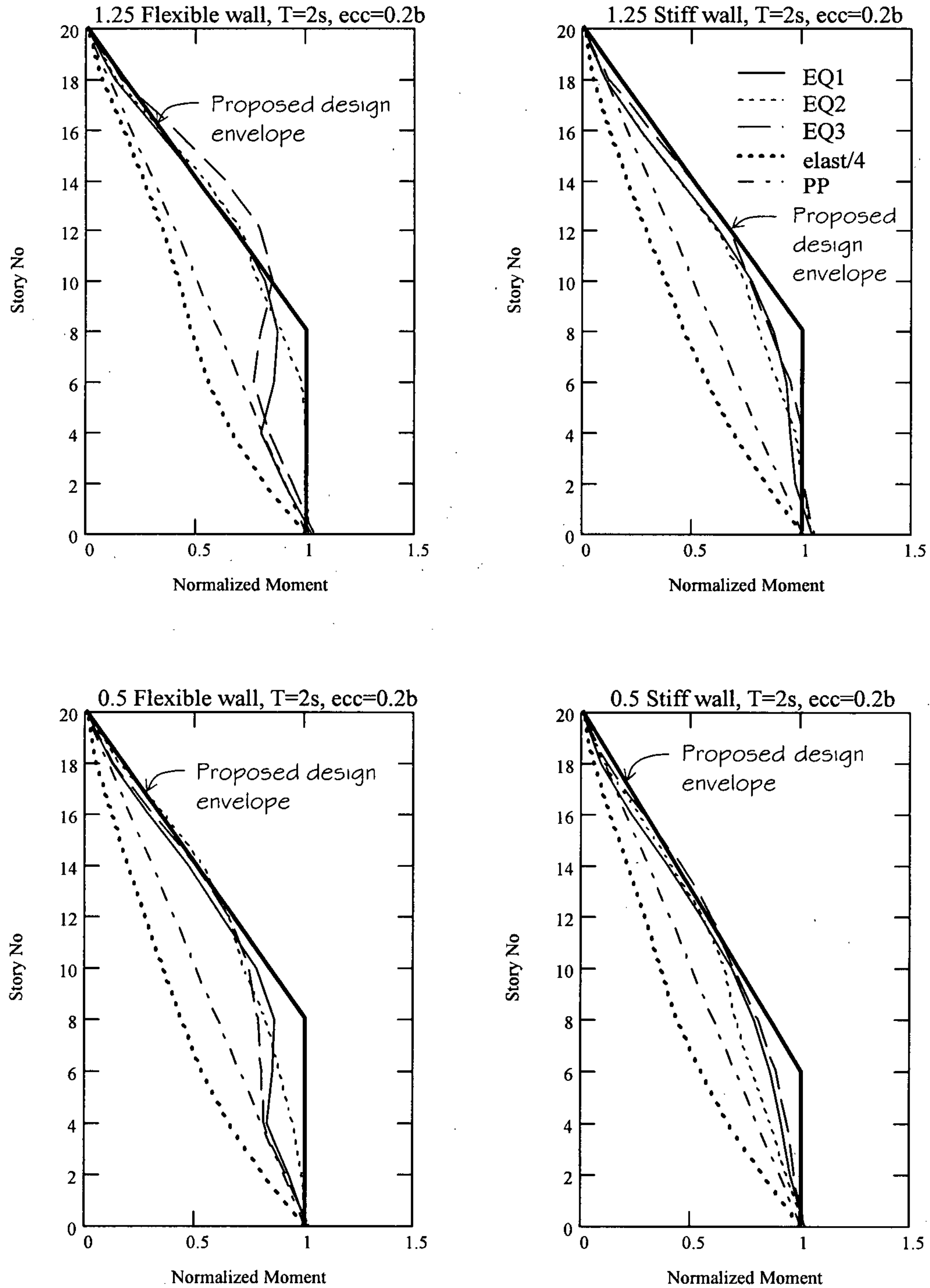

Figure 7.16 Normalized moment envelope of nonlinear TH analyses for *Dyn+T1* design method for $\Omega = 1.25$ (top) and $\Omega = 0.5$ (bottom) for $T_y = 2$ seconds and $e_s = 0.2b$

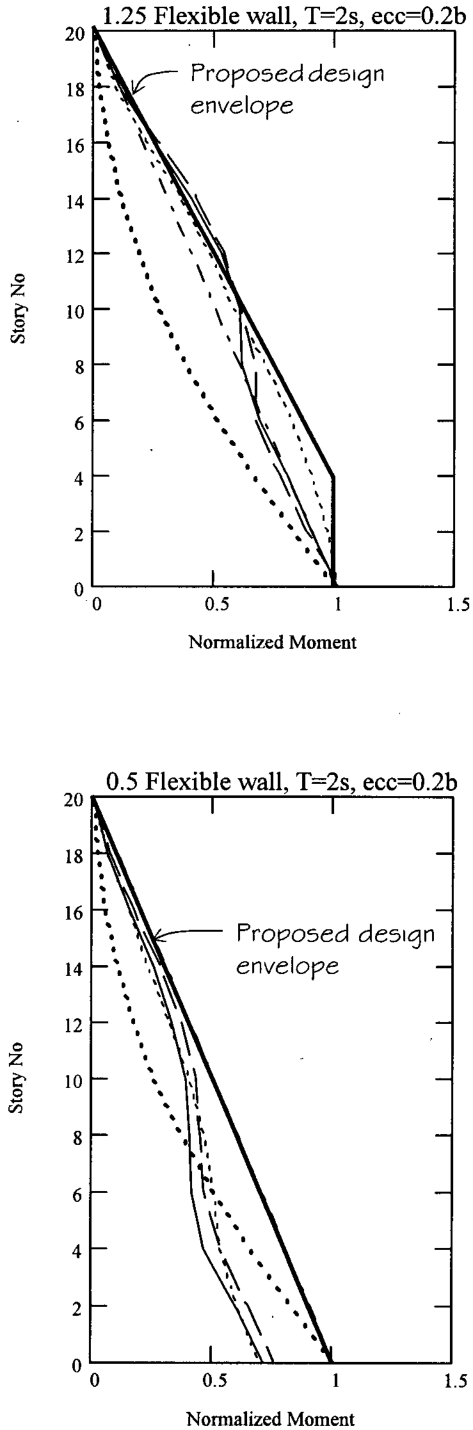

Figure 7.17 Normalized moment envelope of nonlinear TH analyses for *NBC* design method for $\Omega = 1.25$ (top) and $\Omega = 0.5$ (bottom) for $T_y = 2$ seconds and $e_s = 0.2b$

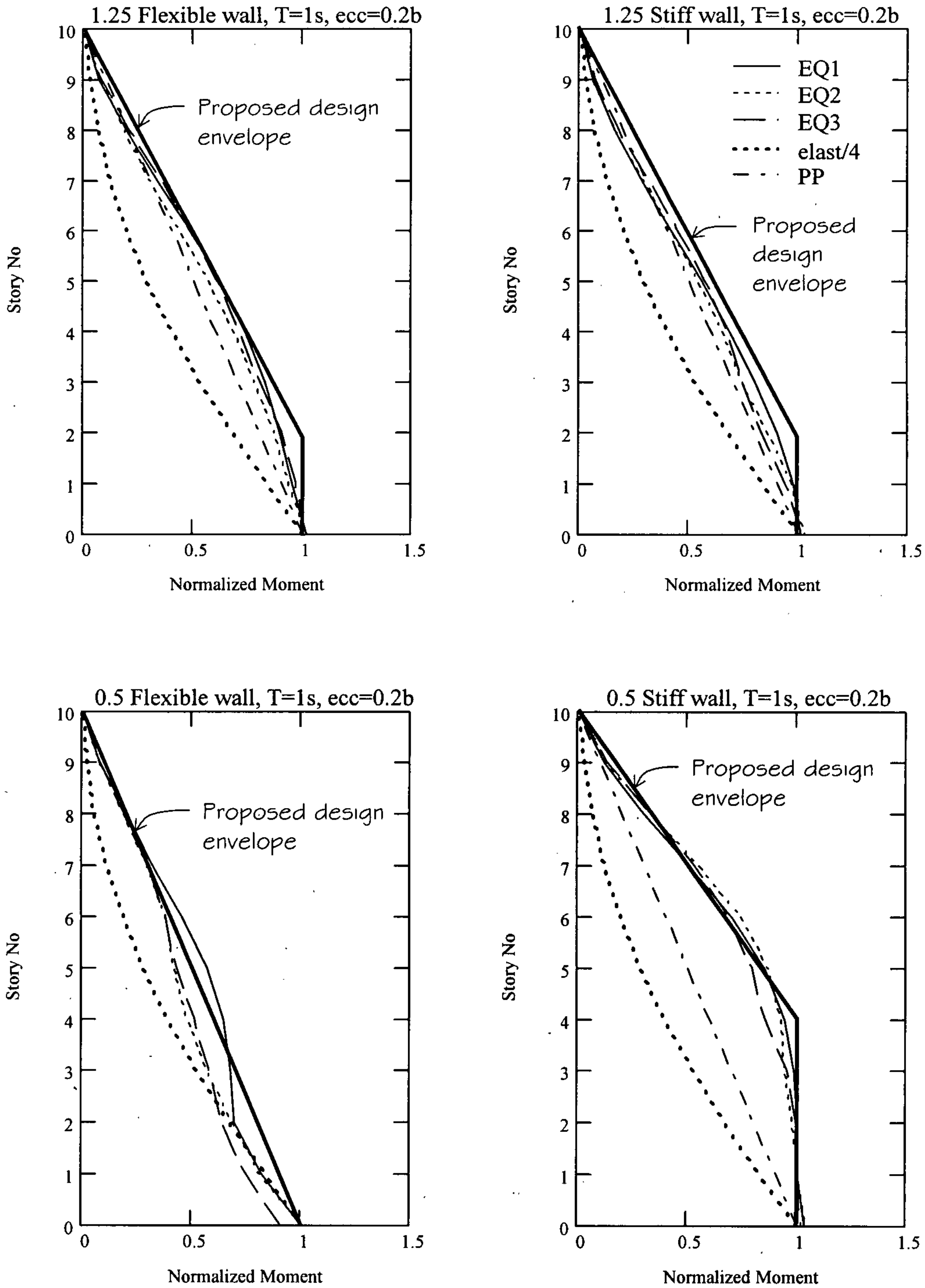

Figure 7.18 Normalized moment envelope of nonlinear TH analyses for *NBC* design method for $\Omega = 1.25$ (top) and $\Omega = 0.5$ (bottom) for $T_y = 1$ second and $e_s = 0.2b$

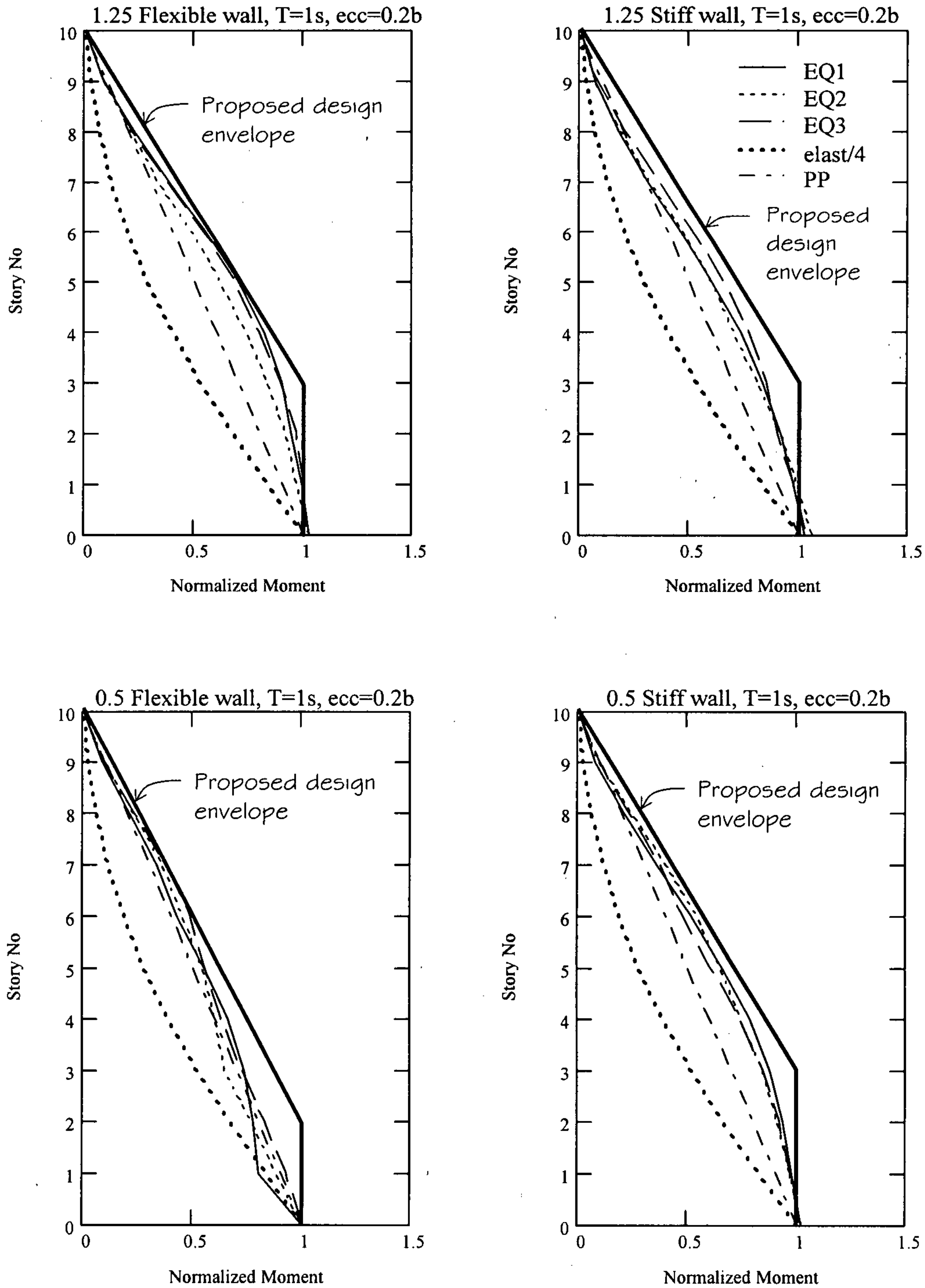

Figure 7.19 Normalized moment envelope of nonlinear TH analyses for *H/K* design method for $\Omega = 1.25$ (top) and $\Omega = 0.5$ (bottom) for $T_y = 1$ seconds and $e_s = 0.2b$

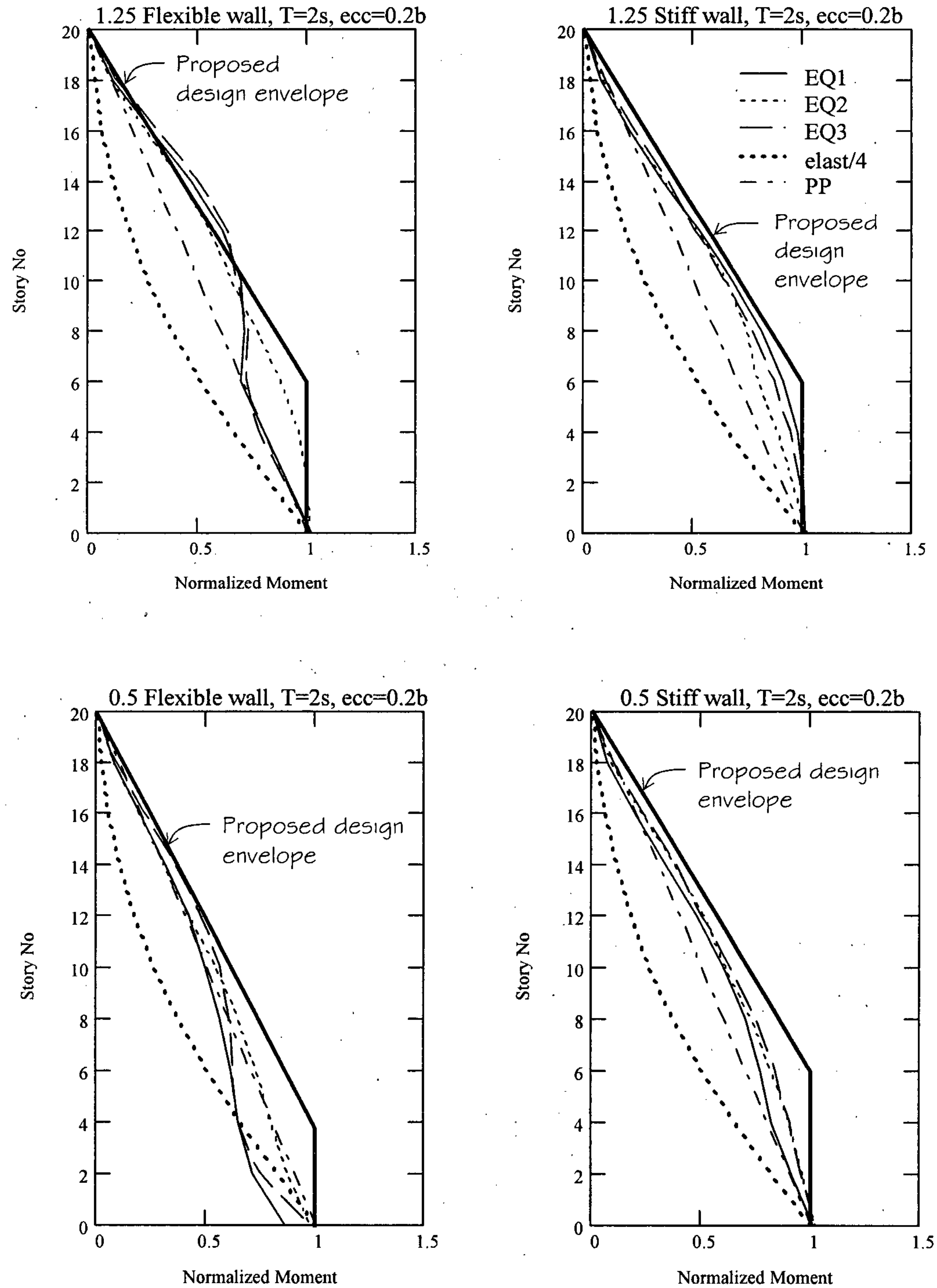

Figure 7.20 Normalized moment envelope of nonlinear TH analyses for *H/K* design method for $\Omega = 1.25$ (top) and $\Omega = 0.5$ (bottom) for $T_y = 2$ seconds and $e_s = 0.2b$

of the probable moment demand. Paulay and Priestley (1992) recommend that the cutoff for the flexural reinforcement be extended a minimum of the length of the wall, l_w, plus the development length, l_d, beyond the linear variation line of moment to account for the effects of the diagonal tension shift of the internal flexural tension forces which is assumed to be equal to the length of the wall, l_w. An increase in the envelope is required to take care of the excess moment demand due to higher mode effects up the height of the building displayed by the nonlinear dynamic response.

A proposed design moment envelope is shown on each plot indicated by the heavy continuous line. For systems designed based on a dynamic response spectrum analysis with statically applied torsional moments, *Dyn+T1*, the design base moment should be extended 30-40% up the height of the building, with a linear approximation continued from that point to the roof level. Systems design to the *NBC* static provisions require a similar envelope but with the base moment extended 20% up the height for a torsionally stiff building. For the torsionally flexible buildings, the base moment should be extended to 40% of the building height for the stiff walls, while the linear approximation proposed by Paulay and Priestley (1992) is adequate to account for the higher mode effects of the flexible walls. The flexible walls require such large strength increases for the torsionally flexible system that, when subjected to strong ground motion, in some instances they do not even yield.

7.5 Shear Response

7.5.1 Peak Base Shear

The desired mode of yield for the systems in this study is in flexure. Therefore, the wall elements need to possess sufficient strength in shear to sustain the maximum shear forces resulting from strong ground motion. As discussed in section 6.3 the magnitude of the dynamic magnification of shear forces is a concern for shear wall structures since at some instances during an earthquake the response of shear wall structures may be strongly influenced by the second and third modes of vibration. It was observed in the time history responses that the peak values of base shear occur virtually simultaneously to the peak moment response and large values may occur more than once over the duration of shaking.

The average normalized peak base shear from the nonlinear time history analysis, to the three ground motions, for each method of design are plotted in Figure 7.21. They are presented as the ratio of the nonlinear response to the perspective elastic design values. The elastic design value is taken as the peak base shear from the 3 methods used for determining wall strengths: the *Dyn+T1* analysis, the *NBC* static analysis or the *H/K* static analysis, divided by the force reduction factor of R = 4. As predicted, the nonlinear base shear response is significantly higher than the elastically estimated design values. Typically the magnification of nonlinear shear response is in the range of 1.3 to 2.3 times that of the elastic prediction. These values are even higher than the maximum of 1.8 proposed by Keintzel (1992) which has been adopted by the New Zealand reinforced concrete design code (Paulay & Priestley, 1992). The *NBC* method produces the lowest magnification for the flexible wall and highest for the stiff wall at

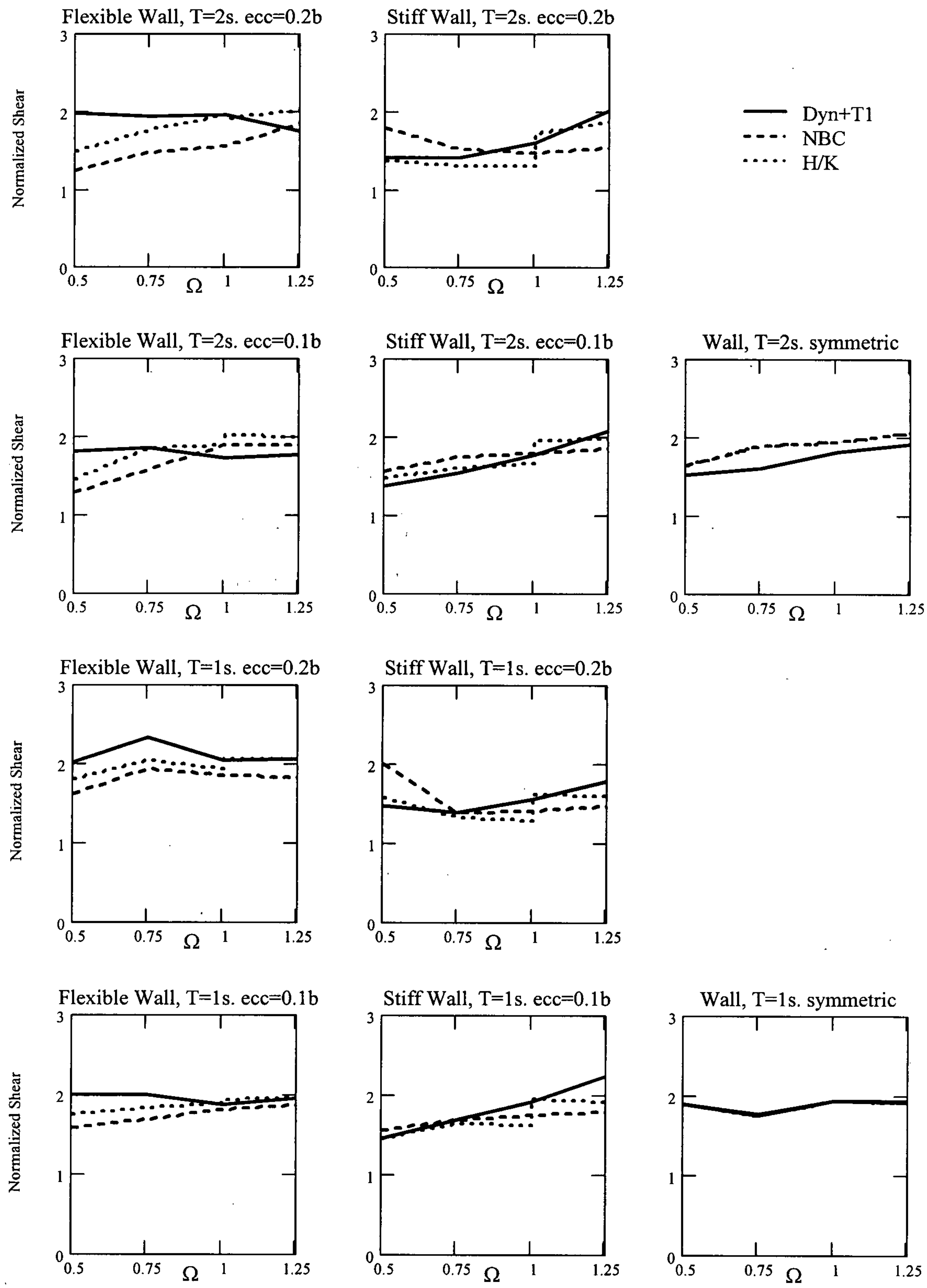

Figure 7.21 Average normalized peak shear for wall elements from TH analyses

low Ω. The opposite holds for the *Dyn+T1* method at low Ω. At high Ω the *Dyn+T1* method consistently experiences the highest magnification for all systems. An amplification factor of two covers most cases for all design methods.

For the structures of this study, according to the New Zealand Standard (NZS, 1992) formulas given in equations 5.1 and 5.3, the values for dynamic magnification of shear due to contributions from higher modes would be $1.3 + 10/30 = 1.63$ for the 10 storey buildings and $1.3 + 20/30 = 1.97 > 1.8 = 1.8$ for the 20 storey buildings. These values would be adjusted for the factored strength of steel and the J factor as specified in the CSA code, but since we are concerned only with the design and not the probable moment capacity in this study, no further adjustments are needed for comparison with the dynamic magnification results found here. The formulas in the NZS are based on a study by Keintzel (1992) on the nonlinear response of stick models over a range of periods. In his study, Keintzel found that the magnitude of shear magnification was a function of building height (or period) and increased with height due to the increase in contribution from higher modes. The results of our study indicate little correlation between building height, ranging from 10 to 20 stories, and magnitude of dynamic magnification of shear. In fact, in many instances higher amplification values were found for the shorter buildings with a lateral period of 1 second than for the taller, 2 second buildings. Also, the magnification appears to be independent of the torsional to lateral frequency ratio except for the stiff walls design using *Dyn+T1* method.

The values of shear magnification found in this study could be somewhat conservative since shear cracking and degradation were not accounted for in the analysis. Only flexural cracking and degradation were taken into consideration since the wall was designed to yield purely in flexure. Similar equations to those proposed by Keintzel (1992) need to be developed applicable to the Canadian code.

7.5.2 Shear Distribution

The distribution of shear up the height of the building does not follow that of the elastic prediction. Examples of the typical distribution of peak shear envelopes for the flexible and stiff walls subjected to the three strong motion records are shown in Figures 7.21and 7.23 for the *Dyn+T1* method, Figures 7.24and 7.25 for the *NBC* method, and Figures 7.27 for the *H/K* method. Higher mode effects are typically visible in the form of small shear near mid height and large shear forces in the upper and lower floors, particularly in buildings with high Ω. Due to the contribution from higher modes, the nonlinear shear forces of the upper stories can be more than double those predicted by elastic analysis regardless of the elastic method employed in determining wall strengths. The flexible wall element does not yield for three building configurations: the *NBC* $\Omega = 0.5$, $T_y = 2$ second and $e_s = 0.2b$ for all earthquakes; the *NBC* $\Omega = 0.5$, $T_y = 1$ second and $e_s = 0.2b$ for EQ3; and *H/K* $\Omega = 0.5$, $T_y = 2$ sec. and $e_s = 0.2b$ for EQ1. The peak nonlinear shear storey forces for these structures follow more closely to those predicted by elastic analysis and the magnitude of dynamic shear magnification is lower as can be seen in Figure 7.25, but even here the shears from the time history analysis are greater than the elastic/4 shears. Also, where the flexible wall yields only slightly, the storey shear forces fall nearer to the elastic predictions, but are still consistently greater except near mid height of the building. The buildings with a static stiffness eccentricity of $0.1b$ behaved similarly to

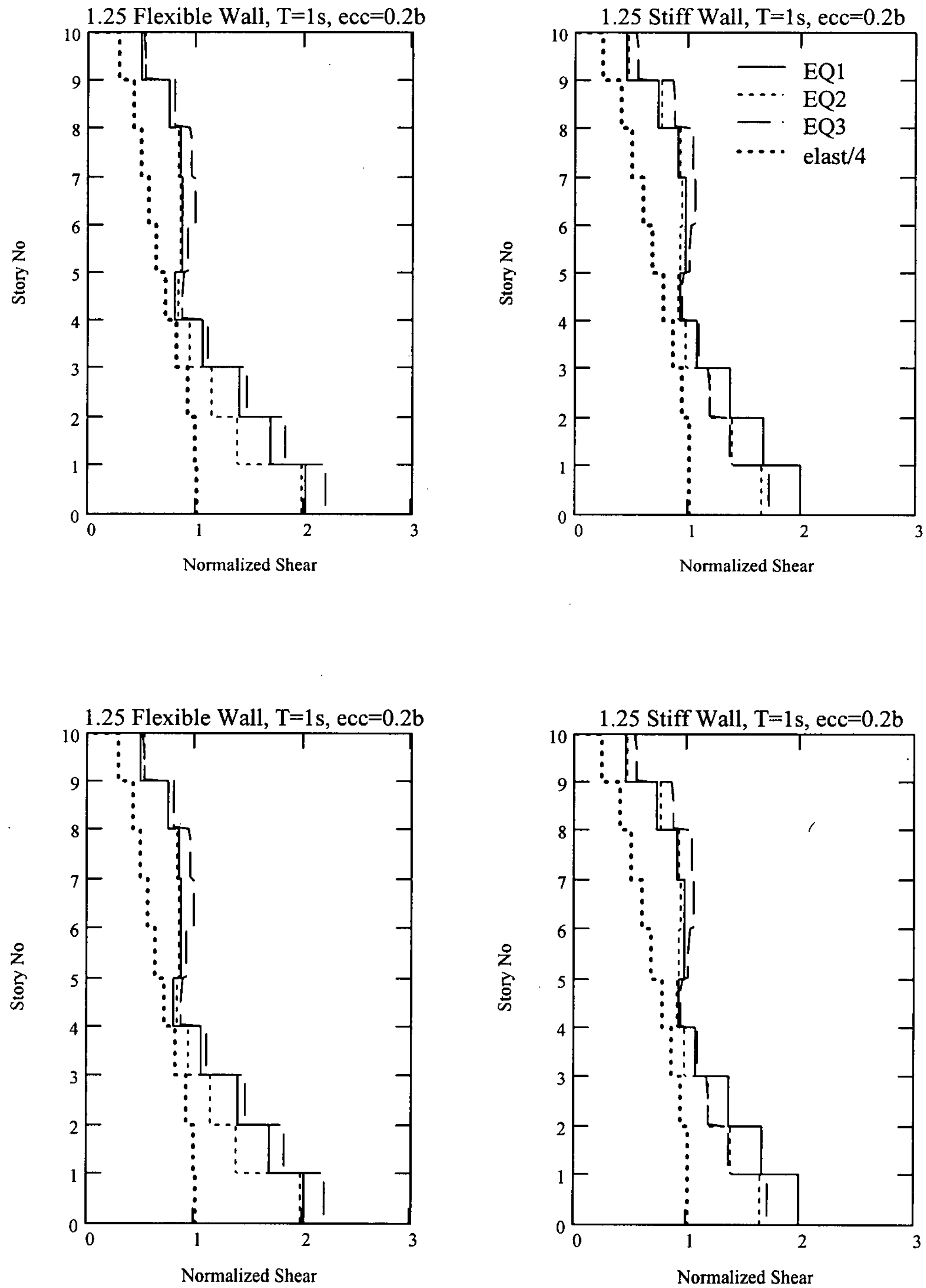

Figure 7.22 Normalized peak shear envelope distribution for *Dyn+T1* method of analysis for $\Omega = 1.25$ (top) and $\Omega = 0.5$ (bottom) for $T_y = 1$ second and $e_s = 0.2b$

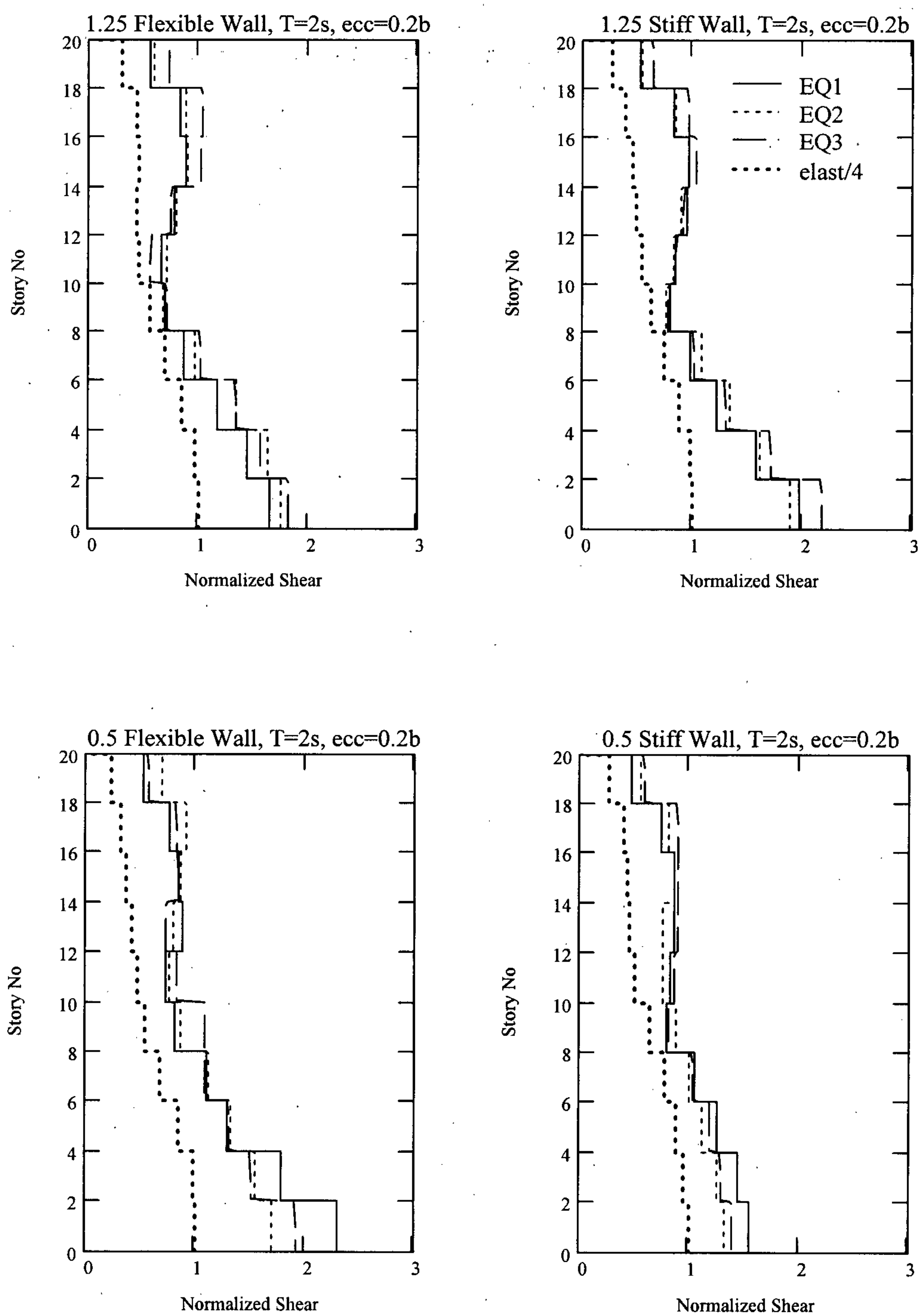

Figure 7.23 Normalized peak shear envelope distribution for *Dyn+T1* method of analysis for $\Omega = 1.25$ (top) and $\Omega = 0.5$ (bottom) for $T_y = 2$ seconds and $e_s = 0.2b$

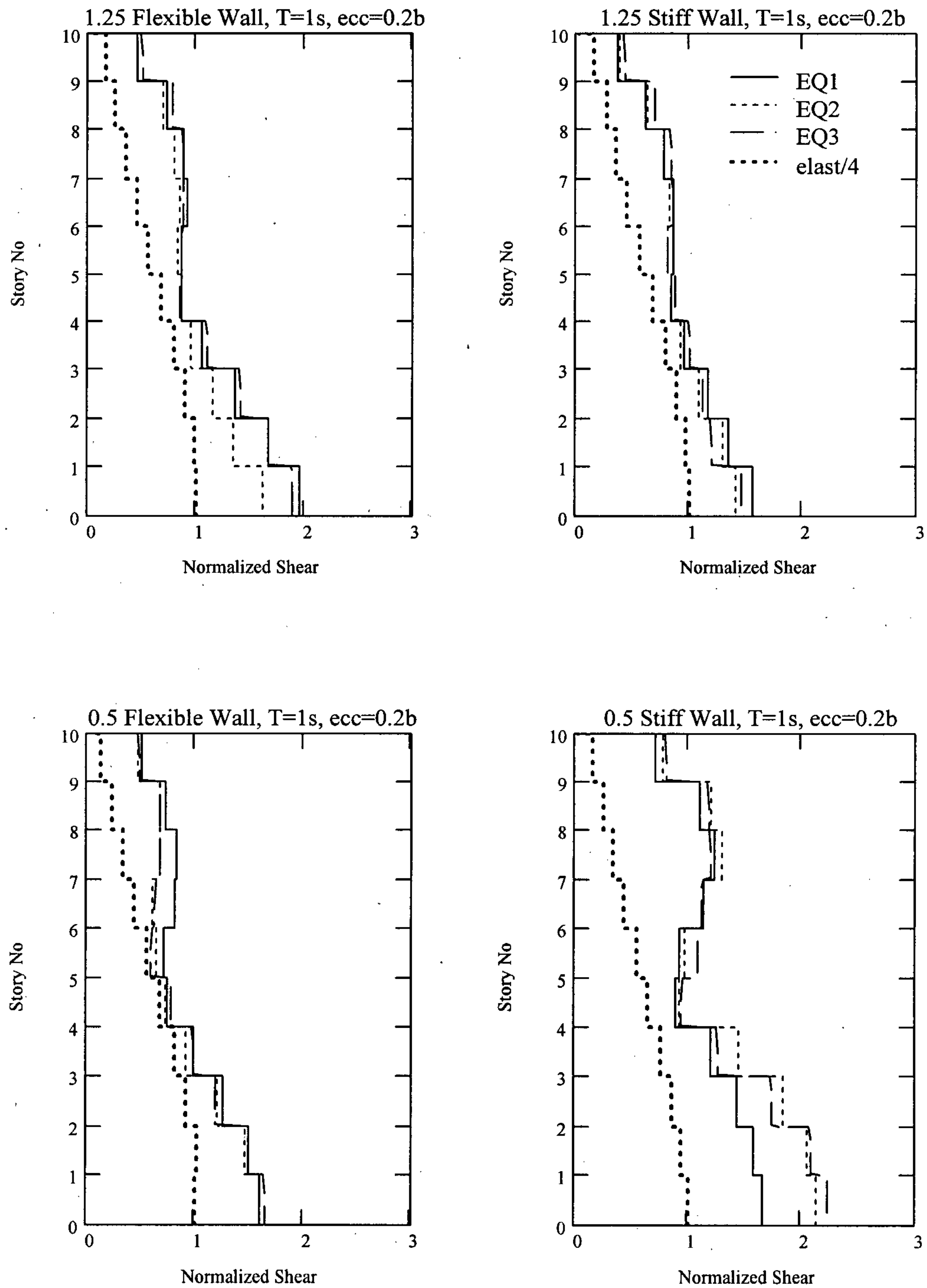

Figure 7.24 Normalized peak shear envelope distribution for *NBC* method of analysis for $\Omega = 1.25$ (top) and $\Omega = 0.5$ (bottom) for $T_y = 1$ second and $e_s = 0.2b$

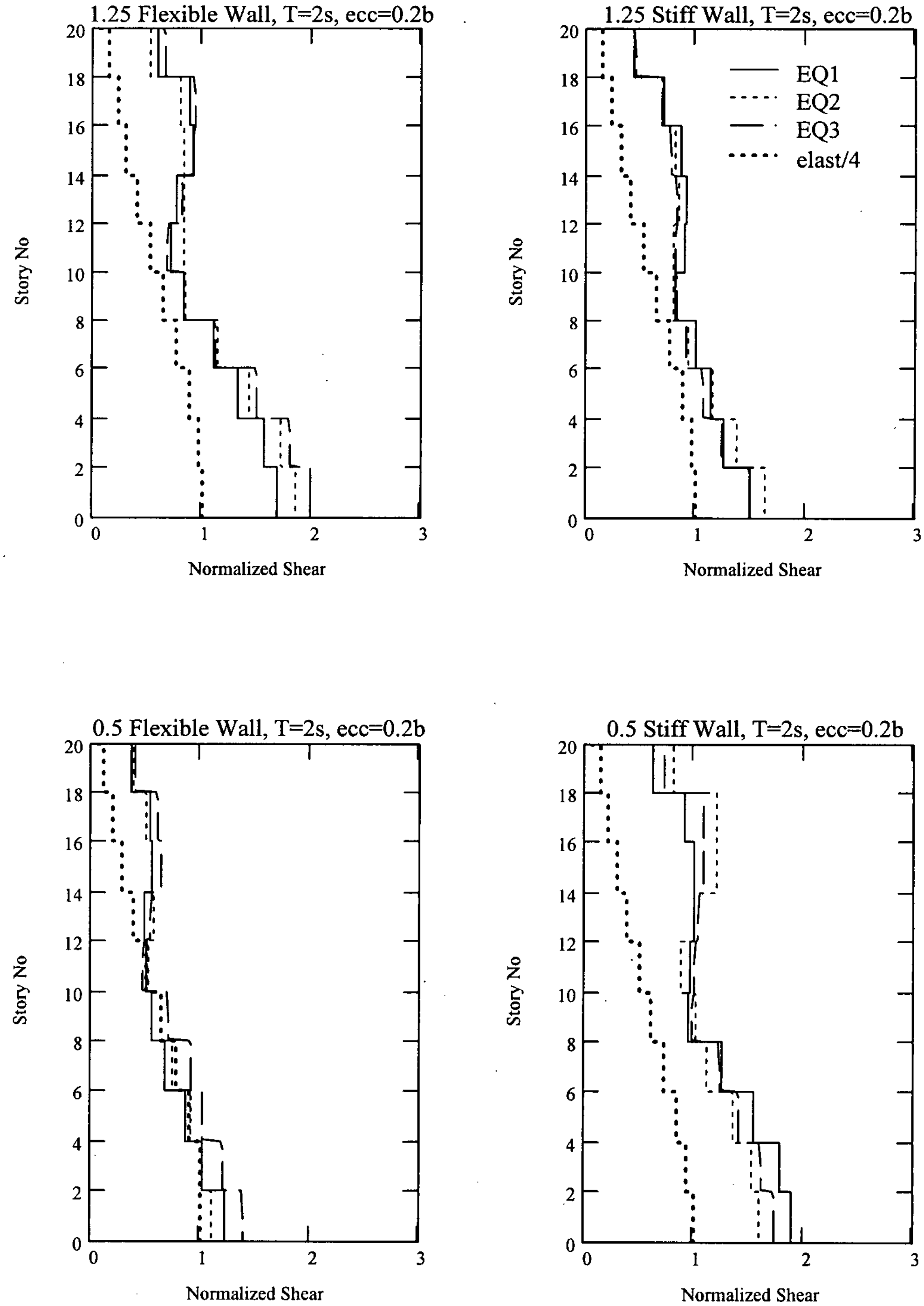

Figure 7.25 Normalized peak shear envelope distribution for *NBC* method of analysis for Ω = 1.25 (top) and $\Omega = 0.5$ (bottom) for $T_y = 2$ seconds and $e_s = 0.2b$

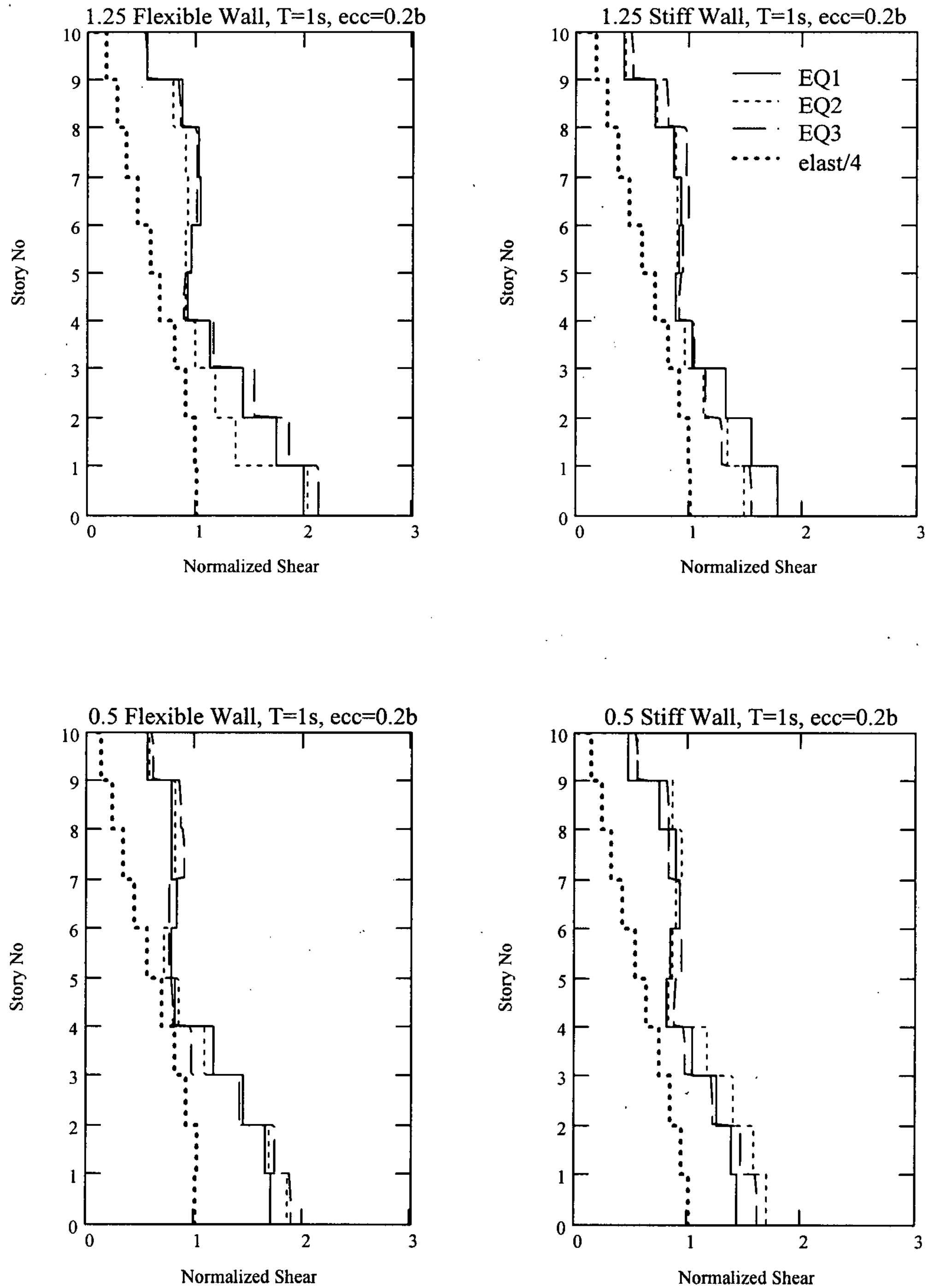

Figure 7.26 Normalized peak shear envelope distribution for *H/K* method for $\Omega = 1.25$ (top) and $\Omega = 0.5$ (bottom); $T_y = 1$ second and $e_s = 0.2b$

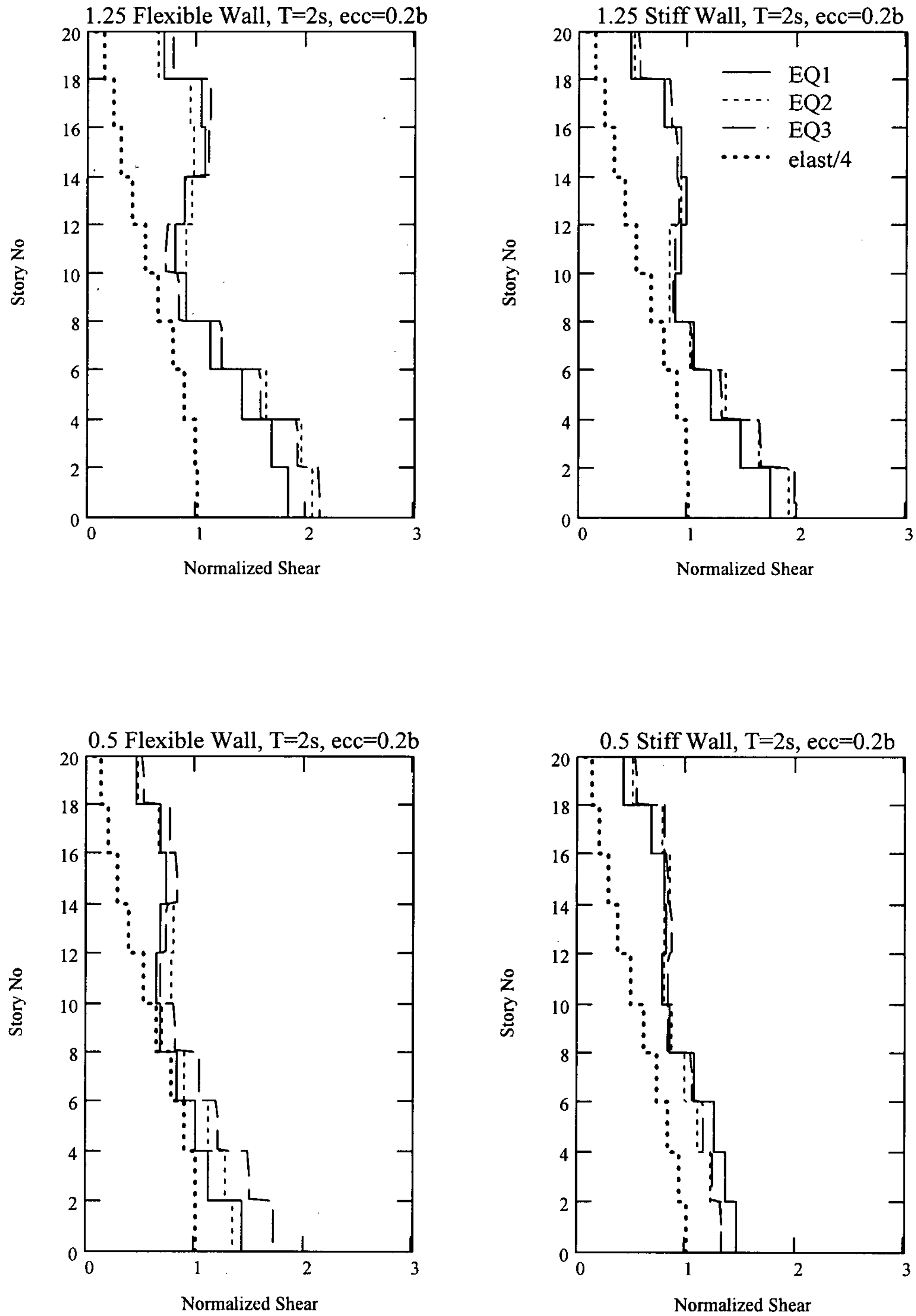

Figure 7.27 Normalized peak shear envelope distribution for *H/K* method for $\Omega = 1.25$ (top) and $\Omega = 0.5$ (bottom); $T_y = 2$ seconds and $e_s = 0.2b$

those included here.

The shear forces shown here are solely based on the design bending capacity of the walls. No increase has been included for wall overstrength. Shear reinforcing should not be curtailed according to the elastic predictions but needs to extend some distance up from the building base and then be gradually deceased towards the top. Adequate reinforcing must be extended full height to provide adequate shear capacity to resist the higher mode contributions.

Further investigation is needed to determine the dynamic magnification of shear forces with lower force reduction factors as well as the influence of peak ground acceleration and building period for the NBCC. Experimentation and/or detailed analysis is required to investigate the influence of shear cracking in the plastic hinge region on reduction of the dynamic shear magnification.

7.6 Summary of Results

The following points present a summary of the main results of this study:

1. Torsionally flexible systems generally exhibit larger peak displacements and interstorey displacements than torsionally stiff systems, however, the displacement and rotational ductility results at low torsional to lateral frequency ratio, $\Omega = 0.5$, are below the target value for all methods of design examined in this study. In contrast, torsionally stiff systems often exhibit displacement and rotational ductilities above the target value although the nonlinear displacements and rotations are quite small.

2. Displacements and interstorey displacements of the flexible-edge increase with increased static stiffness eccentricity regardless of the design method used here to determine element strengths.

3. The elastic dynamic and static designs are based solely on stiffness distribution with the implicit assumption that strength eccentricity would be the same. All design methods examined here result in strength eccentricity which is less than the stiffness eccentricity, and reduce the strength eccentricity to almost zero at $\Omega = 1.25$. In particular the *Dyn+T1* and *H/K* design methods allow large strength reductions for the stiff-edge elements which has the effect of reducing the strength eccentricity. Because of the variation between stiffness and strength eccentricity the elastic time history analyses underestimate inelastic stiff-edge displacements producing misleadingly large displacement and rotational ductility values for the stiff-edge at $\Omega = 1.25$. In contrast, the elastic time history analyses overestimate flexible edge displacements resulting in displacement and rotational ductilities below the target value.

4. At low Ω the dynamic response spectrum analysis with shifted CM, *DynCM±0.05b*, most accurately predicts the inelastic displacements of flexible-edge elements, while the *NBC* and *H/K* static design methods give overly conservative estimates of both flexible- and stiff-edge displacements. At high Ω the elastic *Dyn+T1* method and elastic TH with shifted CM often underestimate stiff-edge displacements while the *NBC* and *H/K* design methods give reasonable estimates of both flexible- and stiff-edge displacements. There is a substantial difference between the displacements determined by a RSA with statically

applied torsional moment of $0.05b$, *Dyn+T05*, and a RSA with shifted CM, *DynCM±0.05b*. The *Dyn+T05* response is always greater than the *DynCM±0.05b* response, particularly at low Ω.

5. The inelastic displacements and interstorey displacements for torsionally flexible structures are relatively insensitive to the design method used for determining element strength distribution. However, for torsionally stiff structures the displacements generally decrease with increase in element strength.

6. Displacement and rotational ductility are the largest for the $T_y = 2$ second system with an static stiffness eccentricity of $e_s = 0.1b$, reaching a magnitude of 10 and 8, respectively, in the stiff walls at $\Omega = 1.25$ for the *Dyn+T1* design method. As described previously, the large ductility values at high Ω are possibly due to the inability of the elastic TH analysis to account for the variation between the stiffness and strength eccentricity, which is also the greatest for this system. The strength eccentricity approaches zero at $\Omega = 1.25$ for all methods of determining element strength examined here. Ductilities calculated from the displacements found by the static methods would likely be more reasonable at $\Omega = 1.25$, however, at low Ω they would become ridiculously low since the elastically predicted displacements by these methods are very large. Despite that the elastic methods do not adequately predict stiff-edge element displacement or ductility, a strength eccentricity near zero is desirable to reduce torsional coupling.

7. Displacement and rotational ductility demand of torsionally flexible systems with $\Omega < 1$

are relatively independent of design method used for determining element strength. However, for torsionally stiff systems with $\Omega > 1$ ductility demand is generally a function of element strength. Ductility demand is adequately controlled for flexible wall elements and stiff wall elements with $\Omega < 1$. For stiff wall elements with $\Omega > 1$ the ductility demand increases with decreased element strength and with increased lateral period and often exceeds the design R value.

8. Displacement and rotational ductility demand in the walls of a symmetric system increase above the target design value for torsionally stiff systems ($\Omega > 1$) with a lateral period $T_y \geq 2$ seconds despite that the nonlinear displacements are relatively small. A design method needs to be developed for the determination of ductility for torsionally stiff asymmetric systems.

9. The revisions to the static torsional design eccentricity equations proposed by Humar and Kumar simplify the calculation of design eccentricity by eliminating the need to determine CR locations for torsionally stiff structure. However, having a separate equation for torsionally flexible structures with $\Omega < 1$ produces a large step in the magnitude of strength increase for the stiff-edge element at $\Omega = 1$. This step is undesirable since estimating frequency ratio is not exact and it is not clear which design equation is applicable for structures with a torsional to lateral frequency ratio in the vicinity of $\Omega = 1$.

10. Dynamic magnification of shear due to the contribution from higher modes can be more than double the estimated base shear or shear storey forces of the upper stories, regardless

of the elastic method employed in determining wall strengths.

11. To ensure that the lateral resisting walls have adequate shear reinforcing to withstand the magnified shear forces, reinforcing steel should not be curtailed according to the elastic predictions. The reinforcing required at the base needs to extend up 20% - 30% of the height from the building foundation and then gradually decrease towards the minimum mid-height requirement. The shear reinforcing for the upper half of the structure should be maintained constant from mid height and not linearly decreased to the top. Some reduction could be allowed for the top storey.

12. The moment demand from the nonlinear dynamic time history analyses varies substantially from that predicted by the elastic analyses. Second mode effects are visible in the flexible walls envelopes and are more apparent with increase in lateral period. An increase in the design moment envelope up the height of the building is necessary to account for the excess moment demand due to higher mode effects. Dependent upon the design method used, the value of the design base moment should be continued up 30-40% of the height of the building and then decreased linearly to zero at the top.

8 Conclusions and Recommendations

8.1 Conclusions

This study of the seismic behaviour of uniformly asymmetric multistorey shear wall structures has lead to the following conclusions which address the questions raised in the scope of this thesis in Section 1.4:

1. All methods examined adequately control the ductility demand of flexible-edge elements with the static methods (*NBC* and *H/K*) giving the most conservative results. The NBCC static torsional provisions best control the additional ductility demand of stiff wall elements, however at high Ω, the ductility demand exceeds the target ductility in some instances. The *Dyn+T1* method exceeds the target ductility by the largest margin for the stiff wall for torsionally stiff buildings due to the combination of permitted strength reductions for stiff wall elements and lower required increases in flexible wall element strength. Stiff wall strength reductions should not be allowed below that of an equivalent TB structure to avoid large increases in stiff-edge displacements and ductility demand.

   The element ductility demand for all systems was calculated using the elastic TH analyses results, therefore, the estimated element yield displacement for a particular model is the same for each design method. In reality the actual element displacement at yield would vary between design methods based on the assigned element flexural strength. Since peak inelastic displacements of torsionally flexible systems ($\Omega < 1$) are relatively insensitive to the method employed for determining element strength and strength reductions are permitted for stiff wall elements of torsionally stiff systems, some allowance should be made for incorporating the proportion of element strength increase into the determination of yield displacements from an elastic TH analysis to provide better approximations of element ductility demand.

2. The NBCC static torsional provisions give consistently conservative estimates of stiff and flexible-edge displacements for all structures examined, however, they substantially overestimate edge displacements of torsionally flexible structures, by as much as three times for flexible-edge elements. The static methods apply larger torsional moments than the dynamic methods in determining element strength and deflections, and therefore, the resulting displacements for both stiff- and flexible-edge elements by the static methods are larger than for the dynamic methods.

   The dynamic modal methods best estimate edge displacements with the *DynCM±0.05b elast* method giving the most accurate results, except for the stiff-edge elements of torsionally stiff structures, where they may underestimate displacements. All design methods examined in this study produce a strength eccentricity that is less than the stiffness eccentricity. The strength eccentricity decreases with increasing frequency ratio, approaching zero at $\Omega = 1.25$. Elastic methods are based solely on stiffness distribution and do not account for a strength eccentricity that varies substantially from the stiffness eccentricity. Because of the difference between the stiffness and strength eccentricity and the reduction in strength allowed for stiff-edge elements, the dynamic modal analyses underestimate inelastic stiff-edge displacements.

Code static provisions try to discourage torsionally flexible structures with large eccentricity by increasing element strength, however, *NBC* and *H/K* static methods excessively increase flexible wall element strength of even minimally eccentric torsionally flexible asymmetric structures to the extent where, in some models, the flexible wall elements do not yield when subjected to intense ground shaking. The *NBC* static method should be revised for asymmetric wall structures to provide a better strength distribution, similar to that of the response spectrum analysis with shifted CM or statically applied torsional moments, for torsionally flexible structures. This would provide adequate strength to limit ductility demand and nonlinear displacements, and enable more accurate estimations of nonlinear displacements and rotations for both stiff and flexible wall elements of flexible structures.

Inelastic displacements increase with torsional flexibility as well as increased eccentricity. The NBCC torsional provisions should integrate some form of the structure's torsional flexibility, or the torsional to lateral frequency ratio, Ω, into the design eccentricity equations. This may be achieved by either (1) approximating Ω by the Rayleigh Ritz method and introducing torsional static design equations as a function of Ω, and, as proposed by Humar, increasing the magnitude of design eccentricity for flexible systems, or (2) implementing a displacement dependent method similar to the UBC. The UBC introduces an amplification factor, A_x, to the accidental eccentricity portion of the design equations, which is a measure of the torsional to lateral frequency and the eccentricity, determined from the ratio of maximum and average diaphragm displacements of the structure under applied design lateral forces. The design eccentricity increases with increased torsional flexibility, thereby penalizing highly flexible and eccentric systems by increasing element design strength.

3. Inelastic displacement demand generally decreases with increase in element strength and lateral period for both stiff- and flexible-edge elements of torsionally stiff buildings. However, the displacement response of torsionally flexible buildings are relatively insensitive to the design method used for determining element strength distribution but increase with increased lateral period.

   Element ductility demand for torsionally flexible systems is relatively insensitive to the lateral period and design method used for determining element strength. For torsionally stiff systems element ductility demand is generally a function of element strength, decreasing with increased element strength but increasing with increased lateral period.

4. The TB inelastic displacement exceeds the TB elastic displacements and the TB displacement ductility demand exceeds the target displacement ductility by approximately 30% for structures with a lateral period $T_y \geq 2$ seconds. These results indicate that the equal displacement rule may not hold for multistorey structures with a lateral period greater than 2 seconds. Because of this, the normalized displacement response or ductility response of an inelastic system to that of an equivalent but torsionally balanced system, Δ/Δ_{TB} and $\mu_\Delta/\mu_{\Delta TB}$, respectively, adopted in previous studies for assessing the adequacy of code torsional provisions, could lead to misleadingly good results when in fact the results are in excess of the target design values.

5. Dynamic magnification of shear could pose a serious problem for shearwall buildings when subjected to strong ground motions. Due to the contribution from higher modes, the nonlinear base shear and the shear storey forces of the upper stories can be more than double those predicted by the elastic analysis, regardless of the method employed in determining wall strengths. Similar equations to those proposed by Keintzel (1992) directly applicable to the Canadian code need to be developed.

   Shear reinforcing should be extended to provide adequate shear capacity to resist the increased forces due to higher mode contributions and should not be curtailed according to the elastic predictions. The steel reinforcing required at the base needs to extend 20% - 30% up the height of the building from the building foundation and then gradually decrease towards the mid-height requirement. The shear reinforcing for the upper half of the structure should be maintained constant from mid height and not linearly decreased to the top, with the exception of perhaps the top storey where some reduction would be acceptable.

In addition to addressing the questions posed in the scope of this study, the following conclusions were drawn:

1. The revisions to the static torsional design eccentricity equations proposed by Humar and Kumar produce a large step in the magnitude of strength increase for the stiff-edge element at $\Omega = 1$. This step is undesirable since the estimate for frequency ratio is not precise and discrepancies could arise as to which is the valid design equation to use for structures that have a torsional to lateral frequency ratio in the vicinity of $\Omega = 1$. A more

gradual transition between the two proposed equations would be an improvement or an alternative method of defining torsionally flexible structures is should be implemented.

2. The moment demand from the nonlinear dynamic time history analyses varies substantially from that predicted by the elastic analyses. Second mode effects are evident in the envelopes of the flexible walls and are more pronounced for the buildings with $T_y \geq$ 2 seconds. An increase in the envelope is required to account for the excess moment demand due to higher mode effects up the height of the building. The magnitude of the base moment should be continued up 30-40% of the building height, depending on the design method implemented, and then decreased linearly to the top of the building.

3. From the extensive literature review it was found that the NBCC is deficient in defining precise definitions of acceptable forms of vertical and plan irregularities to limit the use of the static design procedures to relatively regular structures. Including clear restrictions for the use of the static design provisions would assist the design engineer in choosing the most appropriate means of analysis for each structure and avoid misuse of static procedures.

8.2 Recommendations for Future Research

This study of the elastic and nonlinear response of asymmetric, shear wall, high rise buildings was limited to structures with element strengths distributed according to mainly three design methods, the NBCC static torsional provisions, a dynamic RSA with statically applied torsional moments, and a new static method proposed by Humar and Kumar. The following recommendations for future research would help expand upon the findings of this study on the torsional response of multistorey shear wall buildings.

1. To determine whether limiting the strength reduction of the stiff-edge element to that of the equivalent torsionally balanced (TB) system would improve displacement response for the stiff-edge at $\Omega = 1.25$, further nonlinear time history analyses need to be conducted for adjusted *Dyn+T1*, *H/K* and some *NBC* models.

2. New elastic methods need to be developed to enable more accurate predictions of inelastic displacements and more reasonable element strength increase for torsionally flexible asymmetric structures.

3. Further investigation is needed to develop guidelines for the NBCC to account for the dynamic magnification of shear forces for a broader range of building periods, ground motions and peak acceleration, element strength increase, and R factors. Experimentation and/or detailed analysis is required to investigate the influence of shear cracking in the plastic hinge region on reduction of the dynamic shear magnification.

4. The buildings examined in this study are asymmetric in one direction only. The effects of bi-asymmetric structures on the nonlinear response of torsionally flexible shear wall structures would be of interest.

References

ANSYS Edition 5.3 (1998) Simon & Shuster /A Viacom Company, Upper Saddle River, NJ, Prentice-Hall, Inc.

Atkinson, G. M. and Beresnev, I. A. (1998) "Compatible ground-motion time histories for new national seismic hazard maps." *Canadian Journal of Civil Engineering*, 25, 305-318.

Bertero, R. D. (1995) "Inelastic torsion for preliminary seismic design." *Journal of Structural Engineering, ASCE*, 121 (4), 1183-1189.

Bruneau, M. and Mahin, S. A. (1991) "Seismic response of symmetric structures having unbalanced yield strengths in plan." *Proceedings: 6th Canadian Conference on Earthquake Engineering*, Toronto, Ontario, 109-116.

CPCA Concrete Design Handbook (1995) Ottawa, Canada, Canadian Portland Cement Association.

CANNY-E (1996a) *Technical Manual*, Canny Consultants PTE Ltd., Singapore.

CANNY-E (1996b) *Three-Dimensional Nonlinear Dynamic Structural Analysis Computer Program*, Canny Consultants PTE Ltd., Singapore.

CANNY-E (1996c) *User's Manual*, Canny Consultants PTE Ltd., Singapore.

Chandler, A.M. and Duan, X.N. (1991) "Evaluation of factors influencing the inelastic seismic performance of torsionally asymmetric buildings." *Earthquake Engineering and Structural Dynamics*, 20, 87-95.

Cheung, V.T. and Tso, W.K (1987) "Limitations of Codified Torsional Provisions." *Proc. 5th Canadian Conference of Earthquake Engineering*, Ottawa, Canada, 731-737.

Chopra, A. K. (1995) *Dynamics of structures: theory and applications to earthquake engineering.*, New Jersey, Prentice-Hall, Inc.

Correnza, J.C. Hutchinson, G. L. & Chandler, A. M. (1996) "An evaluation of serviceability limit state seismic torsional provisions of Eurocode 8." *Structural Engineering Review*, 8 (1), 49-63.

Correnza, J.C. Hutchinson, G. L. & Chandler, A. M. (1995) "Seismic response of flexible-edge elements in code-designed torsionally unbalanced structures." *Engineering Structures*, 17 (3), 158-166.

Correnza, J.C. Hutchinson, G. L. & Chandler, A. M. (1992) "A review of reference models for assessing inelastic seismic torsional effects in buildings." *Soil Dynamics and Earthquake Engineering*, 11, 465-484.

De La Llera, J. C., and Chopra, A. K. (1992) "Evaluation of code accidental torsion provisions using earthquake records from three nominally symmetric plan buildings." *Report No. UBC/EERC-92/09*, Earthquake Engineering Research Center, University of California, Berkeley.

De La Llera, J. C., and Chopra, A. K. (1994a) "Accidental and Natural Torsion in Earthquake Response and Design of Buildings." *Report No. UBC/EERC-94/07*, Earthquake Engineering Research Center, University of California, Berkeley.

De La Llera, J. C., and Chopra, A. K. (1994b) "Accidental torsion in buildings due to base rotational excitation." *Earthquake Engineering and Structural Dynamics*, 23 (9), 1003-1021.

De La Llera, J. C., and Chopra, A. K. (1994c) "Accidental torsion in buildings due to stiffness uncertainty." *Earthquake Engineering and Structural Dynamics*, 23 (2), 117-136.

De La Llera, J. C., and Chopra, A. K. (1994d) "Evaluation of code accidental torsion provisions from building records." *Journal of Structural Engineering, ASCE*, 120 (2), 597-616.

De La Llera, J. C., and Chopra, A. K. (1994e) "Using accidental eccentricity in code-specified static and dynamic analyses of buildings." *Earthquake Engineering and Structural Dynamics*, 23 (9), 947-967.

De La Llera, J. C., and Chopra, A. K. (1995a) "Estimation of Accidental Torsion Effects for Seismic Design of Buildings." *Journal of Structural Engineering, ASCE*, 121 (1), 102-114.

De La Llera, J. C., and Chopra, A. K. (1995b) "Understanding the inelastic seismic behaviour of asymmetric-plan buildings." *Earthquake Engineering and Structural Dynamics*, 24, 549-572.

De La Llera, J. C., and Chopra, A. K. (1995c) "A simplified model for analysis and design of asymmetric-plan buildings." *Earthquake Engineering and Structural Dynamics*, 24, 573-594.

De La Llera, J. C., and Chopra, A. K. (1996) "Inelastic Behavior of Asymmetric Multistorey Buildings." *Journal of Structural Engineering, ASCE*, 122 (6), 597-606.

Dempsey, K. M. and Tso, W. K. (1982) "An alternative path to seismic torsional provisions." *Soil Dynamics and Earthquake Engineering*, 1 (1), 3-10.

Duan, X. N. and Chandler, A. M. (1993) "Inelastic seismic response of code designed multistorey frame buildings." *Earthquake Engineering and Structural Dynamics*, 22, 431-445.

Farah, Reina M. (1998) "Torsional Response of Ductile Wall Systems Under Seismic Attack." *Masters Thesis, University of California under N. Priestley,* San Diego, California, USA.

Goel, R. K. and Chopra, A. K. (1990) "Inelastic seismic response of one-storey, asymmetric-plan systems: effects of stiffness and strength distribution." *Earthquake Engineering and Structural Dynamics*, 19, 949-970.

Goel, R. K. and Chopra, A. K. (1991) "Effect of plan asymmetry in inelastic seismic response of one-storey, systems." *Journal of Structural Engineering, ASCE,* 117 (5), 1492-1513.

Goel, R. K., and Chopra, A. K. (1993) "Seismic code analysis of buildings without locating centers of rigidity." *Journal of Structural Engineering, ASCE*, 119 (10), 3039-3055.

Humar, J. L. (1998) "Code Provisions to Account for Earthquake Induced Torsion" To be published.

Humar, J. L. and Kumar, P. (1999) "Effect of orthogonal inplane structural elements on inelastic torsional response" To be published in Earthquake Engineering and Structural Dynamics.

Jain, A. K. and Anniger, S. (1995) "Seismic load distribution in buildings with eccentric setback: Discussion." *Canadian Journal of Civil Engineering*, 22, 840-841.

Kan, C. L. and Chopra, A. K. (1981) "Torsional coupling and earthquake response of simple elastic and inelastic systems." *Journal of Structural Division, ASCE,* 107, 1569-1588.

Keintzel, Einar (1990) "Seismic design shear forces in RC cantilever shear wall structures." *European Earthquake Engineering*, 3, 7-16.

Keintzel, Einar (1992) "Advances in the design of shear of RC structural walls under seismic loading." In *Nonlinear Seismic Analysis and Design of Reinforced Concrete Buildings*, ed. Peter Fajfar and Helmut Krawinkler, Elsevier Applied Science, London and New York, 161-170.

Kumar, P. (1998) "Torsional Response of Buildings During Earthquake" *Ph.D. Thesis, Carleton University*, Ottawa, Canada.

NBCC - National Building Code of Canada. (1995) "Section 4.1.9. Live Loads Due to Earthquakes." National Research Council of Canada, Ottawa, Ontario.

Naumoski, N. (1985) "SYNTH program: Generation of artificial acceleration time history compatible with a target spectrum." *McMaster Earthquake Engineering Software Library*, Dept. of Civil Engineering and Engineering Mechanics, McMaster University, Hamilton, Canada.

NEHRP Recommended provisions for the development of seismic regulations for new buildings. Part 1 - Provisions, Part 2 - Commentary (1994 Edition) Building Seismic Safety Council, Washington, DC.

NEHRP Recommended provisions for the development of seismic regulations for new buildings and other structures. Part 1 - Provisions, Part 2 - Commentary (1997 Edition) Building Seismic Safety Council, Washington, DC.

Newmark, N. M. and Rosenblueth, E. (1971) *Fundamentals of Earthquake Engineering*, Prentice-Hall Inc. Englewood Cliffs, N.J.

NZS 4203 - Code of Practice for General Structural Design and Design Loadings for Buildings, Part 4 - Earthquake Provisions (1992) New Zealand Standard, Standards Association of New Zealand.

Paulay, T. (1997a) "Are Existing Seismic Torsional Provisions Achieving the Design Aims?" *Earthquake Spectra*, 13 (2), 259-279.

Paulay, T. (1997b) "Seismic torsional effects on ductile structural wall systems" *Journal of Earthquake Engineering*, 13 (2), 259-279.

Paulay, T. (1997c) "A behaviour based design approach to earthquake-induced torsion in ductile buildings." To be published.

Paulay, T. and Priestley, M.J.N. (1992) *Seismic design of reinforced concrete and masonry buildings*, John Wiley and Sons, Inc., New York, Chichchester, Brisbane, Toronto and Singapore.

Preumont, A. (1984) "The generation of spectrum comp[atible accelerograms for the design of nuclear power plants." *Earthquake Engineering and Structural Dynamics*, 12, 481-497.

SAP2000 Nonlinear Version 6.11 (1997) Computers and Structures Inc., Berkeley, California.

Sadek, A. W. and Tso, W. K. (1989) "Strength eccentricity concept for inelastic analysis of asymmetrical structures." *Engineering Structures*, 11 (3), 189-194.

Supplement to the National Building Code of Canada (1995) "Commentary J Effects of Earthquakes." National Research Council of Canada, Ottawa, Ontario.

Thomson, W. T. (1971) *Mechanical Vibrations, 2nd Edition*, Prentice-Hall Inc. Englewood Cliffs, N.J.

Tso, W. K. (1983) "A Proposal to improve the static torsional provisions for the National Building Code of Canada." *Canadian Journal of Civil Engineering*, 10, 561-565.

Tso, W. K. (1990) "Static eccentricity concept for torsional moment estimations." *Journal of Structural Engineering, ASCE,* 116 (5), 1199-1212.

Tso, W. K. (1993) "Discussion of 'A review of reference models for assessing inelastic seismic torsional effects in buildings,' by J. C. Correnza et al." *Soil Dynamics and Earthquake Engineering,* 12 (7), 445-447.

Tso, W. K. and Sadek, A. W. (1985) "Inelastic seismic response of simple eccentric systems." *Earthquake Engineering and Structural Dynamics*, 13, 225-269.

Tso, W. K. and Wong, C. M. (1993) "An evaluation of the new zealand code torsional provision." *Bulletin of the New Zealand National Society for earthquake engineering*, 26 (2), 194-207.

Tso, W. K. and Wong, C. M. (1995) "Seismic displacements of torsionally unbalanced buildings." *Earthquake Engineering and Structural Dynamics*, 24, 1237-1387.

Tso, W. K. and Ying, H. (1990) "Additional seismic inelastic deformation caused by structural asymmetry." *Earthquake Engineering and Structural Dynamics,* 19, 243-258.

Tso, W. K. and Yao, Shu (1994) "Seismic load distribution in buildings with eccentric setback." *Canadian Journal of Civil Engineering*, 21, 50-62.

Tso, W. K. and Ying, H. (1992) "Lateral strength distribution specification to limit additional inelastic deformation of torsionally unbalanced systems." *Engineering Structures,* 14 (4), 263-277.

Tso, W. K. and Zhu, T. J. (1992) "Design of torsionally unbalanced structural systems based on code provisions I: Ductility demand." *Earthquake Engineering and Structural Dynamics*, 21, 609-627.

Uniform Building Code. (1997) "Chapter 16 - Structural Design Requirements." International Conference of Building Officials, Whittier, California.

Wong, C.M., and Tso, W. K. (1994) "Inelastic Seismic Response of Torsionally Unbalanced Systems Designed Using Elastic Dynamic Analysis." *Earthquake Engineering and Structural Dynamics*, 23, 777-798.

Wong, C.M., and Tso, W. K. (1995) "Evaluation of Seismic Torsional Provisions in the Uniform Building Code." *Journal of Structural Engineering, ASCE,* 121 (10), 1436-1442.

Zhu, T. J. and Tso, W. K. (1992) "Design of torsionally unbalanced structural systems based on code provisions II: Strength distribution." *Earthquake Engineering and Structural Dynamics*, 21, 609-627.

Appendix A

Computer Input Files

A.1 Sample CANNY-E Input File for Nonlinear Analysis

1999.1, dynamic analysis of 3D 20 story shear wall building T=2s
TU a/b=0.5 ecc=0.1 FR=0.5 CM=-0.05b

// analysis assumptions and output options

title = DYNAMIC ANALYSIS 20-STORY WALL BUILDING TU a/b=0.5 ecc=0.1 FR=0.5
CM=-0.05b T=2s

force unit = kN
length unit = m
time unit = sec
including rigid floor rotation
gravity acceleration is 9.807
output of overall response at floor levels
output of nodal displacement response
output all column response
output of extreme response

// control data of dynamic response
integration 4-step for one acceleration data
start time 0.0, end time 40
check peak displacement 0.05
response limit 1.5
master DOFs for analysis control: 10F XY-translation
binary file output at every 0-step
including Z-translational inertia forces

/*DAMPING
Newmark method using Beta-value 0.25
damping constant 0.05 to first mode
damping constant 0.05 to second mode

/*EARTHQUAKE RECORDS
scale factor 0.001 to X-EQ file =
scale factor 0.001 to Y-EQ file = c:\canny\EQrecords\Miyans.s2O
scale factor 0.015 to Z-EQ file =
scale factor 1.5 to R-EQ file =

//node locations
X1 & X5, Y1 & Y5, 1F to 11F
X2 & X4, Y3, 1F to 11F
X3, Y3, 1F to 11F

X3, Y2 & Y4, 1F to 11F
node at X20, Y3, 2F to 11F, free
node at X40, Y3, 2F to 11F, free
node at X50, Y5, 2F to 11 F, free
node at X55, Y5, 2F to 11 F, free
//

//node DOF
general DOF all component
node X20, Y3, 2F to 11F eliminate all rotations
node X40, Y3, 2F to 11F eliminate all rotations
node X50, Y5, 2F to 11F eliminate all rotations
node X55, Y5, 2F to 11F eliminate all rotations
//

// floor level data
11F(rigid floor): Z=37.0 G(-1.8,0), W=3412.905 Rj=460742.2
10F(rigid floor): Z=33.3 G(-1.8,0), W=3412.905 Rj=460742.2
9F(rigid floor): Z=29.6 G(-1.8,0), W=3412.905 Rj=460742.2
8F(rigid floor): Z=25.9 G(-1.8,0), W=3412.905 Rj=460742.2
7F(rigid floor): Z=22.2 G(-1.8,0), W=3412.905 Rj=460742.2
6F(rigid floor): Z=18.5 G(-1.8,0), W=3412.905 Rj=460742.2
5F(rigid floor): Z=14.8 G(-1.8,0), W=3412.905 Rj=460742.2
4F(rigid floor): Z=11.1 G(-1.8,0), W=3412.905 Rj=460742.2
3F(rigid floor): Z=7.40 G(-1.8,0), W=3412.905 Rj=460742.2
2F(rigid floor): Z=3.70 G(-1.8,0), W=3412.905 Rj=460742.2
1F(fixed support): Z=0
//

// frame locations
X1=-18.0, X2=-3.974, X3=0.0, X4=8.608, X5=18.0, X20=-3.976, X40=8.610, X50=-17.998, X55=17.998
Y1=-9, Y2=-0.3, Y3=0.0, Y4=0.3, Y5=9.0
//

// element data: slab
(X1 Y1)(X1 Y5)(X5 Y5)(X5 Y1) 1F to 11F
//

// element data: column
auto rearrange elements of columns in sequential order
/* 4 - CORNER COLUMNS
X1&X5 Y1&Y5, 2F~11F BU1 TU1 SU100 AU900 r(0.01 0.01)
X1&X5 Y1&Y5, 1F~2F BU1 TU1 SU100 AU900 r(0 0.01)

```
/* 4 - WALLS

/* flexible wall
X2 Y3, 2F~11F  BX1 BY1001 TX1 TY1001 SU101 AU901 r(0.01 0.01)
X2 Y3, 1F~2F   BX1 BY1001 TX1 TY1001 SU101 AU901 r(0 0.01)

/* centre wall
X3 Y3, 2F~11F  BX2 BY1002 TX2 TY1002 SU102 AU902 r(0.01 0.01)
X3 Y3, 1F~2F  BX2 BY1002 TX2 TY1002 SU102 AU902 r(0 0.01)

/* stiff wall
X4 Y3, 2F~11F BX3 BY1003 TX3 TY1003 SU103 AU903 r(0.01 0.01)
X4 Y3, 1F~2F  BX3 BY1003 TX2 TY1003 SU103 AU903 r(0 0.01)

/* walls in x-direction (symmetrical)
X3 Y2&Y4, 2F~11F BX1005 BY5 TX1005 TY5 SU105 AU905 r(0.01 0.01)
X3 Y2&Y4, 1F~2F  BX1005 BY5 TX1005 TY5 SU105 AU905 r(0 0.01)

/*dummy beams to get wall deformations
Y3 X2-X20 2F~11F horizontal column BU2 TU2 SU20 AU200
Y3 X4-X40 2F~11F horizontal column BU2 TU2 SU20 AU200
Y5 X1-X50 2F~11F horizontal column BU2 TU2 SU20 AU200
Y5 X5-X55 2F~11F horizontal column BU2 TU2 SU20 AU200
//

// stiffness and hysteresis parameters
/* outside columns bending, shear and axial properties
U1   EL1  0.5E+8  3.74E-6
U100  EL1  19.25E+6  0.0013
U900  EL1  0.5E+8  2.447E-03

/*dummy beams
U2   EL1  2.0E+4  3.74E-6
U20   EL1  77E+3  0.0013
U200  EL1  2.0E+4  2.44E-03

/* elastic bending stiffness of walls
X1  EL1  6.85E+6  0.0003
X2  EL1  6.85E+6  0.0003
X3  EL1  6.85E+6  0.0003
Y5  EL1  6.85E+6  0.0003

/* trilinear bending stiffness walls
Y1001  CA3  6.85E+6  7.958251   C(4159 4159)  Y(12477 12477)  A(1 1)  B(0.001 0.001)
      P(0.3,0.053)
```

```
Y1002  CA3  6.85E+6  3.183449  C(1286 1286)  Y(3858 3858)   A(1 1)  B(0.001 0.001)
       P(0.3,0.053)
Y1003  CA3  6.85E+6  14.32576  C(6850 6850)  Y(20551 20551)  A(1 1)  B(0.001 0.001)
       P(0.3,0.053)
X1005  CA3  6.85E+6  12.73284  C(3608 3608)  Y(10823 10823)  A(1 1)  B(0.001 0.001)
       P(0.3,0.053)

/* shear stiffness of walls
U101  EL1  2.74E+6  1.89
U102  EL1  2.74E+6  1.39
U103  EL1  2.74E+6  2.30
U105  EL1  2.74E+6  2.21


/* axial stiffness of walls
U901  EL1  6.85E+6  2.27
U902  EL1  6.85E+6  1.67
U903  EL1  6.85E+6  2.76
U905  EL1  6.85E+6  2.66
//

// initial load before TH analysis

/* initial axial load in 4-walls
node X3 Y2&Y4 2F to 11F, Pz = 100
node X2 Y3 2F to 11F, Pz = 100
node X4 Y3 2F to 11F, Pz = 100
//
```

A.2 Sample SAP2000 Input File for Elastic Analysis

```
3DFRAME 10-STORY 3 WALL STRUCTURE CONSTRAINED SLABS ecc=0.1
    Omega=0.5 T=2sec

SYSTEM
 FORCE=N  LENGTH=m  PAGE=SECTIONS

MODE
 TYPE=EIGEN  N=21

JOINT
 1,2,1,1001,100        X=18,18,18                Y=9,-9,9           Z=0,0,37
 3,4,1,1003,100        X=-18,-18,-18             Y=-9,9,-9          Z=0,0,37
 5,7,2,1005,100        X=8.608,-3.974,8.608      Y=0,0,0            Z=0,0,37
 6,8,2,1006,100        X=0,0,0                   Y=-0.3,0.3,-0.3    Z=0,0,37
 9,1009,100            X=0,0                     Y=0,0              Z=0,37

;add joints for locating CM
 110,1010,100          X=0,0          Y=0,0      Z=3.7,37

;NBCC design
;add joints applying load at 1.5e+0.1b
 111,1011,100          X=-5.4,-5.4    Y=0,0      Z=3.7,37
;add joints applying load at 0.5e-0.1b
 112,1012,100          X=5.4,5.4      Y=0,0      Z=3.7,37

;H/K design
;add joints applying load at 1.0e+0.1b
 113,1013,100          X=-3.6,-3.6    Y=0,0      Z=3.7,37
;add joints applying load at -0.1b
 114,1014,100          X=7.2,7.2      Y=0,0      Z=3.7,37

RESTRAINTS
 ADD=1  9  1  DOF=ALL          ;fix base
 ADD=110  1010  100  DOF=U3,R1,R2       ;fix CM joint DOF
 ADD=111  1011  100  DOF=U3,R1,R2
 ADD=112  1012  100  DOF=U3,R1,R2
 ADD=113  1013  100  DOF=U3,R1,R2
 ADD=114  1014  100  DOF=U3,R1,R2

CONSTRAINT
NAME=FLR1  TYPE=DIAPH  AXIS=Z
  ADD=101,114,1
```

```
NAME=FLR2  TYPE=DIAPH  AXIS=Z
  ADD=201,214,1
NAME=FLR3  TYPE=DIAPH  AXIS=Z
  ADD=301,314,1
NAME=FLR4  TYPE=DIAPH  AXIS=Z
  ADD=401,414,1
NAME=FLR5  TYPE=DIAPH  AXIS=Z
  ADD=501,514,1
NAME=FLR6  TYPE=DIAPH  AXIS=Z
  ADD=601,614,1
NAME=FLR7  TYPE=DIAPH  AXIS=Z
  ADD=701,714,1
NAME=FLR8  TYPE=DIAPH  AXIS=Z
  ADD=801,814,1
NAME=FLR9  TYPE=DIAPH  AXIS=Z
  ADD=901,914,1
NAME=FLR10  TYPE=DIAPH  AXIS=Z
  ADD=1001,1014,1

PATTERN
 NAME=DEFAULT

MASSES
 ADD=110,1010,100  UX=348019 UY=348019  RZ=46982625

MATERIAL
 NAME=STL  ;IDES=S  M=7827.099  W=76819.54;steel column material properties
   E=0.5E11            U=0.3
 NAME=CONC  ;IDES=C  M=2400  W=2400*9.81 ;concrete wall material properties
   E=6.85E9            U=0.25

FRAME SECTION
 NAME=WALLX MAT=CONC   SH=R      T=7.586,0.35
 NAME=WALLS MAT=CONC   SH=R      T=0.35,7.89
 NAME=WALLF MAT=CONC   SH=R      T=0.35,6.486
 NAME=WALLM MAT=CONC   SH=R      T=0.35,4.779
 NAME=CCOL  MAT=STL    SH=B      T=0.102,0.102,0.0064,0.0064

FRAME
; number generation is for frame numbers not joints
  1 J=1,101  SEC=CCOL
 GEN=1,4,1,901,100
  5  J=5,105  SEC=WALLS
 GEN=5,905,100
  6  J=6,106  SEC=WALLX
```

```
GEN=6,8,2,906,100
 7 J=7,107  SEC=WALLF
GEN=7,907,100
 9 J=9,109  SEC=WALLM
GEN=9,909,100

LOAD
;apply vertical dead load of structure to walls
 NAME=DL
  TYPE=FORCE
    ADD=105,109,1  UZ=-100000
    ADD=205,209,1  UZ=-100000
    ADD=305,309,1  UZ=-100000
    ADD=405,409,1  UZ=-100000
    ADD=505,509,1  UZ=-100000
    ADD=605,609,1  UZ=-100000
    ADD=705,709,1  UZ=-100000
    ADD=805,809,1  UZ=-100000
    ADD=905,909,1  UZ=-100000
    ADD=1005,1009,1  UZ=-100000

;static loads from dynamic analysis force distribution applied at each floor in N
 NAME=TPOS1
  TYPE=FORCE
    ADD=109  RZ=1314.015E3
    ADD=209  RZ=1792.404E3
    ADD=309  RZ=2101.369E3
    ADD=409  RZ=2265.901E3
    ADD=509  RZ=2271.199E3
    ADD=609  RZ=2106.667E3
    ADD=709  RZ=1788.197E3
    ADD=809  RZ=1428.867E3
    ADD=909  RZ=1479.166E3
    ADD=1009  RZ=2713.691E3

 NAME=TNEG1
  TYPE=FORCE
    ADD=109  RZ=-1314.015E3
    ADD=209  RZ=-1792.404E3
    ADD=309  RZ=-2101.369E3
    ADD=409  RZ=-2265.901E3
    ADD=509  RZ=-2271.199E3
    ADD=609  RZ=-2106.667E3
    ADD=709  RZ=-1788.197E3
    ADD=809  RZ=-1428.867E3
```

```
    ADD=909  RZ=-1479.166E3
    ADD=1009 RZ=-2713.691E3

NAME=TPOS05
  TYPE=FORCE
    ADD=109  RZ=657.008E3
    ADD=209  RZ=896.202E3
    ADD=309  RZ=1050.685E3
    ADD=409  RZ=1132.951E3
    ADD=509  RZ=1135.599E3
    ADD=609  RZ=1053.333E3
    ADD=709  RZ=894.099E3
    ADD=809  RZ=714.434E3
    ADD=909  RZ=739.583E3
    ADD=1009  RZ=1356.845E3

NAME=TNEG05
  TYPE=FORCE
    ADD=109  RZ=-657.008E3
    ADD=209  RZ=-896.202E3
    ADD=309  RZ=-1050.685E3
    ADD=409  RZ=-1132.951E3
    ADD=509  RZ=-1135.599E3
    ADD=609  RZ=-1053.333E3
    ADD=709  RZ=-894.099E3
    ADD=809  RZ=-714.434E3
    ADD=909  RZ=-739.583E3
    ADD=1009 RZ=-1356.845E3

NAME=LAT1
  TYPE=FORCE
    ADD=111  UY=365004
    ADD=211  UY=497890
    ADD=311  UY=583714
    ADD=411  UY=629417
    ADD=511  UY=630889
    ADD=611  UY=585185
    ADD=711  UY=496721
    ADD=811  UY=396908
    ADD=911  UY=410880
    ADD=1011  UY=753803

NAME=LAT2
  TYPE=FORCE
    ADD=112  UY=365004
```

```
  ADD=212 UY=497890
  ADD=312 UY=583714
  ADD=412 UY=629417
  ADD=512 UY=630889
  ADD=612 UY=585185
  ADD=712 UY=496721
  ADD=812 UY=396908
  ADD=912 UY=410880
  ADD=1012 UY=753803

NAME=LAT3
 TYPE=FORCE
  ADD=109 UY=365004
  ADD=209 UY=497890
  ADD=309 UY=583714
  ADD=409 UY=629417
  ADD=509 UY=630889
  ADD=609 UY=585185
  ADD=709 UY=496721
  ADD=809 UY=396908
  ADD=909 UY=410880
  ADD=1009 UY=753803

NAME=LATH1
 TYPE=FORCE
  ADD=113 UY=365004
  ADD=213 UY=497890
  ADD=313 UY=583714
  ADD=413 UY=629417
  ADD=513 UY=630889
  ADD=613 UY=585185
  ADD=713 UY=496721
  ADD=813 UY=396908
  ADD=913 UY=410880
  ADD=1013 UY=753803

NAME=LATH2
 TYPE=FORCE
  ADD=114 UY=365004
  ADD=214 UY=497890
  ADD=314 UY=583714
  ADD=414 UY=629417
  ADD=514 UY=630889
  ADD=614 UY=585185
  ADD=714 UY=496721
```

```
  ADD=814  UY=396908
  ADD=914  UY=410880
  ADD=1014  UY=753803

SPEC     ;response spectrum for elastic analysis in y-direction
 NAME=CQC  DAMP=0.05  MODC=CQC
  ACC=U2  FUNC=VANSPEC  SF=9.81

FUNCTION
 NAME=VANSPEC NPL=1  PRINT=Y  FILE=VanSpec.sap

COMBO
 NAME=RSAPOS1  TYPE=ADD
  LOAD=DL      SF=1
  LOAD=TPOS1   SF=1
  SPEC=CQC     SF=1
 NAME=RSANEG1  TYPE=ADD
  LOAD=DL      SF=1
  LOAD=TNEG1   SF=1
  SPEC=CQC     SF=1
 NAME=RSAPOS05  TYPE=ADD
  LOAD=DL      SF=1
  LOAD=TPOS05  SF=1
  SPEC=CQC     SF=1
 NAME=RSANEG05  TYPE=ADD
  LOAD=DL      SF=1
  LOAD=TNEG05  SF=1
  SPEC=CQC     SF=1

 NAME=ENVRSA1  TYPE=ENVE
  COMB=RSAPOS1  SF=1
  COMB=RSANEG1  SF=1

 NAME=ENVRSA05  TYPE=ENVE
  COMB=RSAPOS05  SF=1
  COMB=RSANEG05  SF=1

 NAME=ENVCODE TYPE=ENVE
  LOAD=LAT1     SF=1
  LOAD=LAT2     SF=1
  LOAD=LAT3     SF=1

 NAME=ENVH  TYPE=ENVE
  LOAD=LATH1  SF=1
  LOAD=LATH2  SF=1
```

```
 LOAD=LAT3   SF=1

OUTPUT
 ELEM=JOINT  TYPE=DISP,REAC   COMB=ENVRSA05, ENVRSA1, ENVCODE, ENVH
 ELEM=FRAME  TYPE=JOINTF      COMB=ENVRSA05, ENVRSA1, ENVCODE, ENVH
 ELEM=JOINT  TYPE=DISP,REAC    SPEC=CQC
 ELEM=FRAME  TYPE=JOINTF       SPEC=CQC

END
```